Genetic and Functional Studies on the Conserved IRG (Immunity-related GTPase) Protein IRGC (CINEMA)

Inaugural-Dissertation

zur

Erlangung des Doktorgrades

der Mathematisch-Naturwissenschaftlichen Fakultät

der Universität zu Köln

vorgelegt von

Christoph Rohde

aus Köln

Köln, 2007

für meine Eltern

Table of contents

Abbreviations

Ade	adenine
APS	ammoniumpersulfate
ATP	adenosine triphosphate
bp	base pair
BSA	bovine serum albumine
C-terminal	carboxy terminal
cAMP	cyclic adenosine monophosphate
CRE	cAMP response element
CREM	cAMP response element modulator
C. psittaci	*Chlamydia psitacci*
C. trachomatis	*Chlamydia trachomatis*
DEPC	diethyl pyrocarbonate
DMEM	Dulbecco Modified Eagles Medium
DNA	desoxyribonucleicacid
E. coli	*Escherichia coli*
EDTA	ethylendiamintetraacetic acid
EF cells	embryonic feeder cells
EGFP	enhanced green fluorescent protein
ER	endoplasmatic reticulum
ES cells	embryonic stem cells
EST	expressed sequence tag
EtBr	ethidium bromide
EtOH	ethanol
FCS	fetal calf serum
GAP	GTPase activating protein
GAPDH	Glyceraldehyde-3-phosphate dehydrogenase
GAS	γ-activated site
GBP	guanylate binding protein
GEF	guanine nucleotide exchange factor
GDI	guanine nucleotide dissociation factor
GDP	guanosine diphosphate
GMP	guanosine monophosphate
GTP	guanosine triphosphate
His	histidine
IC	immunocytochemistry
IF	immunofluorescence
IFN	interferon
IFGR	interferon-γ receptot
IFAR	interferon-α receptor
IRF9	interferon regulatory factor 9
IRG	Immunity-related GTPase
ISH	*in situ* hybridization
ISRE	interferon-stimulated response element
JAK	Janus kinase
kb	kilo base
kDa	kilodalton
Leu	leucine
LIF	leukaemia inhibitory factor

L. major	*Leishmania major*
L. monocytogenes	*Listeria monocytogenes*
LMD	laser microdissection
MEF	mouse embryonic fibroblast
MMC	mitomycine C
MOPS	3-[Morpholino-]propansulfonsäure
M. avium	*Mycobacterium avium*
M. tuberculosis	*Mycobacterium tuberculosis*
N-terminal	amino terminal
OD	optical density
ON	over night
ORF	open reading frame
p.p.	postpartum
PBS	phosphate buffered saline
PCR	polymerase chain reaction
PEG	polyethylene glycol
PFA	paraformaldehyde
RNA	ribonucleicacid
RNAse	ribonuclease
rpm	rounds per minute
RT	room temperature
RT-PCR	reverse transcriptase-PCR
SDS	sodium dodecylsulfate
SDS-PAGE	SDS polyacrylamide gel electrophoresis
STAT	signal transducer and activator of transcription
S. typhimurium	*Salmonella typhimurium*
TCE	translational control element
TEMED	N,N,N',N'-Tetramethyldiamine
Trp	tryptophane
T. cruzi	*Trypanosoma cruzi*
T. gondii	*Toxoplasma gondii*
WB	Western blot
WT	wild type
YRS	Y-box recognition sequence

1. Introduction

1.1. The testis

The testis is the reproductive organ of male animals. Its main functions are the production of spermatozoa and hormones, especially the androgen testosterone. Covered by a tough fibrous capsule the testis is divided in two major compartments: the intertubular or interstitial compartment (interstitium) and the seminiferous tubule compartment (Russel 1991).

The interstitium contains blood and lymphatic vessels and different types of cells. The most abundant cells are Leydig cells (Mori 1982), which produce a wide variety of hormones including the male sex hormone testosterone. Other cells located in the inerstitium are macrophages.

The other compartment of the testis are the seminiferous tubules. This is the place, where the spermatozoa are made from spermatogonia in a process called spermatogenesis, which will be explained in detail in the next chapter (Russel 1991).

1.2. Spermatogenesis

The haploid spermatozoa develop from diploid stem cells, the spermatogonia, in a process called spermatogenesis. It takes place in the seminiferous tubules and is a spatially and temporally highly structured process. It can be divided into three distinct phases. The proliferative phase, the meiotic phase and the spermiogenic phase, which is also called spermiogenesis. During the whole development, which takes 35 days in the mouse (Clermont 1969) the germ cells are in close contact to the Sertoli cells (Figure 1). These cells nurture the germ cells with nutrients and supply different signals regulating the spermatogenesis.

In the proliferative phase the spermatogonia undergo repetitive mitotic divisions and thus laying the basis for the production of millions of spermatozoa every day. The spermatogonia are located on the basal lamina on the periphery of the seminiferous tubule. Three different types of spermatogonia are known.
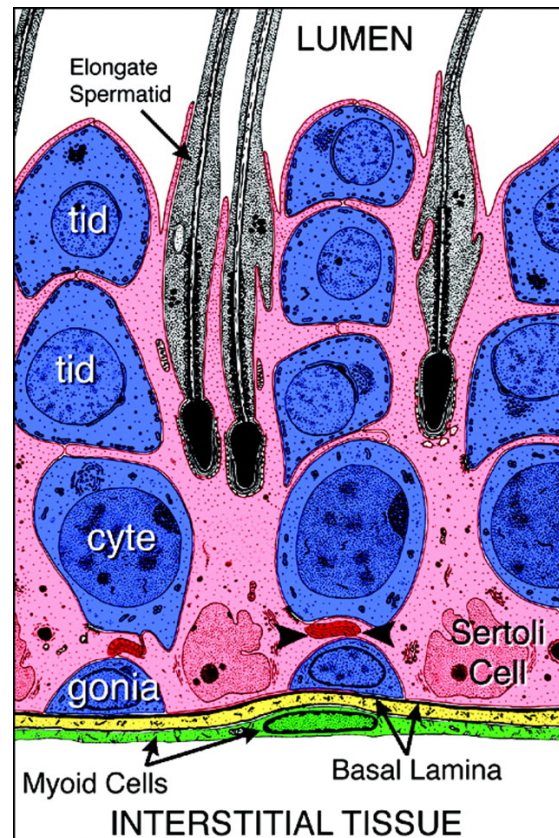
Figure 1. **Scheme of the organization of germ cells and somatic cells in the seminiferous tubule (from Brinster 2002).** Differentiation of germ cells during spermatogenesis proceeds from spermatogonia (gonia) through spermatocytes (cyte), round and elongated spermatids (tid) to spermatozoa. These are released into the lumen of the seminiferous tubules. Through the whole spermatogenesis the germ cells are embedded in Sertoli cells, which are joined continuously around the tubule by tight junctions (black arrowheads).

The spermatogonial stem cells share two crucial characteristics with other adult stem cells. They can self renew their own population and provide differentiating daughter cells. These daughter cells form the second type of spermatogonia, the proliferative spermatogonia. Their development is synchronized via intercellular bridges (Fawcett 1959, Weber 1987). The third type are the differentiating spermatogonia, which have lost their stem cell character and start differentiating. After a last division at the end of this phase the spermatogonia differentiate into preleptotene spermatocytes and the meiotic phase starts.

In the primary spermatocytes (ploidy: 4n) the homologous chromosomes align at the cell equator. During this chromosomal alignment recombination can occur. During the first meiotic division the homologous chromosomes are randomly distributed between the two daughter cells, the secondary spermatocytes (2n). The second meiotic division leads to the separation of the sister chromatids as in mitotic divisions. The products of this division are the haploid round spermatids (1n).

In the last phase, the spermiogenesis, the spermatids undergo a drastic change in morphology to form the spermatozoa. During this process, which takes 13 days in the mouse, the flagellum and acrosome develop, the nucleus gets condensed and reshaped and most of the cytoplasm is eliminated. Spermiogenesis is separated into 16 steps in the mouse, describing the different developmental changes (Leblond 1952, Oakberg 1956, Russell 1991).

The chromatin in the nucleus gets packed in a very condensed way by the replacement of histones against transition proteins and protamines (Ando 1973). A consequence of this tight packaging of the DNA is that transcription stops. The size of the nucleus decreases drastically and takes on a hook-like shape in mice.

The spermatids eliminate approximately 75% of their cytoplasm during spermiogenesis (Sprando 1987). Three different mechanisms are involved in this reduction. Firstly, during the elongation of the spermatids water from the nucleus and cytoplasm gets eliminated. Secondly, some cytoplasm is eliminated via the so-called tubulobulbar complexes, which project from the spermhead into the Sertoli cells and get phagocytosed by them (Russell 1979). Thirdly, the so-called residual body, a cytoplasmic package containing packed RNA and organelles, gets released from the neck-region of the spermatozoa when it is released into the lumen. The residual body is transported to the basis of the tubule and gets phagocytosed by Sertoli cells (Kerr 1974). When the spermatozoa are released a small amount of cytoplasm, the cyoplasmic droplet, is still attached to the neck of the spermatozoa. This droplet gets removed during the maturation of the spermatozoa in the epididymis.

The spermiogenesis ends with the spermiation, the release of the spermatozoa from the Sertoli cells into the lumen of the seminiferous tubules. The fluid stream inside the tubules transports the still non-motile spermatozoa into the epididymis, where the maturation of the spermatozoa is completed.

The progress through spermatogenesis is tightly regulated. Crossections of seminiferous tubules always show a well defined composition of spermatocytes and spermatids at specific phases of development. In the mouse there are 12 defined arrangements of germ cells, the stages. A schematic representation of the different stages is shown in Figure 2. The series of all 12 stages in a given segment of a seminiferous tubule is called the cycle (Russell 1991).
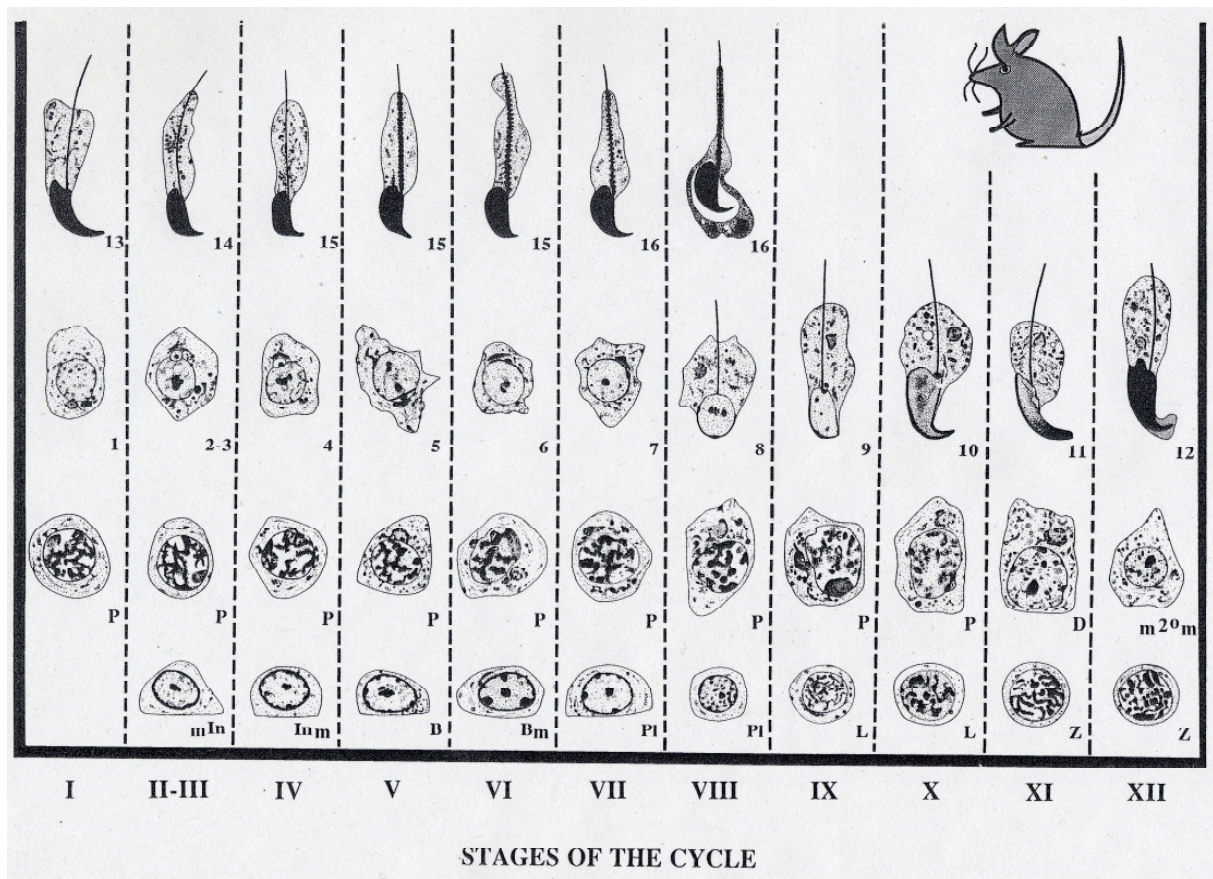
Figure 2. **Cycle map of spermatogenesis in the mouse (from Russell 1991).** The vertical columns, designated by Roman numerals I to XII, depict the stages of mouse spermatogenesis. The developmental progression of a cell is followed horizontally until the right hand border of the cycle map is reached. Cell progression continues on the left side one row up. Stage with the first appearance of round spermatids is defined as Stage I. Stage II and III are combined into a single stage called II-III. Numbers 1-16 indicate spermatids at respective step of spermiogenesis. In: Intermediate spermatogonia, B: Type B spermatogonia, Pl: preleptotene spermatocytes, L: leptotene spermatocytes, Z: zygotene spermatocytes, P: pachytene spermatocytes, D: diplotene spermatocytes, 2°: secondary spermatocytes, m: mitotic or meiotic cell division.

1.3. Germ cell-specific gene expression

A large fraction of the transcripts detected in spermatogenic cells are found exclusively there. These specific transcripts can be divided into three different groups (Eddy 2002, Dadoune 2004). The first group consist of germ-cell-specific homologues of genes expressed in somatic cells. Examples for this group include the *testis-specific glyceraldehyde-3-phosphate dehydrogenase* (*GAPDHS*), a homologue of the somatic *GAPDH* gene (Mori 1992), or the *phosphoglycerate kinase-2* (*pgk-2*), which is transcribed after the inactivation of *pgk-1* during meiosis (Boer 1987, McCarrey 1987).

Second, alternate transcripts derived from the same gene as the transcripts in somatic cells. These transcript variants originate from the same gene as the somatic transcript, but differ in the transcription start due to an alternate promoter or transcription factors, the splicing pattern or usage of alternate polyadenylation sites and signals. One remarkable example for this

group of transcripts is the transcription factor cAMP-responsive element modulator (CREM). By alternative splicing the testis-specific isoform CREMτ is generated in spermatocytes, which is a potent activator of transcription, while the somatic isoforms CREMα, -β and –γ are repressors (Foulkes 1992, Kimmins 2004).

The third group includes genes that are expressed in a testis-specific manner. It includes a wide variety of genes mediating the specialized functions necessary for the formation of spermatozoa. Examples are the transition proteins and protamines that confer the tight packaging of the DNA in the nucleus (Dadoune 2003) or the outer dense fiber (ODF) proteins (Oko 1998) that are essential for the formation of the sperm-tail.

Several members of all three groups are expressed only in haploid spermatids during early spermiogenesis. A list of genes expressed in testis only postmeiotically in haploid spermatids is presented in Table 1.

Table 1. **List of genes expressed only postmeiotically in haploid spermatids.**

Function	Gene	Reference
Remodelling and condensation of nucleus	Protamine 1/2 (Prm1/2)	Tanaka 2005
	Transition protein 1/2 (Tnp1/2)	
	spermatid-specific linker histone H1-like protein (Hils1)	Yan 2003
Sperm tail/flagellum, motility	Outer dense fiber protein 1/2 (ODF1/2)	Burmester 1996, Brohmann 1997
	A kinase anchoring protein 3/110 (AKAP3/AKAP110)	Mandal 1999, Vijayaraghavan 1999
	A kinase anchoring protein 4 (AKAP4)	Carrera 1994, Fulcher 1995
	Spermatid-specific Thioredoxin-1/2 (SPTRX-1/2)	Jimenez 2002, Miranda-Vizuete 2003
Acrosome	Acrosin	Kashiwabara 1990, Klemm 1990
Sperm-egg interaction	Sperizin	Fujii 1999
Testis specific homologues	spermatogenic cell-specific glyceraldehyde 3-phosphate dehydrogenase (Gapds)	Mori 1992
	Testis-specific phosphoglycerate kinase (Pgk2)	Fujii 2002
not defined or unknown function	Multi PDZ-domain protein 1 (MUPP1)	Heydecke 2006
	Testis-specific serine kinase 1 (Tssk-1)	Kueng 1997
	T-ACTIN 1/2	Tanaka 2003
	Beta-Chimaerin	Leung 1993
	Testicular haploid expressed gene (Theg)	Mannan 2003

1.4   Transcriptional and translational regulation in haploid spermatids

There have been a number of transcription factors identified, which play a crucial role in the transcriptional activation of genes in haploid spermatids, but due to the lack of spermatid cell lines many questions concerning the haploid expression are still unanswered.

Many genes with essential functions in spermatogenesis contain the cAMP response element (CRE) in their proximal promoter (Sassone-Corsi 1998). This is recognized by the CRE

modulator (CREM), a master controller of gene expression in spermatogenesis. Targeted deletion of CREM leads to an arrest of spermatogenesis at the round spermatid stage (Blendy 1996, Nantel 1996). CREM requires the association with ACT (activator of CREM in testis) to mediate the transcriptional activation in postmeiotic spermatids. Many CREM containing promoters lack a TATA-box and require the TATA-box-binding protein-like factor (TLF), a transcription factor massively upregulated in spermatogenic cells (Kimmins 2004).

Fractions of 25% to 100% of some mRNA species in spermatogenic cells are stored in translationally inactive free-messenger ribonucleoprotein particles (free-mRNPs) (Kleene 2003). This implies specific mechanisms for translational repression, which are poorly understood so far.

The best characterized example for translationally repression is protamine 1. The mRNA is stored in inactive free-mRNPs in round spermatids and is translationally activated in elongated spermatids, which are transcriptionally inactive. The repression is mediated by the translational control element (TCE) in the 3'-UTR of the mRNA (Zhong 2001). The protein binding the TCE is not identified yet. Another element in the 3'-UTR of protamine mRNA implicated in translational repression is the Y-box recognition sequence (YRS), which is bound by MSY2 and MSY4 (Fajardo 1997, Giorgini 2001, 2002). For other genes like the sperm mitochondria-associated cysteine-rich protein (Smcp) the importance of the 3'-UTR in translational repression has been demonstrated, but not characterized in detail (Hawthorne 2006).

The regulation of the length of the poly(A) tail of mRNAs is also used to control translation. The cytoplasmic polyadenylation element binding protein (CPEB) (Tay 2001) and the testis-specific cytoplasmic poly(A) polymerase (TPAP) (Kashiwabara 2002) activate the translation of various testis-specific transcripts in round spermatids by elongation of the poly(A) tail.

During the studies for my diploma thesis first indications for the expression of Irgc, a member of the Immunity-related GTPases (IRG), in the testis were obtained (Rohde 2003). These were mainly based on the large number of Irgc expressed sequence tags (ESTs) derived from the testis of mouse and human. However, the experimental results of Western blot analysis and immunocytochemical stainings of testis sections were ambiguous and could not verify the expression of Irgc in the testis. Therefore further investigations on the expression profile of Irgc were necessary.

The Immunity-related GTPases belong to the interferon-induced GTPases, which will be introduced in the following chapters starting with short summary of interferon signalling pathway.

1.5   Interferons

Interferons (IFNs) are small inducible cytokines secreted by different cells upon infection or tissue damage. The family of IFNs consists of three subfamilies: type I, type II and type III IFNs. Type I IFNs include IFN-α (van Pesch 2004, Pestka 2004), IFN-β (Mogensen 1999), IFN-δ (Lefevre 1998), IFN-ε (Conklin 2001), IFN-κ (LaFleur 2001), IFN-τ (Roberts 2007), IFN-ω (Hauptmann 1985) and limitin (Oritani 2000). They are secreted by a wide range of different cells mainly as response to viral infection, although their action is not restricted to viruses. Three different IFN-λ proteins form the group of type III IFNs and are also implicated in the antiviral response (Kotenko 2003, Sheppard 2003).

The group of type II IFNs consists only of IFN-γ, which is secreted by activated T-cells (Mosmann 1989, Sad 1995), natural killer (NK) cells (Trinchieri 1995) and macrophages (Puddu 2005). IFN-γ and type I interferon stimulation regulates the transcription of hundreds of genes (Boehm 1997, Halonen 2006, Kota 2006, Zocco 2006). The complex response affects both innate and adaptive immunity.

Type I and type II IFNs signal through similar but distinct pathways (Figure 3) (Platanias 2005). IFN-γ is recognized by the IFN-γ receptor (IFNGR). The binding of an IFN-γ homodimer leads to the formation of the heterodimer of IFNGR1 and IFNGR2. The dimerization activates a tyrosine phosphorylation cascade involving the receptor associated Janus-activated kinases (JAK) 1 and 2, which ultimately phosphorylate the signal transducer and activator of transcription 1 (STAT1). STAT1 dimerizes upon phosphorylation and the dimer called Gamma activated factor (GAF) translocates to the nucleus. There it binds to Gamma activated sequence (GAS) elements in the promoter of IFN-γ inducible genes and initiates their transcription.

Type I interferons signal through one common receptor, the heterodimeric IFN-α receptor (IFNAR), which consists of the two subunits IFNAR1 and IFNAR2. They are associated with the kinases TYK2 and JAK1, respectively. The activation of these receptors leads to the phosphorylation of STAT1 and STAT2, forming a complex called IFN-stimulated gene factor 3 (ISGF3) together with the IFN-regulatory factor 9 (IRF9). After translocation into the

nucleus ISGF3 binds to IFN-stimulated response elements (ISREs) and activates the transcription of the respective genes.
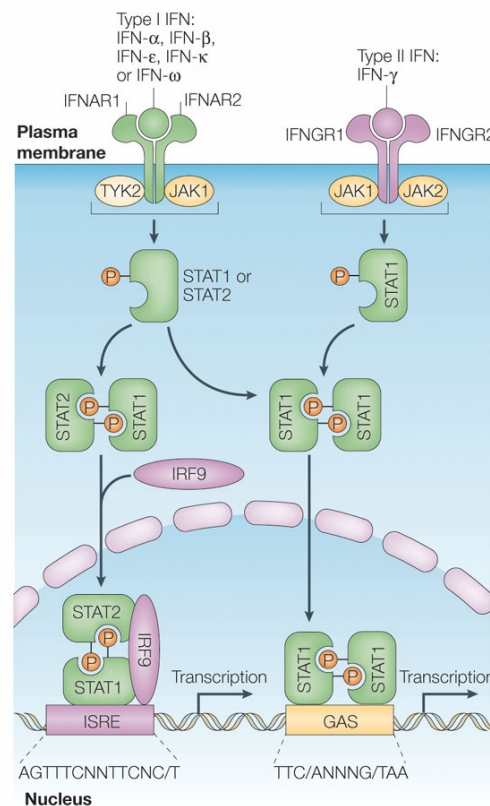
Figure 3. **Interferon receptors and activation of JAK–STAT pathways by type I and type II interferons (from Platanias 2005).** Type I IFNs bind the common type I IFN receptor on the cell surface, which consists of two subunits, IFNAR1 and IFNAR2. They associate with TYK2 and JAK1, respectively. Type II IFN-γ binds to the type II IFN receptor, composed of two subunits, IFNGR1 and IFNGR2, which are associated with JAK1 and JAK2, respectively. Activation of the JAKs that are associated with the type I IFN receptor results in tyrosine phosphorylation of STAT2 and STAT1; this leads to the formation of STAT1–STAT2–IRF9 complexes, which are known as ISGF3 complex. These complexes translocate into the nucleus and bind ISREs in the promoter to initiate transcription of the respective gene. Both type I and type II IFNs also induce the formation of STAT1–STAT1 homodimers that translocate to the nucleus and bind GAS elements, thereby initiating the transcription of these genes. The consensus GAS element and ISRE sequences are shown. N, any nucleotide

1.6 IFN-inducible GTPases

The arsenal of genes upregulated by interferon-induction includes 4 families of GTPases: the Mx proteins, the p65 guanylate-binding proteins (GBPs), the very large inducible GTPases (VLIGs) and the Immunity-related GTPases (IRGs), formerly known as p47 GTPases (Martens 2006).

In mouse and human, two Mx genes, called Mx1 and Mx2 (Staehli 1986, 1988) and MxA and MxB (Staeheli 1985, Aebi 1989), respectively, are known. All Mx genes are strongly

upregulated upon stimulation with type I and type III interferon (Horisberger 1987). Mx GTPases have a molecular weight of approximately of 70-80 kDa and show a clear homology to dynamins. Mx GTPases form large oligomers in the presence of GTP and hydrolyze GTP cooperatively (Melen 1992, Kochs 2002a). The GTP maximum hydrolysis rate is high (Richter 1995). Whether these biochemical properties are functionally important was put in question by the mutant MxA (L612K) that is unable to oligomerize and hydrolyze GTP *in vitro* but was still able to confer its antiviral effect (Janzen 2000). The possibility remains that this mutant is partially active in nucleotide binding under *in vivo* conditions.

Mouse Mx1 carries a nuclear localization signal leading to the nuclear localization of the protein (Noteborn 1987, Melen 1992), while Mx2 is a cytoplasmic protein (Meier 1988). In humans both Mx proteins are localized in the cytoplasm. MxA was shown to bind to the smooth endoplasmic reticulum and tubulate synthetic lipid vesicles in nucleotide dependent manner (Accola 2002).

Especially Mx1 and its homologues are implicated in resistance against a wide range of RNA viruses (Haller 2007) and are major effectors against influenza (Hefti 1999, Grimm 2007). Mx1 was discovered as a dominant locus conferring resistance against influenza virus infection to the mice strain A2G (Lindemann 1963). Interestingly, most inbred laboratory mouse strains do not carry a functional *Mx1* allele while out bred strains do (Jin 1998). Mx2 from rodents inhibits the replication of the vesicular stomatitis virus and LaCrosse virus, which replicate in the cytosol (Haller 2007).

The mechanism by which Mx proteins mediate their antiviral effect is still not understood completely. MxA was shown to interact directly with viral nucleocapsids (Kochs 1999a), leading to a block of nuclear import (Kochs 1999b) probably by immobilization and missorting of viral components (Kochs 2002b, Reichelt 2004). The nuclear Mx1 mediates its function, corresponding to its localization, in the nucleus (Pavlovic 1992).

The family of p65 guanylate-binding proteins (GBPs) is well conserved throughout the vertebrates (Robertsen 2006) with seven known members in human, *hGBP1-7* (Cheng 1991, Luan 2002, Fellenberg 2004, Olszewski 2006) and mouse, *mGBP1-7* (Cheng 1991, Wynn 1991, Boehm 1998, Han 1998, Olszewski 2006). They are massively induced upon stimulation with interferon-γ and to a lesser extent by interferon-α/-β (Cheng 1983, 1985, Boehm 1998, Nguyen 2002).

The crystal structure of hGBP1 shows an N-terminal G domain and C-terminal helical domain (Prakash 2000). All GBPs analyzed so far bind GMP, GDP and GTP with the same affinity

(Cheng 1983, 1985, Staeheli 1984) and hydrolyze GTP in two consecutive cleavage reactions into GMP (Schwemmle 1994, Neun 1996, Praefcke 1999, Ghosh 2006).

hGBP1, mGBP1 and mGBP-2 are largely cytosolic. mGBP2 shows a granular distribution in the cytosplasm, also associated with vesicular structures (Vestal 2000). Activated hGBP1 relocates to the Golgi apparatus (Modiano 2005). GBP targeting to membraneous structures requires isoprenylation at the C-terminus (Vestal 2000, Modiano 2005).

Little is known about the function of GBPs and a link between the massive interferon-γ induction and the proposed functions could not be offered. Although weak antiviral effects of GBPs against vesicular stomatitis virus (VSV) and encephalomyocarditis virus (ECMV) have been reported (Anderson 1999, Carter 2005), it is questionable if they are specific or secondary effects to other physiological changes induced by GBPs (Vestal 2005). Besides these antiviral effects GBPs have been implicated in the regulation of fibroblast proliferation (Gorbacheva 2002) and the control of angiogenic capabilities of endothelial cells (Guenzi 2001, 2003).

The family of very large inducible GTPases (VLIGs) has at least six members in the mouse and one in human (Klamp 2003). VLIGs have a molecular weight of 280 kDa and are strongly induced by type I and type II interferons. Based on the canonical G-domain, VLIG-1 shows highest homology to other interferon-induced GTPases, which suggests a role in cell-autonomous resistance (Klamp 2003).

The fourth family of interferon-induced GTPases are the Immunity-related GTPases (IRGs), which will be described in the next chapter.

1.7   Immunity-related GTPases (IRGs)

The immunity-related GTPases (IRG), also known as p47 GTPases, are important factors mediating resistance against numerous intracellular pathogens in the mouse (Taylor 2007).

Irgd (IRG-47), the first IRG to be discovered and founder of the family name, was detected as part of the interferon-γ response in B-cells (Gilly 1992). Consecutively other members of the family have been identified in type II interferon stimulated cells, including Irgb6 (TGTP/Mg21) (Carlow 1995, Lafuse 1995), Irgm1 (LRG-47) (Sorace 1995), Irgm3 (IGTP) (Taylor 1996), Irgm2 (GTPI) and Irga6 (IIGP1) (Boehm 1998). In total the mouse possesses at least 23 (possibly) different IRGs including 2 pseudogenes (Bekpen 2005, Bernstein-Hanley 2006, Jonathan Howard personal communication). IRGs have been found in all

classes of vertebrates except for birds (MacMicking 2004, Bekpen 2005, Julia Hunn personal communication). A phylogeny of the IRGs from *Mus musculus domesticus* is shown in Figure 4. As suggested by the phylogenetic tree, mouse IRGs can be divided in two subfamilies. The GKS-subfamily consists of the IRGAs, IRGBs, Irgc and Irgd. The IRGMs form the second subfamily, informally called the GMS-subfamily. They are characterized by a unique substitution in the G1 motif of the GTPase domain. The universally conserved lysine in the GxxxxGKS motif is replaced by a methionine leading to the sequence GxxxxGMS.

Most mouse *IRG*s are located in two clusters on chromosome 11 and one cluster on chromosome 18. Chromosome 18 harbours all eight *Irga* genes, the *Irgb*, *Irgd* and *Irgm* genes are located on chromosome 11 (Bekpen 2005). In contrast *Irgc*, also known as *CINEMA*, is an isolated gene on chromosome 7 (Rohde 2003, Bekpen 2005).

The new nomenclature of the IRG genes/proteins was introduced 2005 by Bekpen and coworkers and is based on the phylogenetic relationships of the different genes (Bekpen 2005). IRGs written with a capital I in the beginning, followed by small letters (e.g. Irgc, Irgm1) always refer to the genes or proteins from the mouse. For all other mammals or the gene/protein in general, only capital letters are used (e.g. IRGC).
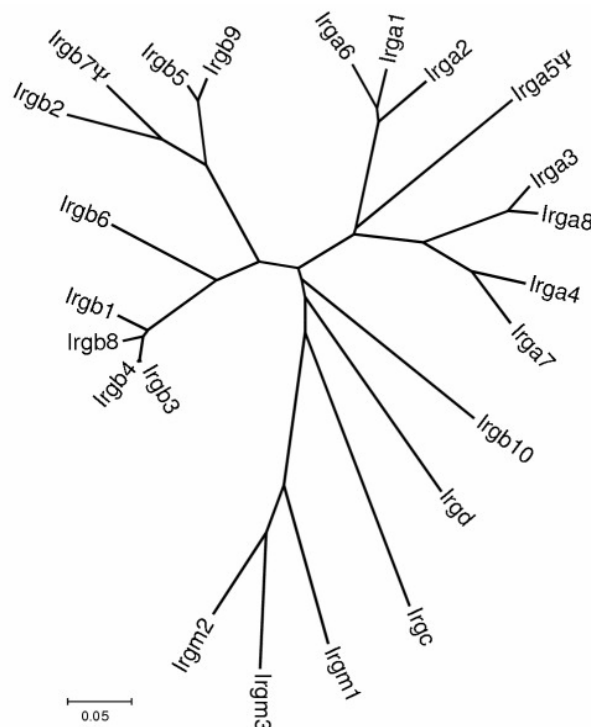
Figure 4. **Phylogenetic tree of mouse IRGs (from Bekpen 2005).** The unrooted tree (p-distance based on neighbour-joining method) is based on the alignment of the nucleotide sequences of the G-domains of the 23 IRGs and was performed with the MEGA2 software.

A characteristic property of most *IRG* genes is that they are massively induced by type II interferons (Boehm 1998, Bekpen 2005) and to lesser extent by type I interferons (Zerrahn 2002). This inducibilty is conferred by multiple ISRE (interferon-stimulated response element) and GAS (γ-activated sequence) sites located in the promoter regions of the responsive IRGs (Gilly 1996, MacMicking 2003, Bekpen 2005).

The role of different IRG proteins in infection by a wide variety of pathogens has been studied. The results obtained demonstrate that different IRG proteins are crucial resistance factors, which act in a non-redundant manner (MacMicking 2004, 2005, Taylor 2007). The results are summerized in Table 2. Targeted deletion of Irgm1 or Irgm3 leads to a complete loss of resistance against the intracellular pathogen *Toxoplasma gondii* and infected mice die within a few days (Taylor 2000, Collazo 2001). The short time between infection and death of the Irgm1$^{-/-}$- and Irgm3$^{-/-}$-mice suggest that the deleted proteins are part of the innate immune system. Indications that IRG proteins are part of the cell-autonomous response of the innate immune system come from studies showing, that primary astrocytes from Irgm3-deficient mice were unable to restrain *T. gondii* growth after interferon-γ stimulation while wildtype astrocytes could (Halonen 2001). Hela cells expressing Irgb6 or Irgm3 are less susceptible to VSV (Carlow 1998) or Coxsackievirus B3 (Zhang 2003), respectively. Nevertheless, recently a regulatory effect of Irgm1 in differentiation of bone marrow has been suggested, based on the expression of *IRG* genes in hemopoietic stem cells (Terskikh 2001, Venezia 2004) and the development of a striking leukopenia in Irgm1-deficient mice infected with Mycobacteria or Trypanosoma (Feng 2004, Santiago 2005).

Table 2. **Summary of evidence supporting roles for IRG proteins in host resistance (modified after Taylor 2007).**

IRG protein	defined role in host resistance		possible mechanism(s)
	In vivo	In cultured cells	
Irgm1	*T. gondii* (Collazo 2001)	*T. gondii* (Butcher 2005)	- Lysosome fusion (MacMicking 2003, Deghmane 2007)
	L. major (Santiago 2005)	*T. cruzi* (Santiago 2005)	- Autophagy (Gutierrez 2004)
	T. cruzi (Santiago 2005)	*M. tuberculosis* (MacMicking 2003)	- Haematopoiesis (Feng 2004, Santiago 2005)
	L. monocytogenes (Collazo 2001)	*S. typhimurium* (Taylor 2007)	
	M. tuberculosis (MacMicking 2003)		
	M. avium (Feng 2004)		
	S. typhimurium (Taylor 2007)		
Irgm3	*T. gondii* (Taylor 2000)	*T. gondii* (Ling 2006, Butcher 2005, Halonen 2001)	- Vacuole vesiculation (Martens 2004, Ling 2006)
	L. major (Taylor 2007)	*C. trachomatis* (Bernstein-Hanley 2006)	- Lysosome fusion (Ling 2006) - Autophagy (Ling 2006)
Irgm2	*C. psittaci* (Miyairi 2007)	*C. psittaci* (Miyairi 2007)	
Irga6		*T. gondii* (Martens 2005)	- Vacuole vesiculation (Martens 2004)
		C. trachomatis (Nelson 2005)	- Membrane trafficking (Nelson 2005)
Irgd	*T. gondii* (chronic) (Collazo 2001)	*T. cruzi* (Koga 2006)	
Irgb10	*C. psittaci* (Miyairi 2007)	*C. trachomatis* (Bernstein-Hanley 2006)	

The crystal structure of Irga6 (IIGP1) revealed a Ras-like G-domain, which is preceded by a N-terminal domain composed of three α–helices (Ghosh 2004). A short linker helix connects the G-domain to the C-terminal domain, which contains seven α–helices. Secondary structure predictions and sequence alignments lead to the conclusion that the structure of Irga6 is representative for the whole family of IRG proteins (Ghosh 2004).

So far Irga6 is the only IRG protein analyzed in detail for its biochemical properties (Uthaiah 2003, Ghosh 2004). It binds nucleotides in the µM range with a higher affinity for GDP than GTP. In the presence of GTP Irga6 oligomerizes and shows cooperative GTP hydrolysis activity. These biochemical features are also seen in dynamins and other dynamin-like GTPases (Praefcke 2004). Although GDP-bound Irga6 crystallizes as a dimer, the crystal dimer interface is probably not a biological relevant interface (Martens 2006, Niko Pawlowski personal communication). The primary interface for the formation of the oligomers localizes to the G domain, suggesting a G domain:G domain dimer (Niko Pawlowski personal communication). The alternate use of this interface and a second, not completely characterized, interface would provide a mechanism for the construction of oligomers.
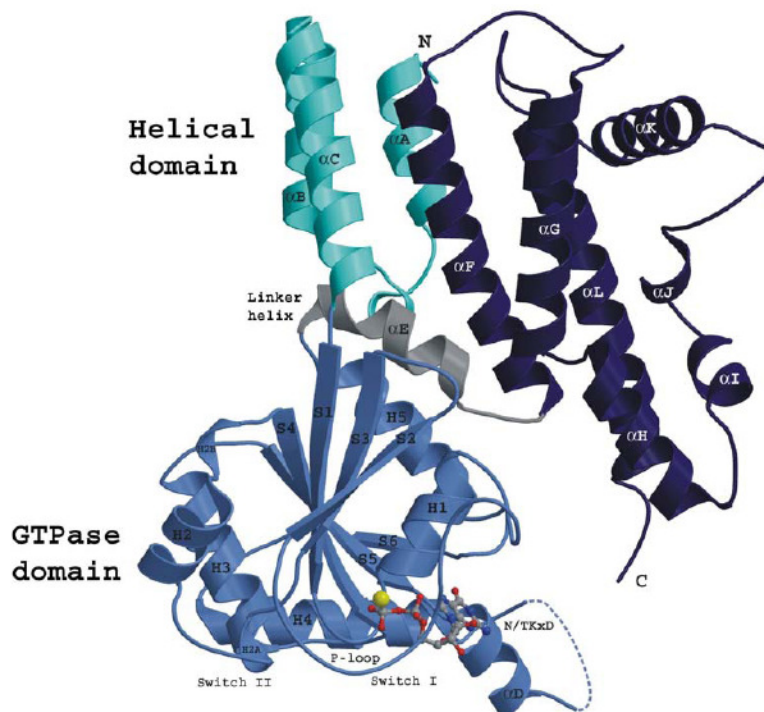
Figure 5. **Crystal structure of Irga6 (IIGP1) in the GDP bound form (from Ghosh 2004).** The N-terminal domain (cyan) is composed of the α-helices A, B and C. This is followed by the Ras-like GTP binding domain (light blue). A linker helix (grey) connects the C-terminal domain (dark blue) to the G-domain. The first 13 amino acids are not resolved in the crystal structure and not shown in the model.

Except for Irgd, which is largely if not completely cytosolic, all studied IRGs are distributed between specific membrane compartments and the cytosol (Martens 2004). Membrane binding of Irga6 is mediated by an N-terminally myristoyl group. The membrane-targeting signal of Irgm1 corresponds to the αK helix and localizes the protein to the Golgi apparatus and the lysosomal compartment (Martens 2004, Bagshaw 2005, Yang Zhao personal communication).

Upon infection all IRGs get relocated from their resting compartment. After infection with *T. gondii* all IRGs except Irgm1 relocalize to the parasitophorous vacuole (Martens 2005). Nevertheless, Irgm1 was reported to bind to the phagosome containing *M. tuberculosis* (MacMicking 2003). Different mechanisms have been suggested, how the IRGs located around the pathogen containing vacuoles mediate their antimicrobial effects. Irgm1 has been suggested to induce autophagy (Gutierrez 2005) and promote phagosome maturation (MacMicking 2003). Irga6 may vesiculate the parasitophorous vacuole and thus expose *T. gondii* to effectors located in the cytosol (Martens 2005).

Recently complex interactions between different IRG proteins have been revealed. Proper intracellular localization of Irga6 and Irgb6 requires the action of all three IRGs from the GMS subfamily (Julia Hunn, Stephanie Könen-Waisman, Sascha Martens, Nina Schröder personal communication). Therefore the IRGM proteins act as regulators of GKS IRG proteins. These regulations may involve hetero-oligomeric interactions.

1.8   IRGQ (FKSG27) – the quasi-GTPase

The mammalian IRGQ proteins are homologous to the IRGs, but radically modified in the GTP binding site. The conserved GTP binding motifs G1, G3 and G4 are missing or mutated. Thus IRGQ is not a GTPase. Therefore the classification of IRGQ as IRG, as done by Singh and coworkers, is arguable (Singh 2006).

Mouse and human IRGQ are 70% identical on amino acid level. Compared to the other IRGs they are N-terminally extended by about 150 amino acids. The remaining 420 amino acids are encoded by one exon. Aligned to other IRGs the homology of the N- and C-terminal part of the protein becomes obvious, while the G domain shows the lowest similarity.

The quasi-GTPase *IRGQ* is located in close proximity to the *IRGC* gene (Figure 6). This is the case not only in mouse and human (Bekpen 2005), but also in all other mammals that contain an *IRGC* orthologue that can be mapped (Julia Hunn personal communication). There is no experimental data published on IRGQ yet.

The zebrafish contains three different *irgq* genes (*irgq1-3*) (Bekpen 2005). They show different degrees of mutations away from the conserved GTP binding motifs. While the mammalian *IRGQ* genes are monophyletic, the *irgq* genes in zebrafish are of polyphyletic origins.

1.9   *IRG* genes in human

There is a striking difference between the *IRG* genes in the mouse and in humans. While the mouse possesses 23 different *IRG* genes, the human genome contains only one full-length *IRG* gene, which resides on chromosome 19. This is *IRGC*, an orthologue of the mouse *Irgc* (Rohde 2003, Bekpen 2005). Mouse and human *IRGC*, which are 90% identical on amino acid level, are located in chromosomal regions syntenic between the mouse chromosome 7 and human chromosome 19, respectively (Figure 6) (Bekpen 2005).
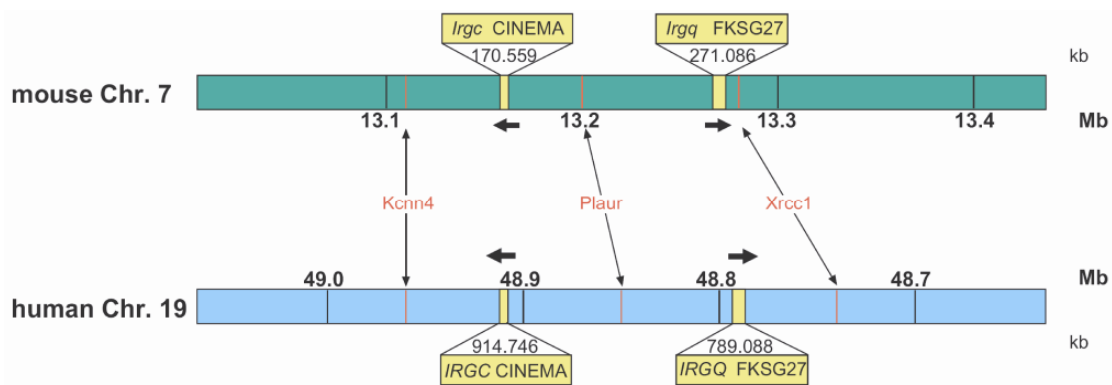
Figure 6. **Synteny relationship between mouse *Irgc* and human *IRGC* (modified after Bekpen 2005).** Synteny between regions of mouse chromosome 7 and human chromosome 19 containing the respective *IRGC* gene. Mouse *Irgq* and human *IRGQ* are located close to the respective *IRGC* gene. Numbers indicate distance from the centromere in megabases. Location of the synteny markers Kcnn4, Plaur and Xrcc1 is shown. Black arrows show orientation of the gene. (modified figure kindly provided by Julia Hunn)

In addition to the full-length gene *IRGC* and the highly anomalous, IRG-related sequence *IRGQ* the human genome contains *IRGM*, an amino- and carboxyl-terminally truncated G-domain homologous to the IRGM subfamily of mouse *IRG* genes (Bekpen 2005). *IRGM* is located on chromosome 5 in a region that is syntenic to the regions on the mouse chromosomes 11 and 18 containing the *IRG* gene clusters. This suggests that *IRGM* is a fragment of an ancestral *IRG*, which was partly lost with the other inducible IRGs during evolution in all higher primates (Bekpen 2005, Julia Hunn personal communication). Transcription of 5 isoforms of *IRGM* differing in their 3' splicing pattern was shown in

cultured cells and different human tissues (Bekpen 2005). The expression of *IRGM* is driven by the long terminal repeat (LTR) of the endogenous retrovirus ERV9 and is not inducible by interferons. Nevertheless, the translation of *IRGM* transcripts in various human cell lines has been shown and the resulting protein has been implicated in the induction of autophagy as a mechanism to eliminate intracellular mycobacteria (Singh 2006), analogous to the function of mouse Irgm1 (Gutierrez 2004). Recently polymorphisms in the *IRGM* gene have been connected to an increased susceptibility in Crohn's disease (Parkes 2007, WTCCC 2007).

1.10   The aim of this study

In recent years it became evident, that the family of *IRG* genes are essential mediators of resistance against a wide range of intracellular pathogens in the mouse. With only *IRGC* and the fragment *IRGM* left, humans seem to have lost their repertoire of *IRG* genes. Also the isolated chromosomal location of mouse *Irgc* on chromosome 7 outside of the clusters containing all other members of the family makes *Irgc* an exceptional *IRG*. However, nothing is known about the function of *IRGC*. In order to investigate the functions of IRG proteins in humans, meaning IRGC, it is crucial to define the role and functions of the strongly conserved mouse orthologue Irgc.

Different approaches were chosen to study this gene and elucidate its role among the *IRG* genes. An *in silico* analysis of *IRGC* included the search of orthologues and the definition of the gene and promoter structure. Different techniques were applied to elucidate the expression pattern of mouse Irgc in detail. To answer the question, if the highly conserved IRGC orthologues have also a conserved expression profile, IRGC expression was analyzed in different mammals including human. The function of Irgc was investigated in Irgc deficient mice and analysis of their putative phenotypes. Additional possible interaction partners of mouse Irgc were searched by a yeast two-hybrid screen.

2.   Methods

2.1 Material

2.1.1   Chemicals and reagents

All chemicals used were graded p.A. and purchased from Aldrich (Steinheim), Applichem (Darmstadt), Baker (Deventer, Netherlands), Boehringer Mannheim (Mannheim), GE Healthcare (München), GERBU (Gaiberg), Gibco BRL (Eggelstein), Merck (Darmstadt), Riedel de Haen (Seelze), Roth (Karlsruhe), Serva (Heidelberg), Sigma-Aldrich (Deisenhofen), ICN biochemicals, Oxoid (Hampshire, UK)

Buffers and solutions were prepared with deionised and sterile water or Ultra pure water derived from Beta75/delta UV/UF from USF Seral Reinstwasserysyteme GmbH (Baumbach) equipped with UV and ultrafiltration or from Milli-Q-Synthesis (Millipore, Schwalbach). All solutions used for techniques designed to isolate, process or detect RNA were treated with DEPC.

2.1.2   Enzymes and proteins

All restriction enzymes were purchased from New England Biolabs (Frankfurt/Main); T4 DNA ligase (New England Biolabs); RNase A (Sigma); shrimp alkaline phosphatase (SAP) (USB, Staufen; Amersham, Freiburg); Proteinase K (Merck); *Thermus aquaticus* (*Taq*) polymerase was prepared by Rita Lange; *Pyrococcus furiosus* (*Pfu*) DNA Polymerase (Promega, Mannheim); SP6 RNA polymerase, T7 RNA polymerase (Roche, Mannheim)

2.1.3   Kits

Plasmid Midi kit, RNeasy Mini kit, RNeasy Lipid Tissue, RNeasy Micro kit, Oligotex mRNA isolation kit (QIAGEN, Hilden), Terminator-cycle Sequencing kit version 3.1 (ABI, Foster City, CA, USA), Rapid PCR product purification kit (Roche), SuperScript First-Strand Synthesis System for RT-PCR (Invitrogen, Karlsruhe), Strip-EZ DNA kit (Ambion, TX, USA), pGEM-T easy Vector System I (Promega, Madison, USA)

2.1.4   Vectors

pGEM-T easy (Promega, Mannheim)

pGBD-C1 (James 1996)

pGAD-C1 (James 1996)

pGBKT7 (Clontech, Mountain View, CA, USA)

pACT1 (Clontech)

2.1.5   Media

Luria Bertani (LB) medium

10g bacto tryptone, 5g yeast extract, 10g NaCl, 1 l dH2O, for plates additionally 15g agar

YPD

10g yeast extract, 20g peptone, 20g glucose, 1 l dH2O, for plates additionally 20 g agar

SD minimal media

6,7 g yeast nitrogen base without amino acids, 20 mg arginine, 10 mg isoleucine, 40 mg lysine, 10 mg methionine, 60 mg phenylalanine, 50 mg threonine, 40 mg uracil, depending on selection: 20 mg adenine (not in –Ade), 10 mg hisitidine (not in –His), 60 mg leucine (not in –Leu), 40 mg tryptophane (not in –Trp), 1 l dH2O, for plates additionally 20 g agar

IMDM (Iscove's Modified Dulbecco's Medium)

Supplemented with 10 % FCS, 2 mM Glutamine, 1 mM sodium pyruvate, 100 U/ml Penicillin, 100 µg/ml Streptomycin, 1x non-essential amino acids

DMEM (Dulbecco's Modified Eagle Medium)

Supplemented with 10% FCS, 100 U/ml Penicillin, 100 µg/ml Streptomycin, 1x non-essential amino acids

EF medium

DMEM (Dulbecco's Modified Eagle Medium) with Glutamax (no sodium pyruvate, 4500 mg glucose, with pyridoxine), supplemented with 10 % FCS, 1 mM sodium pyruvate, 100 µg/ml penicillin/streptomycin

ES medium

DMEM (Dulbecco's Modified Eagle Medium), supplemented with 15 % ES FCS (tested for ES cell culture), 1 mM sodium pyruvate, 2 mM L-glutamine, 1x non-essential amino acids, 1 mM β-mercaptoethanol, LIF (leukaemia inhibitory factor; supernatant from LIF-transfected CHO cells line 8/24 720 LIFD(.1) from Genetics Institute, Cambridge, MA, USA; amount of LIF used depends on the concentration of the batch)

Freezing medium

10 % DMSO in FCS, sterile filtered

2x freezing medium for 96-well plates: 20 % DMSO in FCS, sterile filtered

2.1.6 Serological reagents

Primary antibodies and antisera

name	immunogen	species	dillution	origin
α-Irgc 39/3°	mouse Irgc aa 421-435 and 449-463	rabbit polyclonal	WB: 1:10.000 IC: 1:1.000 IF: 1:1.000	Eurogentec (Köln) double X programm, Rohde 2003
α-Calnexin	Calnexin	rabbit polyclonal	WB: 1:5.000	Biomol (Hamburg)
BD Living Colors A.v. Peptide Antibody	peptides corresponding to central and C-terminal portions of GFP	rabbit polyclonal	WB: 1:400	BD biosciences (Palo Alto, USA)
Anti-Digoxigenin-AP, Fab fragments	Digoxigenin (DIG label on RNA probes)	sheep	ISH: 1:4.000	Roche (Mannheim)

Secondary antibodies and antisera

Goat-anti-rabbit Alexa 546 (Molecular Probes, Karlsruhe), donkey-anti-rabbit HRP (Amersham)

2.1.7 Bacterial strains

E. coli DH5α: *80dlacZΔM15*, recA1, endA1, gyrA96, thi-1, hsdR17 (r_B^-, m_B^+), supE44, relA1, deoR, *Δ(lacZYA-argF)*U169

2.1.8 Yeast strains

Saccharomyces cerevisiae:

- PJ69-4a-a: *MATa trp1-901 leu2-3,112 ura3-52 his3-200 gal4Δ, gal80Δ, LYS2::GAL1-HIS3 GAL2-ADE2 met2::GAL7-lacZ* (James 1996)

- PJ69-4a-α: *MATα trp1-901 leu2-3,112 ura3-52 his3-200 gal4Δ, gal80Δ, LYS2::GAL1-HIS3 GAL2-ADE2 met2::GAL7-lacZ* (James 1996)

- AH109: *MATa, trp1-901, leu2-3, ura3-52, his3-200, gal4Δ, gal80Δ, LYS2::GAL1$_{UAS}$-GAL1$_{TATA}$-HIS3, GAL2$_{UAS}$-GAL2$_{TATA}$-ADE2, URA3::MEL1$_{UAS}$-MEL1$_{TATA}$-lacZ, MEL1* (Clontech)

- Y187: *MATα, ura3-52, his3-200, ade2-101, trp1-901, leu2-3, 112, gal4Δ, met-, gal80Δ, MEL1, URA::GAL1$_{UAS}$-GAL1$_{TATA}$-lacZ* (Clontech)

2.1.9 Eukaryotic cell lines and primary cells

- mouse: L929 (fibroblast cell line), V6.5 (F1 ES cell line), embryonic feeder (EF) cells (prepared from day 13-14 embryos of 129 mouse strain harbouring pSV2 neo (Müller 1991)

- human: Hela (cervix carcinoma cell line), HepG2 (liver cancer cell line), Hs27 (primary foreskin fibroblasts), MCF7 (breast adenocarcinoma cell line), SW480 (colon adenocarcinoma), T2 (lymphoblastoma cell line), THP1 (monocytic leukaemia cell line)

2.1.10 Animals and human tissue samples

Mice were provided by the Center for Mouse Genetics in the Institute for Genetics in Köln. Adult male Sprague Dawley rats were purchased from Harlan-Winkelmann (Borchen). Testis from 22 months old bulls were obtained from the Schlachthof Euskirchen with the kind help of Dr. Junker. Testis from an eight months old cat and an eleven months old dog (Golden Retriever) were kindly provided by the veterinary Monika Morlak (Köln). Sections of paraffin embedded human testis were kindly provided by Prof. Andreas Meinhardt (Giessen).

2.2 Molecular biology

All methods were carried out according to standard procedures according to Sambrook et al 1989 and Ausubel et al 1998 if not stated otherwise.

2.2.1   Agarose gel electrophoresis

DNA was analyzed by agarose gel electrophoresis in 1x TAE buffer (0,04 M Tris, 0,5 mM EDTA, pH adjusted to 7,5 with acetic acid). Migration of the samples was visualized by using bromphenol blue and xylene-cyanol. The DNA was stained with ethidium bromide (0,3µg/ml), exposed to UV-light and documented with the BioDocAnalyze 2.1 equipment (Biometra, Göttingen).

2.2.2   PCR (polymerase chain reaction)

PCR applications were used for the amplification of the inserts of the yeast two-hybrid vectors, the *in situ* hybridization probes, typing of mice and detection of gene-specific transcripts in cDNA. For the first application Pfu DNA polymerase was used, for the other ones Taq DNA polymerase.

The standard reaction mix included various amounts of template DNA, 10 pmol of each primer, 2,5 U Taq DNA polymerase, 200 pmol dNTP-mix, 2,5 µl 50mM $MgCl_2$, 5 µl 10x PCR buffer (200mM HEPES pH8,4, 500mM KCl), ad 50 µl H_20. 5 U of enzyme was added when Pfu DNA polymerase was used and 5 µl of the supplied buffer was included into the reaction mix instead of HEPES buffer and $MgCl_2$. Primers were bought by Invitrogen and Operon (Köln) are listed in the chapters of their respective use.

2.2.3   Ligation

1-3 µg of the vector was cut with the chosen restriction enzyme(s) (10U/µg DNA). The reaction was incubated for 1-2 h under the appropriate conditions. Then the same amount of restriction enzyme and 0,1U of SAP were added and incubated for another 1-2 h. The insert was cut in the same way without the use of SAP. Following restriction the DNA was separated by agarose gel electrophoresis. The DNA was cut out of the gel and purified using the Rapid PCR purification kit (Roche). Yield of DNA was estimated by agarose gel electrophoresis. Vector and insert were mixed at a ratio of 1:3 and ligated in a total volume of 10 µl with T4 DNA ligase ON at 16°C.

2.2.4   Preparation of competent cells

2 ml LB medium supplemented with 20 mM $MgSO_4$, 10 mM KCl were inoculated with one E. coli colony and cultured ON at 37°C. The culture was diluted 1:100 and incubated at 37°C for approximately 2 h until a OD_{600} density of 0,45 was reached. The Culture was incubated 10 min on ice and cells collected by centrifugation for 5 min at 6.000 rpm at 4°C. Cells were resuspended in TFB 1 (30 mM KOAc, 50 mM $MnCl_2$, 100 mM RbCl, 10 mM $CaCl_2$, 15% (w/v) glycerine, pH 5,8; 30 ml for 100 ml culture) and incubated for 10 min on ice. Then the cells were pelleted by centrifugation for 5 min at 6.000 rpm at 4°C and resuspended in TFB 2 (10 mM MOPS, pH 7,5, 75 mM $CaCl_2$, 100 mM $RbCl_2$, 15 % w/v glycerine; 4 ml for 100 ml culture). Aliquots a 100 µl of competent bacteria were frozen at -80°C.

2.2.5   Transformation of bacteria

A 100 µl aliquot of competent bacteria was thawed on ice. The ligation reaction or 5 ng of plasmid was added and mixed well before incubating for 20 min on ice. Then cells were heat-shocked for 2 min at 42°C, followed by 5 min incubation on ice. 1 ml of LB medium supplemented with 20 mM MgSO4, 10 mM KCl was added and cells were incubated for 30-45 min on roller at 37°C. 100-500 µl of this culture were plated on LB agar plates containing the appropriate antibiotics for selection.

2.2.6   Plasmid DNA isolation from bacteria

An alkaline lysis method was applied to isolate plasmid DNA from bacteria. 1,5 ml of 3 ml ON LB cultures supplemented with the appropriate antibiotics were harvested by centrifugation for 1 min at 13.000 rpm. Cells were resuspended in 100 µl P1 (50 mM Tris-Cl, pH 8,0, 10 mM EDTA, 100 µg/ml RNase A) and lysed after the addition of 100 µl P2 (200 mM NaOH, 1 % SDS) for 5 min at RT. Lysis was stopped by adding 130 µl P3 (3 M KAc, pH 5,5). Cellular debris and genomic DNA were pelleted by centrifugation for 20 min at 13.000 rpm. The supernatant was transferred into 700 µl 100% EtOH. After mixing the precipitated plasmid DNA was pelleted by centrifugation for 15 min at 13.000 rpm. The pellet was washed with 1 ml 70% EtOH and spun again for 5 min at 13.000 rpm. The supernatant was removed and the pellet air dried before resuspending in 50 µl Tris pH 8,0. For larger bacterial cultures the Plasmid Midi kit (QIAGEN) was used according to the suppliers instructions.

2.2.7   Determination of DNA concentration

The DNA concentration was determined with a spectrophotometer at 260 nm. The concentration was calculated according to the following formular. c = A260 x 50 µg/ml x dilution factor. The purity of the DNA was tested using the ratio of A260/A280, which should be 1,8 for pure DNA.

2.2.8   RNA isolation from tissues

Mice were sacrificed and organs were taken. They were stored in the RNA stabilizing solution RNAlater (QIAGEN) under appropriate temperature conditions until further processing. Total RNA from tissues was extracted using the RNAeasy Lipid Tissue Kit for testis and brain and the RNAeasy Mini Kit (QIAGEN) for other organs. Isolated total RNA was eluated with 80 µl DEPC-$H_2$0. Integrity of total RNA was tested on agarose gels. Total RNA from human brain, liver and testis was purchased from Biochain (Hayward, CA, USA).

2.2.9   IFN induction and RNA isolation from cultured cells

Mouse L929 fibroblasts were stimulated for 24 h with 200 U/ml IFN-β (Calbiochem-Novabiochem Corporation, La Jolla, CA, USA) or 200 U/ml IFN-γ (R&D System GmbH, Karlsruhe). Human cell lines were stimulated for 24 h with 2000 U/ml IFN-β (PBL Biomedical Laboratories, NY, USA) or 200 U/ml IFN-γ (Peprotech, Rocky Hill, NJ, USA). Total RNA was extracted using the RNAeasy Mini kit (QIAGEN). Poly(A) RNA was isolated from total RNA using the Oligotex mRNA kit (QIAGEN).

2.2.10 cDNA synthesis and reverse transcriptase-PCR (RT-PCR)

The „SuperScript First-Strand Synthesis System for RT-PCR" (Invitrogen, Karlsruhe) with oligo(dT) primers was used for generating cDNA from total RNA or mRNA. If not stated differently, 1 µl of cDNA solution was used in each following RT-PCR reaction as template. For detection of transcripts in the cDNA primers located in different exons were used. They generate a specific product only on cDNA and not on genomic DNA (Table 3). All PCR-products were verified by sequencing.

Table 3. **Primers used for detection of gene-specific transcripts from cDNA.**

primer name	primer sequence 5'-to-3'	fragment size
bull GAPDH	GCTCACTTGAAGGGTGGCGCC	427 bp
	GTTTCTCCAGGCGGCAGGTCAG	
bull IRGC	GGAGAGTGAAGGGGAGAGGGAGAG	604 bp
	GCACGAAATAGAACTTCTTGCCCTG	
cat GAPDH	GAGATCCCGCCAACATCAAATG	519bp
	CAGCTTTCTCCAGGCGGC	
cat IRGC	GCAGGGAGAGTGTGAGGGGAC	615 bp
	GCAGGACGGTCGCCTCG	
dog GAPDH	GCGAGATCCCGCCAACATC	521bp
	CAGCTTTCTCCAGGCGGC	
dog IRGC	CCAGCGGGGAAAGTGTGAG	645bp
	CACGAGGAAGATGCGCGG	
human GAPDH	ATGACAACTTTGGTATCGTGGAAGG	495 bp
	GAAATGAGCTTGACAAAGTGGTCGT	
human GBP1	CTGTATCCGGAAATTCTTCCCAAAG	428 bp
	CTTCAATGGCCTCTCTCTCACTGTC	
human IRGC	GGAGATCCTATCAGTGGGGAGAGTGTGAGGG	682 bp
	CCTCTCTGAAGCCCGACGGCCG	
mouse GAPDH	GTCTACATGTTCCAGTATGACTCCACTCACGG	837 bp
	GTTGCTGTAGCCGTATTCATTGTCATACCAGG	
mouse GORASP2	CGAAGCAAAGCCCCTGAAGCTCTAC	878 bp
	CTGAAGCATCTGCATCAGACACAGGC	
mouse tsv GORASP2	CGAAGCAAAGCCCCTGAAGCTCTAC	586 bp
	GGAGGGTAAGGCATGCAACATACCC	
mouse Irga2	TAAGAAGAAGCTCAGTAGCC	963 bp
	ACCGAGGGCTATTCTTCTCT	
mouse Irgc	GCCTCTAGCTGCTGGGACCTGTCTCAGGTCACATCTGAG	622 bp
	GCGGGTGGCCGCCAGATCCTCGTCCACC	
mouse Irgq	CGCGTTATGCGGTAAGAATGTGGAC	534 bp
	GTCTCGAAGGCCTCACGAACAGCTT	
rat GAPDHS	GGAGAAGGGCGTTCGGGTAGTAG	769 bp
	GTCCTCTGTATAAGCAAGGATGCCAG	
rat Irgc	GGTCAGTGCATAGAGACCCAGGC	665bp
	GCCTCGCTGAAGCCCGAG	

2.2.11 DNA-Sequencing

DNA was sequenced according to the dideoxy-chain termination method (Sanger 1977). The ABI 3730 sequencer of the Cologne Center for Genomics (CCG) was used with the *ABI*[R] *Prism™ BigDye* V3.1 Terminator Cycle Sequencing Reaction kit (PE Applied Biosystems) following the protocols of the CCG.

2.2.12 Lysis of mouse tissues

Mice were sacrificed and organs were taken. For each mg of tissue 10 µl RIPA buffer (150 mM NaCl, 50 mM Tris, 1% NP-40, 0,1% SDS, 0,5% deoxycholate, 5 mM EDTA, 1% Triton X-100, pH 8,0, one Complete Mini Protease Inhibitor tablet per 10 ml buffer (Roche)) was added and the tissue was homogenized with rotor-stator homogenizer T10 basic (IKA,

Staufen). The homogenized lysate was incubated for 50 min on ice and then centrifuged for 30 min at 23.000 g. The supernatant was taken and analyzed by Western blot (2.2.14).

2.2.13 Hypotonic lysates

Seminiferous tubules were isolated from the testis and homogenized with a rotor-stator homogenizer T10 basic (IKA) and then lysed for 1 h on ice in hypotonic buffer (10 mM HEPES, 5 mM $MgCl_2$, pH 7,5). Cells were disrupted by 50 strokes with a Dounce homogenizer (Wheaton, Millville, NJ, USA). The nuclei were removed by a low speed centrifugation at 1.000 g for 5 min at 4°C. The supernatant was ultracentrifuged for 30 min at 100.000 g at 4°C. The membrane containing pellet was washed with hypotonic buffer and centrifuged for another 15 min at 100.000g at 4°C. The pellet was resuspended in 0,5% SDS in PBS.

By the short centrifugation step to remove the nuclei approximately 50% of the Irgc is removed from the lysate and found in the pellet (fraction T). This pellet was resuspended in the following buffers in order to test, under which conditions this Irgc fraction could be solubilised again. PBS; 1 M NaCl; 100 mM Na_2CO_3 (pH 11,75); 2 M, 4 M, 6 M Urea; 1% Triton X-100 in PBS. The soluble and non-soluble fractions were separated by centrifugation at 100.000g for 30 min at 4°C. The supernatant was taken and the pellet washed with the respective buffers and centrifuged for 15 min at 100.000g at 4°C. The pellet was resuspended in 0,5% SDS in PBS and equal volumes of all samples were analysed by SDS-PAGE and Western blot.

2.2.14 Western blot analysis

Protein and lysate samples were separated by 10% SDS-PAGE and then transferred to a nitrocellulose membrane by electroblotting. After transfer the membrane was stained with Ponceau S (0,1 % (w/v) Ponceau-S in 5 % (v/v) acetic acid) to locate protein size standard Page Ruler™ on the membrane. Then unspecific protein binding sites on the membranes were blocked by incubation for 1 h at RT in 5 % milk powder, 0,1 % Tween20 in PBS. Antisera/antibodies were diluted in 10 % FCS, 0,1 % Tween20 in PBS. Protein bands were visualized using the enhanced chemiluminescence (ECL) substrate.

2.2.15 Genomic Southern blot

Genomic DNA was cut with an endonuclease and separated on an agarose gel. The gel was treated subsequently with 0,25 M HCl and 0,4 M NaOH for 20 min each and placed on Hybond N+ nylon membrane (Amersham) on a stack of paper towels and Whatman paper (Labomedic, Bonn). 3 prewetted sheets of Whatman paper were put on top of the gel and connected to a reservoir of transfer buffer (0,4 M NaOH, 0,5 M NaCl) via a bridge of Whatman paper. DNA was transferred downwards onto the membrane ON. The membrane was prehybridized in hybridization buffer (5x SSC, 5x Denhardt's solution, 10 % dextransulfate, 0,5% SDS 250µg/ml denatured salmon sperm DNA) ON at 65°C in a hybridization oven (Techne Hybridizer HB-1D, Techne, Big Lake, USA). Probes labelled with [α-^{32}P]dCTP were synthesized using redi prime II labelling kit (Amersham) according to the manufacturer's instructions. Not incorporated nucleotides were removed with ProbeQuant G-50 Micro Columns (Amersham). The labelled probe was denatured for 10 min in a boiling waterbath, added to the hybridization solution and incubated at 65°C ON in the hybridization oven. Then the blot was washed for 10 min at 65°C with buffers containing decreasing concentrations of SSC (2x, 1x 0,5x, 0,1x) and 0,1x SDS. Signals were detected by autoradiography on X-ray films (X-omat AR, Kodak, Stuttgart).

2.2.16 Northern blot

The FirstChoice Northern Blot Mouse I was purchased from Ambion (Austin, TX, USA). It contains 2 µg of poly(A) RNA from ten mouse tissues of 8-10 weeks old Swiss Webster mice, except for embryo which are 14 days old. The [α-^{32}P]dATP labelled DNA probe was synthesized using the Strip-EZ DNA Kit (Ambion) and taking the ORF of Irgc as template. Hybridization in ULTRAhyb – Ultrasensitive Hybridization Buffer (Ambion) and washing was performed according to the manufacturer's instructions. The probed blot was exposed to X-ray film (X-omat AR, Kodak) for 24 h at -80°C.

2.3   Histology

2.3.1   Paraffin embedding of tissues and sectioning

The paraffin embedding of tissues was performed in 6-well tissue culture plates. Testis were taken and fixed overnight in Bouin's solution at 4°C. Other tissues were fixed in 4%

paraformaldehyde in PBS. Tissues dehydrated with the following series (1 h at 4°C PBS, 1 h at 4°C 0,86% NaCl, 6 h at 4°C 50% EtOH, ON at 4°C 70% EtOH, 4 h at 4°C 90% EtOH, 6 h at 4°C 96% EtOH, ON at 4°C 96% EtOH, 8 h at RT Isopropanol). Then the tissues were incubated in a paraffin:isopropanol 1:1 mixture overnight at 60°C. After evaporation of the isopropanol fresh liquid paraffin was added and incubated ON at 60°C. The paraffin was removed and fresh liquid paraffin was added and incubated for another hour at 60°C. The paraffin was exchanged again and the embedded tissues were kept at RT until the paraffin hardened completely.

The embedded tissues were cut with a microtome RM 2065 (Leica Microsystems, Wetzlar) into 6 µm thick serial sections, put on SuperFrost slides (Menzel, Braunschweig) and incubated at 40°C overnight.

Before staining, sections were dewaxed with Xylene (2x 10 min), then rehydrated by an EtOH series (100%, 95%, 90%, 70%, 30%, PBS each step 3-5 min) and postfixed for 1 h in 4% paraformaldehyde in PBS.

2.3.2   Hematoxylin and eosin (H&E) staining

Sections of paraffin embedded tissues were dewaxed (2.3.1). The sections were incubated in Meyer's hematoxylin for 2 to 5 min at RT, washed briefly with tab H_2O and then incubated for 5 min in tab H_2O. Afterwards the tissues were stained for 30 sec in eosin and washed 3 times for 30 sec with tab water. The slides were dried and mounted with Entellan (Merck, Darmstadt). The stained sections were analyzed and documented with an Axiophot microscope (Zeiss, Jena) equipped with the Spot Advanced Version 3.0.3 documentation system (Diagnostic Instruments, Sterling Heights, MI, USA).

2.3.3   *In situ* hybridization (ISH)

The templates for the probe were amplified from the vector pGW1H-CIN and cDNA from human testis, respectively, using the primers listed in Table 4 and cloned into the vector pGEM-T-easy (Promega). From this vector the templates for the sense and antisense probe were amplified with the respective primers. The respective template includes either the promoter of the Sp6- or T7-RNA-polymerase. The RNA-probe was synthesized using the proper RNA-polymerase and labelled with DIG using the DIG labelling reaction mix (Roche). Then the probe was purified by ethanol precipitation and resuspended in DEPC H_2O.

Table 4. **Primers used to generate *in situ* hybridization probes.**

probe	primer name	primer sequence 5'-to-3'	size
N-Irgc template	mCIN N5.1	ATGGCAACTTCCAGGTTGCCCGCCG	811 bp (N-terminal part of Irgc ORF
	CIN811-787 bw	CCAAGGCAGTCTTAAGCACCTGCTC	
N-Irgc antisense	mCIN N5.1	ATGGCAACTTCCAGGTTGCCCGCCG	Probe transcribed with SP6
	M13 rev	GGAAACAGCTATGACCATG	
N-Irgc sense	CIN811-787 bw	CCAAGGCAGTCTTAAGCACCTGCTC	Probe transcribed with T7
	M13 fw	TGTAAAACGACGGCCAGT	
hIRGC template	hCINEx1fwb	GGAGAGGGAGAGCCTGCAGGGCAG	852 bp (90 bp of 5'-UTR and 762 bp of hIRGC ORF)
	hCINEx2bwb	CTCCAGCGAGATGTCGGGGAGCG	
hIRGC antisense	hCINEx1fwb	GGAGAGGGAGAGCCTGCAGGGCAG	Probe transcribed with SP6
	M13 rev	GGAAACAGCTATGACCATG	
hIRGC sense	hCINEx2bwb	CTCCAGCGAGATGTCGGGGAGCG	Probe transcribed with T7
	M13 fw	TGTAAAACGACGGCCAGT	

All solutions for ISH were prepared with DEPC treated H_2O. Bouin's solution fixed and paraffin embedded 6μm thick sections of testis of different species were used for ISH. After dewaxing and postfixation the sections were digested with Proteinase K (10 μg/ml in 0,1 M Tris pH 7,5) for 10 min at 37°C. The digestion was stopped by incubation in 0,2% glycine in PBS for 10 min at RT and slides were washed two times with PBS, once with 0,2 N HCl and then again with PBS. Positively charged amino acids were blocked by incubation in 0,1 M triethanolamine pH 8,0, 0,25% acetic acid anhydrate. After washing with PBS and H_2O the samples were prehybridised for 2 hours at 70°C with prehydridization buffer (50% formamide, 5x SSC pH 7,0, 1x Denhardt's solution, 0,1% Tween20). 1-5 μl of the proper probe was preheated to 70°C mixed with 50 μl prehybridization buffer and 2 μl yeast tRNA (final concentration 0,1 mg/ml) and put on ice immediately. 55 μl of the hybridization solution was added on the slide, covered with a coverslip and incubated in humid chamber overnight at 70°C. After hybridization the samples were first washed 3 times for 30 min at 70°C with Solution I (50% formamide, 5x SSC pH 7,0, 1% SDS) and then 3 times for 30 min at 65°C with Solution II (50 % formamide, 2x SSC pH 7,0, 0,2% SDS). Following 3 washes for 5 min at RT with MAB (100 mM maleic acid, 150 mM NaCl, 0,1% Tween20, 2 mM Levamisole, adjust to pH 7,5 with NaOH) the slides were blocked for 2-3 hours at RT with 1% blocking reagent (Roche) in MAB. The Anti-Digoxigenin-AP Fab fragments (Roche) were dilluted 1:4000 in MAB/block and 100 μl were put on each slide, which were covered with a coverslip and incubated in a humid chamber at 4°C overnight. Unbound antibody was washed away with MAB (3 times 10 min and 3 times 30 min at RT) and 3 washes for 10 min at RT with NTMT (100 mM Tris pH 9,5, 50 mM $MgCl_2$, 100 mM NaCl, 2 mM Levamisole, 0,1% Tween20). For detection of the antibody the slides were incubated in 0,5 ml BM purple

substrate (Roche) with 2 mM Levamisole. After 2 days the old substrate was removed and fresh BM purple was added. The colour reaction took 2 to 5 days. When the staining was finished the slides were washed with H_2O and mounted with Kaiser's glycerine (Merck).

2.3.4 Immunohistochemistry

Dewaxed and postfixed 6 µm thick paraffin sections were used for immunohistochemistry. In order to demask the epitopes for the antibody, the sections were incubated 10 min in boiling 10 mM citrate buffer pH 6,0 and washed 5 min with PBS. Unspecific protein binding sites and endogenous peroxidases were saturated by a 20 min incubation in Quenching buffer (1 % BSA, 0,3 % H_2O_2 in PBS). After 3 times washing for 1 min at RT with PBS the sections were incubated in a humid chamber for 1hour at RT or overnight at 4°C with the primary antibody, which was dilluted in DAKO diluent (DAKO, Hamburg). Unbound antibody was washed away with PBS 3 times for 2 min at RT. Then the sections were incubated with the secondary antibody, which was coupled to horse radish peroxidase, in a humid chamber for 1 hour at RT. Unbound secondary antibody was removed by washing 3 times for 2 min at RT with PBS. HistoGreen (Linaris, Wertheim-Bettingen) (Thomas 2005), a peroxidase substrate, was applied on the sections and icubated for 3-8 min at RT. The colour reaction was stopped by washing the sections 3 times 2 min with H_2O. The nuclei were counterstained for 3-5 min with Nuclear Fast Red and the sections were washed 5 min at RT with H_2O. Because the substrate HistoGreen is watersoluble the sections had to be dehydrated (3 times 30 sec 100% Ethanol, 2 times 30 sec Xylene at RT) before mounting with Entellan (Merck).

2.3.5 Squash preparation of cells from the *tubuli seminiferi*

A mouse was sacrificed and the testis transferred into PBS. The capsule of the testis was opened and the seminiferous tubules released. Small pieces with a length of 2 to 4 mm of single tubules were cut out and transferred in a small drop of PBS on a slide. A coverslip was put on the tubule and pressed with gentle pressure on the tubule until the cells inside the tubule were squashed out of the tubule. The coverslip and the remains of the tubule were removed and the cells air dried on the slide. Then they were fixed for 20 min in 4 % PFA in PBS, followed by three washing steps in PBS. Afterwards the immunofluorescence protocol was applied (2.3.7).

2.3.6 Preparation of spermatozoa from the epididymis

The epididymis was isolated from mature 8 to 10 weeks old mice. The whole isolation procedure was performed at 4°C. The epididymis was transferred into homogenization buffer (10 mM Tris-Cl pH 7,4, 250 mM Sucrose, 1 mM EDTA, 1 mM Pefabloc SC Inhibitor (Roche)) and the caput of the epididymis was opened. Afterwards the content of the caput was flushed with homogenization buffer and a syringe. The resuspended content of the caput was filtered through a fine mesh. The spermatozoa were pelleted with a low speed centrifugation for 40 min at 600 g and then resuspended in 500 µl homogenization buffer.

For staining 30 µl of the sperm-suspension was put on a slide and air dried. Then the spermatozoa were fixed ON at 4°C in 4% PFA in PBS. After fixation the spermatozoa were washed with PBS. For analysis the fixed spermatozoa were observed under the microscope and the immunofluorescence protocol (2.3.7) was applied.

2.3.7 Immunofluorescence

All steps were performed at RT if not stated otherwise. Fixed cells were permeabilized by 0,1 % Saponin in PBS (washing buffer) for 10 min and unspecific binding sites were blocked with 3 % BSA in PBS (blocking buffer) for 1 h. Three washes for 5 min with washing buffer were followed by the incubation with the primary antibody diluted in blocking buffer for 1 h in a humid chamber. Subsequently the cells were washed three times with washing buffer to remove unbound antibodies. The secondary goat-anti-rabbit IgG Alexa 546 antibody was diluted 1:1000 in blocking buffer and 300 nM DAPI for DNA staining was added. The samples were incubated for 1 h in a humid chamber. Following three washing steps with washing buffer the slides were air dried, mounted with Prolong Gold antifade reagent (Invitrogen) and sealed with nail polish. Samples were analysed using a Zeiss Axioplan II fluorescence microscope (Zeiss, Jena) equipped with a cooled Quantix CCD camera (Photometrics, Tucson, AZ, USA) and the Metamorph software (Molecular Devices, Downingtown, PA, USA) for taking images.

2.3.8 Laser microdissection (LMD)

Testes were taken and immediately snap frozen in liquid nitrogen. 10 µm thick cryosections were prepared on a cryotome CM 3050S (Leica Microsystems, Wetzlar) and put on PALM MembraneSlides (P.A.L.M. Microlaser Technologies, Bernried), which was covered with a

PEN membrane. Samples were fixed for 20 min at -20°C in 70 % EtOH and then washed with H_2O for 5 min. The Nuclei of the cells were stained with Nuclear Fast Red for 5 min and washed briefly with H_2O. Then the samples were dehydrated by an EtOH series (70%, 96%, 100% each step 2 min) and afterwards dried for 10 min at 50°C. Sections were made according to the descriptions in 3.9 using the Laser Microdissection (LMD) equipment of the Institute for Pathology (University Clinic, Köln) consisting of an Interface Microbeam Mini laser (P.A.L.M Microlaser Technologies) and an Axiovert 135 microscope (Zeiss, Jena). The cut samples were collected in a small drop (less than 1µl) of mineral oil in the cap of LPC Microfuge tubes (P.A.L.M. Microlaser Technologies).

Total RNA from the dissected samples was extracted using the RNeasy Micro kit (QIAGEN), using the 10fold amount of carrier RNA and eluting the RNA in the smallest volume possible (12 µl). cDNA was prepared as described in 2.2.10 using 8 µl of the isolated total RNA as template.

2.4   Generation of Irgc$^{-/-}$ -mice

2.4.1   Targeting strategy for Irgc

The targeting vector pCinema EGFP neo and the probes used to detect homologous recombinant ES cell clones by Southern blot analysis were designed and cloned during my diploma thesis (Rohde 2003). By homologous recombination the ORF of Irgc is replaced by the ORF of the Enhanced Green Fluorescent Protein (EGFP). Hence, the reporter protein is expressed under the control of the Irgc promoter (Figure 7). In order to select for homologous recombination the vector contained a neomycin-cassette, which allows positive selection against G418. The *HSV thymidine kinase* is integrated only in case of random integration of the whole vector into the genome and not in homologous recombination. Negative selection against this random integration was performed with Ganciclovir.

With the recombinant ES cells generated with *Bruce4* ES cells (Kontgen 1993) from C57BL/6J mice during my diploma, germline transmission could not be obtained even after multiple trials. Hence, new recombinant ES cells were generated in the F1-ES cellline V6.5, which originates from a C57BL/6 x 129sv/Jae breeding (Rideout 2000).

In order to remove the loxP flanked neomycin-cassette from the genome, the Irgc$^{+/-}$-mice were mated with C57BL/6 Cre-deleter mice (Schwenk 1995). All experiments presented in this thesis were performed with mice without neomycin-cassette.
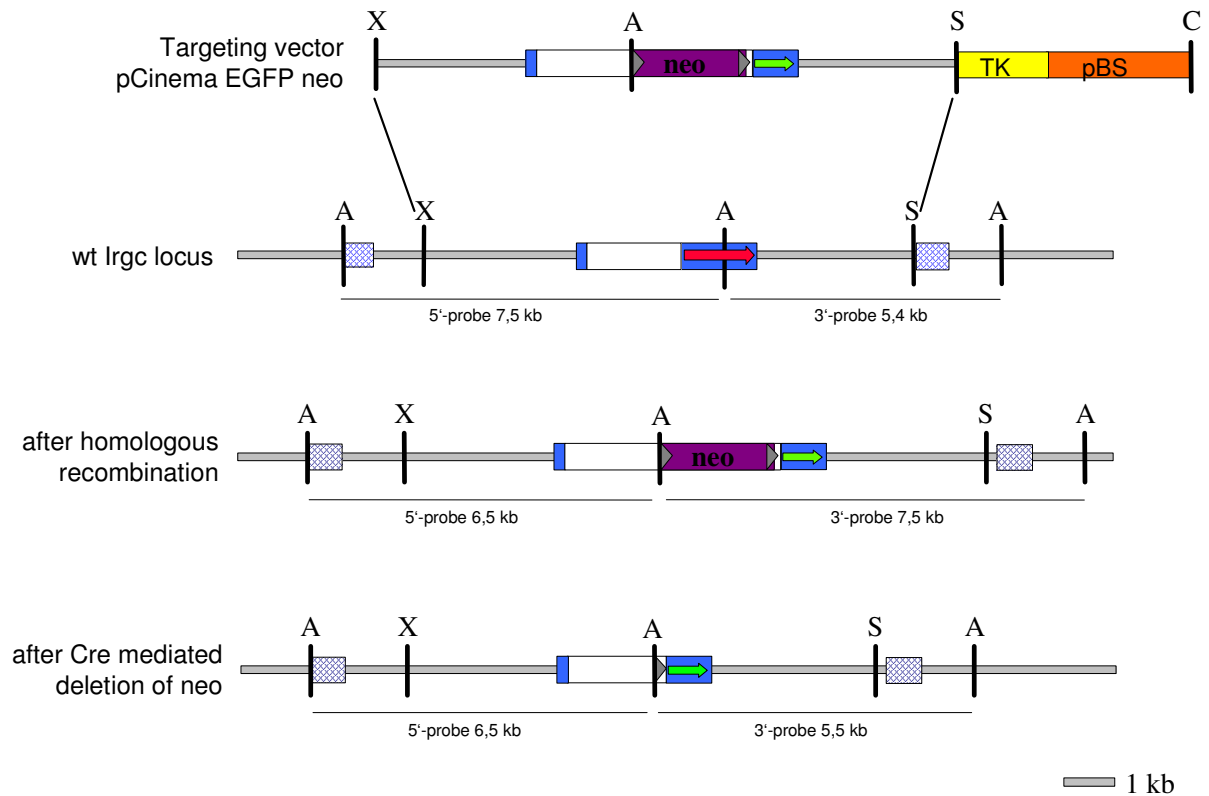
Figure 7. **Targeting strategy for Irgc.** The ORF of Irgc is replaced by the EGFP ORF in the targeting vector pCinema EGFP neo. For positive selection a neo-cassette flanked by two loxP sites is integrated in the intron. After integration of the targeting vector by homologous recombination the signal generated by the 5'- and 3'-probe in Southern blot after *Afl*II restriction shifts from 7,5 kb and 5,4 kb, respectively, to 6,5 kb and 7,5 kb, respectively. blue box: exon, white box: intron, yellow box: HSV Thymidin kinase (TK), orange box: pBlueScript II KS+ (pBS), violette box: neomycine resistance cassette (neo), grey triangle: loxP site, red arrow: Irgc ORF, green arrow: EGFP ORF, blue checkered box: location of probe for Southern blot, restriction sites: A: *Afl*II, C: *Cla*I, S: *Spe*I, X: *Xma*I

2.4.2   ES cell culture

ES cell culture was performed according to the protocols published in *Laboratory Protocols for Conditional Gene Targeting* (Torres 1997) with modifications used in the laboratory of Ari Waisman. ES cells were always cultivated on a layer of MMC-treated EF cells in ES medium (see below).

2.4.2.1 Mitomycin C treatment of EF cells

Embryonic fibroblasts had to be mitotically inactivated with mitomycin C (MMC) before usage as feeder cells for ES cells. EF cells were incubated for 3 h in EF media containing 10µg/ml MMC. Then they were washed 2x with PBS, trypsinized and plated on gelatinized.

2.4.2.2 Transfection of ES-cells with pCinema EGFP neo

100 µg of the targeting vector pCinema EGFP neo was linearized using the restriction endonuclease *Cla*I, purified by phenol/chloroform extraction and resuspended in 0,8 ml RPMI without phenol red. ES cells were fed 4 h before transfection with fresh ES media. Then they were trypsinized for 5 min at 37°C and counted. 10^5 ES cells were plated to control their viability. Two separate transfections with aliquots of 10^7 cells were performed. The ES cells were centrifuged for 10 min at 1.200 rpm at 4°C and resuspended in 0,4 ml RPMI without phenol rot and mixed with 0,4 ml RPMI containing the DNA. The mixture was put in an electroporation cuvette, incubated for 10 min at RT and then electroporated at 240V/500µF. 10^3 cells from each transfection were plated on 6 cm tissue culture plates to control the survival rate of ES cells after transfection, which was approximately 11%. The other ES cells were plated on 10 cm tissue culture plates (5 plates per transfection).

2.4.2.3 Positive and negative selection of ES cells

The day of transfection was counted as day 0. Positive selection with G418 for ES cells containing the neo cassette started from day 2. The activity of the G418 batch had been experimentally tested before and was 70% active. Thus 1,4 ml G418 were added to each 600ml bottle of ES media. At day 5 the negative selection with gancyclovir (GANC) against ES cells, which randomly integrated the whole targeting vector and thus contain also the hsv-thymidin kinase, started. 10µl of the GANC stock (2x10-1 M) was diluted 1:100 in ES media, filtered sterile through a 0,22 µm filter and was further diluted 1:1.000 in ES media containing G418 to obtain the final working concentration of GANC.

2.4.2.4 ES colony picking

On day 8 after selection surviving colonies were picked under a sterile hood. Plates with ES cells were washed three times with PBS. Individual colonies were taken with a P20 pipette and transferred into 50 µl trypsin/EDTA in the wells of a 96 well round bottom tissue culture plate. After 20 min of picking the plates were incubated for 3 min at 37°C. 150 µl of ES media were added to stop trypsinization and picking continued. After 1 h of picking the trypsinized ES cells were distributed on three 96 well flat bottom tissue culture plates and 200 µl ES media was added. In total 288 colonies were picked.

The ES cells were cultivated for 2 to 3 days. Two replica plates were frozen on subsequent days. Therefore they were washed two times with PBS and then trypsinized by adding 50 µl

trypsin/EDTA and incubated 5 min at 37°C. Then 50 µl ice cold 2x freezing media was added. The plates were wrapped in parafilm, placed on ice and slowly frozen at -80°C.

The third plate was trypsinized in the same way, but then the trypsinized cells were distributed on three gelatinized 96 well flat bottom tissue culture plates without EF cells. These cells were grown to complete confluence, washed two times with PBS and then frozen at -20°C. The cells on these plates were used to screen for homologous recombination by Southern blot analysis. Therefore 50 µl lysis buffer (10 mM NaCl, 10 mM Tris-Cl pH 7,5, 10 mM EDTA, 0,5% Sarcosyl, 0,4 mg/ml Proteinase K [freshly added each time]) was added to each well and in parafilm wrapped 96 well plate was incubated ON at 56°C in a humidified chamber. Then the plate was cooled to RT for 1 h and 100 µl 100% EtOH was added to each well. The DNA was precipitated for 1 h at RT. The EtOH was removed by inverting the plate carefully. The DNA remains attached to the bottom of the plate during this procedure. The plate was washed three times with 70% EtOH and dried at room temperature. 35 µl of *Afl*II restriction mix (30 U *Afl*II, 3,5µl NEB2, 1 mM spermidine, 1 mM DTT, 100µg/ml BSA, 50 µg/ml RNase A) was added to each well and incubated ON at 37°C in humidified chamber. Samples were separated by agarose gel electrophoresis and analyzed by Southern blot.

2.4.2.5 Thawing and expansion of ES cell clones

Recombinant ES cell clones identified in the Southern blot had to be thawed and expanded. For this purpose the frozen 96 well tissue culture plates were thawed on a 37°C heating block and immediately after thawing cells were transferred into tubes containing 5 ml ES media to dilute the DMSO. The cells were centrifuged for 5 min at 1.200 rpm at 4°C and the cell pellet was resuspended in 1 ml ES medium. These were plated in the wells of a 24 well tissue culture plate and incubated at 37°C. Clones were expanded every 2 to 3 days by subsequent transfer to 6 well tissue culture plates and 10 cm culture dishes. From each clone three aliquots were frozen. Additionally the thawed clones were analyzed by Southern blot again to confirm the results of the initial analysis. Of the 22 thawed clones homologous recombination could be confirmed in 18 clones (Figure 8). For the 288 clones picked in the beginning the resulting recombination frequency is 6,3 %. Thus the recombination rate was even higher than the 3,7 % for the first transfection performed with *Bruce4* ES cells during my diploma (Rohde 2003).
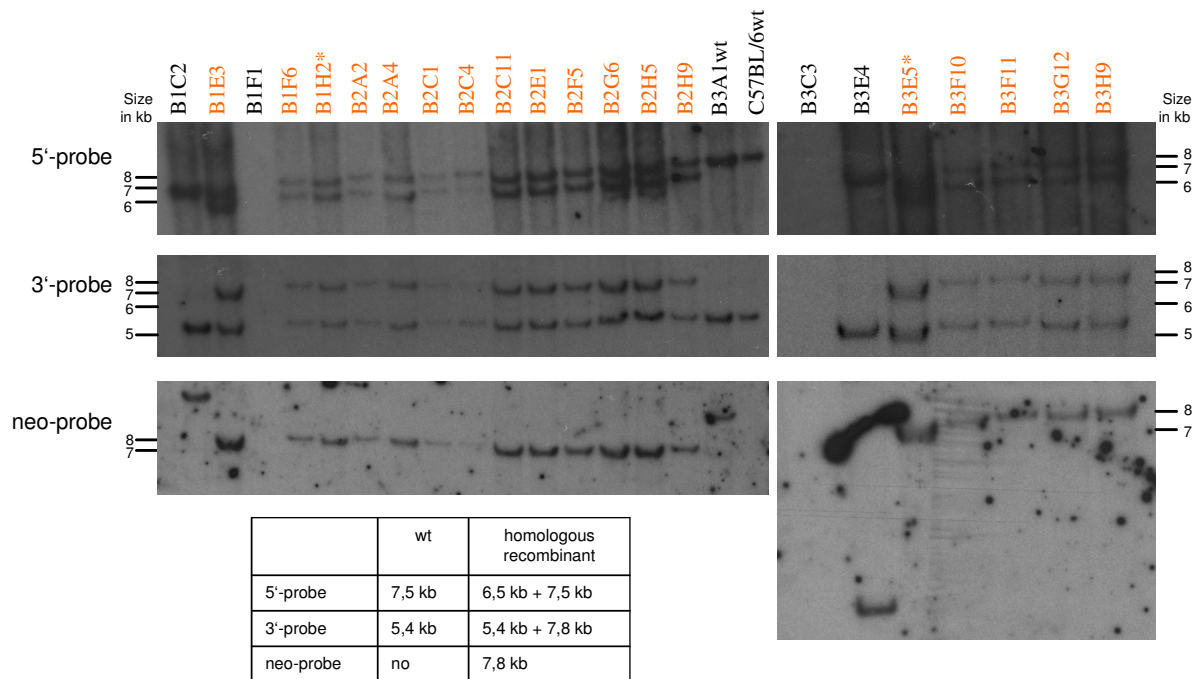
Figure 8. **Verification of homologous recombinant ES cell clones by Southern blot.** Clones identified as homologous recombinants in the initial Southern blot screen were thawed, expanded and tested again by Southern blot. Autoradiographies using the radio-labelled 5'-, 3'- and neo-probe are shown. The expected signals for the respective probe are given in the table. 18 out of 22 clones were positive for all three probes (in red). Clone B3A1wt, which was negative in the first screen and genomic DNA from C57BL/6 mice were used as controls. The * indicates clones used in blastocyte injection and yielding germline transmission.

2.4.2.6 Preparation of ES cells for blastocyst injection

ES cells were thawed two days prior injection and cultured on 10 cm culture dishes. On the day of injection the cells were washed two times with PBS and then trypsinized for 5 min at 37°C. The reaction was stopped by the addition of an equal volume of ES media. Cells were centrifuged 10 min at 1.200 rpm at 4°C and then resuspended in 10 ml ES media. The cell suspension was plated on a gelatinized 10 cm culture dish and incubated for 30 min at 37°C. Since the EF cells sediment faster than the ES cells, the supernatant contains mainly ES cells and is depleted from EF cells. This supernatant is taken and centrifuged for 10 min at 1.200 rpm at 4°C and resuspended in 1 ml injection media. The plate was washed with 10 ml ES media to harvest loosely attached ES cells and the cell pellet after centrifugation resuspended in 1 ml injection media. The injection into CB20 derived blastocysts was performed by Sonja Becker (Center for Mouse Genetics, Institute for Genetics, Köln).

2.4.3 Breeding of mice

Chimeras generated by injection of recombinant ES cells into blastocysts were bred with CB20 mice (see Appendix I for all injections). The chimeras #13 ($\male$, 90% chimerism) and #14 ($\male$, 80%) from the injection of clone B1H2 and #45 ($\male$, 85%) and #46 ($\female$, 75%) derived from clone B3E5 produced 100% germline transmission of the recombinant ES cells as seen by the brown coat colour of all the offspring. Transmission of the recombinant Irgc$^-$ allele was demonstrated by Southern blot analysis and PCR (not shown). The breeding lines were derived from the ES cell clone B1H2.

In order to exclude any effects of the neomycin-cassette located in the intron, it was deleted by breeding the chimeras to C57BL/6 Cre-deleter mice (Schwenk 1995). The resulting offspring were screened for heterozygote Irgc$^{+/-}$/neo$^-$-mice, which were crossed to produce homozygote Irgc$^{-/-}$-mice. The latter breeding produced all expected genotypes (Irgc$^{+/+}$, Irgc$^{+/-}$, Irgc$^{-/-}$). For further breedings Irgc$^{+/-}$- and Irgc$^{-/-}$-mice which did not carry the *Cre* gene were chosen. Therefore all experiments presented in this thesis were carried out with neo$^-$/Cre$^-$-mice.

2.4.4 Generation of Hook1$^{azh/azh}$/ Irgc$^{-/-}$-mice

C57BL/6 Hook$^{azh/azh}$-mice were kindly provided by Dr J. Neesen (Göttingen). Irgc$^{-/-}$-males were crossed to Hook$^{azh/azh}$-females. The resulting double heterozygote mice were crossed and Hook1$^{azh/azh}$/ Irgc$^{-/-}$-mice were obtained.

2.4.5 Typing of mice for Irgc and Hook1 genotype

Mice were typed using a three primer PCR. The tip of the tail of the mouse was cut and lysed overnight at 56°C in 500 µl lysis buffer (100 mM Tris-Cl pH 8,5, 5 mM EDTA, 0,2 % SDS, 200 mM NaCl, 300 µg Proteinase K). After 10 min centrifugation at 13.000 rpm the supernatant was taken and 500 µl Isopropanol added to precipitate the genomic DNA. The DNA was pellet by centrifugation (10 min at 13.000 rpm) and washed with 500 µl 70% Ethanol. Then the sample was centrifuged, the supernatant removed and the DNA-pellet air dried. The DNA was resuspended in 50 µl TE buffer and 1 µl was used as template in the typing PCR. The primers used for genotyping are listed in Table 5.

PCR-protocol: 90 sec 95°C; 35x (30 sec 95°C; 30 sec 66°C; 20 sec 72°C); 3 min 72°C

Table 5. **Primers used for genotyping of mice.** Primers used in 3 primer PCRs amplifying specific bands for wt and homologous recombinant genomic DNA.

gene	primer name	primer sequence 5'-3'	band size in wt	band size in homolog recombinant
Irgc	EGFP fw1	GACTTCAAGGAGGACGGCAACATCC		802 bp
	Hom rec bw2	CCTGGGATATGATGCTGGACCTACCAG		
	CIN 3-point fw	GGAAGCTCGGCCTCCTCCTCAAG	542 bp	
Hook1	HK Del F	GCCAGATGTTGGTCAGAGGCAGTAA		
	HK Del R	GGCCAAATCTAGGAGAGCGGAGCAT	505 bp	
	HK Del Rev2	CAGGGAAACCTGAAGAGCTCAGTAA		343 bp
Neomycin cassette	del neo fw	GCATACCTCAGCTTCAGAACGATCCTACC	+ neo: 951 bp - neo: 638 bp	
	del neo bw	CCGGACACGCTGAACTTGTGGC		
	del neo middle bw	CGAATAGCCTCTCCACCCAAGCG		
Cre	5' deleter	GAAAGTCGAGTAGGCGTGTACG	+ Cre: 600 bp - Cre: no band	
	Mx-Cre R	CGCATAACCAGTGAAACAGCAT		

2.5 Yeast

2.5.1 Preparation of yeast two-hybrid vectors

The ORF of Irgc was amplified from the vector pGW1H-CIN (Rohde 2003) using primers flanked by *Sal*I restriction sites. The cDNA clone Accession number BC080294, which contains the complete Irgq ORF, was obtained from the Deutsches Ressourcenzentrum für Genomforschung (RZPD, Berlin). The complete ORF of Irgq and the fragment of Irgq encoded by the last exon (IrgqE4) were amplified from this clone using primers flanked with *Sal*I restriction sites. All primers used are listed in Table 6. The amplified fragments were cloned according to the instructions in 2.2.3 into the vectors pGAD-C1 and pGBD-C1.

The Hook1 containing yeast two-hybrid vectors pGBK-Hook1 and pGAD-Hook1 were kindly provided by Dr J. Neesen (Göttingen).

Table 6. **Primers used for preparation of yeast two-hybrid vectors.** *Primer is called E3 (Exon3) but refers to E4 (Exon4), because the existence of the untranslated Exon1 was unknown at the time the primer was ordered.

	primer name	primer sequence 5'-3'
Irgc ORF	mCIN Sal 5'	CCCCCCCCCGTCGACATGGCAACTTCCAGGTTGCCC
	8.3	CCCCCCCCCGTCGACTTATTTGTCTGAC
Irgq ORF	IrgqORFSalfw	CCCCCCCCCGTCGACATGCCTCTGCCTCAGGGTGACG
	IrgqORFSalbw	CCCCCCCCCGTCGACTCATTGGTTGGGCTCTGGGGGTCC
IrgqE4	IrgqE3ORFSalfw*	CCCCCCCCCGTCGACAGGCTCCTGCCTCCTGCCCAGG
	IrgqORFSalbw	CCCCCCCCCGTCGACTCATTGGTTGGGCTCTGGGGGTCC

2.5.2 Lithium/Acetate-transformation of *Saccharomyces cerevisiae*

One big colony of *S. cerevisiae* was resuspended in sterile H_2O. Yeast were sedimented by centrifugation for 10 sec at 1000 rpm and washed with 1 ml 100 mM LiAc. Subsequently they were centrifuged again and the pellet was resuspended in 50 µl 100 mM LiAc. In the following order 240 µl 50% PEG, 36 µl 1 M LiAc, 5 µl calf thymus DNA, which has to be denatured for 10 min at 95°C prior to use, 1 µg plasmid DNA, ad 400 µl H_2O was added, well mixed and incubated for 30 min at 30°C. A heatshock was conducted for 20 min at 42°C. Afterwards the yeast were collected by centrifugation for 15 sec at 6000 rpm. The supernatant was removed and the pellet resuspended in 200 µl dH_2O. Cells were plated on SD-Leu or SD-Trp plates, depending on the vector transformed. Then they were incubated for 2-3 days at 30°C until colonies grown to a diameter of approximately 1 mm. Colonies were streaked out on SD-Leu or SD-Trp plates, respectively, for single colonies.

2.5.3 Plasmid preperation from *Saccharomyces cerevisiae* after Robzyk (1992)

A 3 ml overnight culture was harvested by centrifugation, washed with H_2O and resuspended in STET-solution (8% Saccharose, 50 mM Tris pH 8,0, 50 mM EDTA, 5% Triton-X 100). Glass beads (diameter 0,45 mm) were added to reach the level just under the meniscus and the cells were shaked for 5 min on an IKA-Vibrax-VXR (IKA, Staufen). Another 100 µl of STET solution was added and incubated for 3 min at 95 °C. Then the yeast cells were chilled for 10 min on ice and then centrifuged for 10 min at 15.800 g at 4°C. The supernatant was taken and half the volume of 7,5 M NH_4-Acetate was added, mixed and incubated for 1 hour at -20°C. After centrifugation for 10 min at 15.800 g at 4°C 100 µl of the supernatant was taken, 200 µl 100% Ethanol was added to precipitate the plasmid DNA, which was pelleted by centrifugation. The pellet was washed with 70% EtOH and centrifuged again. The supernatant was removed and the pellet dried before resuspending the plasmid in 20 µl 10 mM Tris pH 8,5.

2.5.4 Yeast two-hybrid selection after James (1996)

Haploid yeast strains of the opposite mating type were crossed with each other on YPD plates and incubated for 24 h at 30°C. One strain carried the bait vector, where the protein is expressed as a fusion with the GAL4 DNA binding domain (BD), the other vector contained the putative partner expressed as a fusion with the GAL4 activation domain (AD). If these

two proteins interact with each other, DNA-BD and AD are brought into proximity, leading to the transcription of different reporter genes (Fields 1989, Chien 1991). Both strains carried plasmids with different auxotrophic markers, either *LEU2* or *TRP1*. A replica-plating on SD-Leu/-Trp plates was performed to select for diploid yeast containing both vectors. The diploid yeast were streaked out on different selective media, SD-Leu/-Trp/-Ade, SD-Leu/-Trp/-His/+1 mM 3-AT and SD-Leu/-Trp/-His/-Ade, and cultured at 30°C. Growth of yeast under this selective conditions indicated interaction of the two proteins tested.

2.5.5   Yeast two-hybrid library screen

A Pretransformed Mouse Testis MATCHMAKER cDNA Library was purchased from BD Biosciences (Palo Alto, USA) and the library screen performed according to the manual. It contains a cDNA library from normal, whole testes pooled from 200 8-12 weeks old BALB/c males, cloned into the vector pACT2. Thus, the whole library is expressed as a fusion protein with the GAL4 activation domain (AD), which is transformed into the *Saccharomyces cerevisiae* strain Y187 (*MAT*α). The library containing Y187 are mated to AH109 (*MAT*a) transformed with pGBD-Irgc as bait protein and selected on high stringency SD-Leu/-Trp/-His/-Ade plates. Colonies growing under these conditions were isolated and its plasmids purified. Then these vectors were transformed into *E. coli.* After mini prep of the plasmid DNA, clones containing the pACT2 vector were identified by restriction digest using *Hind*III. Afterwards the insert of the vector was identified by sequencing using the primers listed in Table 7.

To test the specificity of the interaction between the bait- and the library protein, the pACT2 [library protein] was transformed into PJ69-4a-a and mated to PJ69-4a-α [pGBD-empty]. Then the mated yeast strains were cultured under selective conditions on SD-Leu/-Trp/-His/-Ade plates. Yeast growth under these selective conditions indicated, that the library protein interacts directly with the GAL4 AD. Thus, the interaction is unspecific. Only library proteins which did not grow under the conditions described above were regarded as true positives in the yeast two-hybrid screen.

Table 7. **List of sequencing primers for Irgc interaction partners detected in the yeast two-hybrid library screen.** Primers for sequencing of inserts in the vector pACT2.

primer name	primer sequence 5'-3'
pACT2insert5'bw	CTATTCGATGATGAAGATACCCCACCAAACCC
pACT2insert5'bw2	GCTAGCTTGGGTGGTCATATG
pACT2ins3fw2	GTGAACTTGCGGGGTTTTTCAGTATCTACG
pACT2ins3fw3	GTGCACGATGCACAGTTGAAGTGAAC

2.6 Evolutionary and phylogenetic analysis

2.6.1 Database resources

All available public databases were screened with the Basic local alignment search tool BLAST (Altschul 1990) for genomic and mRNA-derived IRGC sequences. These included the databases of NCBI (http://www.ncbi.nlm.nih.gov), ENSEMBL (http://www.ensembl.org) and the Sanger Institute Sequencing Genomics projects (http://www.sanger.ac.uk/Projects/).

2.6.2 Alignments and phylogeny

Sequence alignments were performed with Vector NTI and the BCM Search Launcher (http://searchlauncher.bcm.tmc.edu/multi-align/multi-align.html) and edited manually. Shading of alignments and the amino acid identity and similarity matrix shown in Table 9 were conducted with GeneDoc (Version 2.6.002) (http://www.nrbsc.org).

Phylogenetic analysis is based on the neighbor-joining method (Saitou 1987) and p-distances for construction of phylogenetic trees. The analysis was performed with Molecular Evolutionary Genetics Analysis Version 4 (MEGA 4) (Tamura 2007).

2.6.3 Identification of transcription factor binding sites

The region 10 kb upstream of the transcription start point were designated as the putative promoter regions and screened for transcription factor binding sites. The sequence was searched with the Transcription Element Search System TESS (http://cbil.upenn.edu/tess) (Schug 1997) and confirmed manually. Putative conserved transcription factor binding sites in the promoters of IRGC from different species were identified ConSite (http://www.phylofoot.org) (Lenhardt 2003, Sandelin 2004). ConSite is a bioinformatic tool searching for conserved binding sites on the basis of phylogenetic footprinting.

3. Results

3.1 Phylogenetic distribution of IRGC

IRGC was reported to be present in mouse and human and is highly conserved between the two species (Rohde 2003, Bekpen 2005). To find out which other species contain an orthologue of IRGC, the public genome libraries of a wide variety of species were searched for IRGC. The complete sequence of IRGC was detected in 12 different species and fragments of it in 9 further species, all of which belong to the class of mammals. Among the mammals, IRGC was found in all subclasses, namely the *Monotremata*, the *Marsupialia* and the *Eutheria* (Table 8). The amino acid sequence of Irgc is highly conserved through the mammals as shown in the alignment of the 21 Irgc orthologues in Figure 9. In a comparison between all available full-length IRGC sequences the amino acid identity values range between 100 % (human – chimpanzee) and 88 % (bull – human/chimpanzee) (Table 9). The GTP-binding domain is highly conserved among all IRGCs with only very few amino acid exchanges. The GTP-binding motifs G1 (GxxxxGKS), G3 (DxxG) and G4 (N(T/Q)KxD) were identified in all species, where sequence information on the G-domain of the protein is available. The most divergent region of the protein are the 60 amino acid located on the C-terminus, although this region is nevertheless also well conserved.

The strong conservation within the IRGC orthologues is demonstrated by the phylogentic tree presented in Figure 10. It shows the phylogenetic relationship of the 12 IRGC proteins from whom the complete sequence is available to the 21 IRG proteins present in the mouse excluding the pseudo genes *Irga5* and *Irgb7*. Mouse Irgc is much closer related to all other IRGC orthologues than to any other mouse IRG protein. The relationship within the mammalian IRGCs is closer than within the Irgas, Irgbs and Irgms, respectively, in the mouse.

The *IRG* genes with the closest relationship to the IRGC clade are the *IRGC-like* genes. They form a separate clade of IRG proteins and are closely related to the IRGC proteins. They were discovered in diverse species including dog, shrew, cat, horse, microbat, pig, opossum and platypus, but they are not present in mouse, rat and human (Bekpen 2005, Julia Hunn personal communication). Outside the mammals they were found in reptiles (*Anolis carolinensis*) and amphibians (*Ambystoma tigrinum*). The *IRGC-like* genes are considerably more divergent than the *IRGC* genes.

Table 8. **List of all species which possess IRGC.**

Order	Species		length in amino acids	genomic sequence / Accession nr.	cDNA / ESTs	chromosomal location	poly(A)-Signal in Stop-Codon
Monotremata	*Ornithorhynchus anatinus*	platypus	219 from middle	AAPN01212630	ENSOANT00000022749	-	AATAAA
Marsupialia	*Monodelphis domestica*	opossum	41 from middle	AAFR03064171	-	4	AATAAA
Edentata	*Dasypus novemcinctus*	armadillo	254 from N-terminus	AAGV01591351	ENSDNOT00000002351	-	-
Rodentia	*Mus musculus*	mouse	463	AC073810 (RP23-57J6)	XM_920441 complete mRNA	7: 24.140.914 – 24.142.150	AATAAA
	Rattus norvegicus	rat	463	NW_047556	NM_001014016 complete mRNA	1 : (+) 79.675.029- 79.678.711	AATAAA
	Cavia porcellus	guineapig	304 from C-terminus	AAKN01452559	-	-	AATAAA
	Spermophilus tridecemlineatus	squirrel	114 from N-terminus	Scaffold_35033 Contig_393048	-	-	-
Primates	*Macaca mulatta*	macaque	463	AANU01219337	DY745356, EB518177 from M. nemestrina	19:	AATAAA
	Pan troglodytes	chimpanzee	463	NW_001228236	XM_524291 complete mRNA	19: (+) 49.283.399 – 49.288.075	AATAAA
	Homo sapiens	human	463	AC005622 ENSG00000124449	NM_019612 complete mRNA	19: (+) 48.912.078 – 48.916.004	AATAAA
	Otolemur garnetti	bushbaby	403 from N-terminus	AAQR01370437	-	-	-
	Microcebus murinus	gray mouse lemur	463	ABDC01255415 contains 1 frameshift	-	-	AATAAA
Chiroptera	*Myotis lucifugus*	microbat	395 with gap in the middle	AAPE01124004	-	-	-
Insectivora	*Sorex araneus*	shrew	350 from the middle	AALT01094692	-	-	-
	Echinops telfari	lesser hedgehog tenrec	207 from N-terminus	Contig_323550 Scaffold_270855	-	-	-
Carnivora	*Felis catus*	cat	465	AANG01188477	-	-	AAGTGACC
	Canis familiaris	dog	464	NW_876270	ESTs CX989998 BM537262 cover 576-1395	-	AAGTGAAAG
Artiodactyla	*Sus scrofa*	pig	465	-	ESTs CV875009 CV870591 CO955047 CV865494 only putative G855 not covered	-	AAATGAAAA
	Bos taurus	cattle	465	NW_001493616	NM_001076146 complete mRNA	18: (-) 49.142.304 – 49.146.206	AAATGAAA
Perissodactyla	*Equus caballus*	horse	464	AAWR01029205	-	-	AAGTAAA
Proboscidea	*Loxodonta africana*	elephant	463	AAGU01530220	-	-	AAATGAAAA

```
                          *         20        *         40        *         60        *         80        *        100        *        120
armadillo*  : MAGARSP-GPREEETTILMAKEELEALRTAFESGDIPQAASRLRELLASSESTRLEVGVTGESGAGKSSLINALRGLGAEDAGAALTGVVETTMNPSPYPHPQFPDVTLWDLPGAGAPGCPADKY : 124
mouse       : MATSRLPAVP--EETTILMAKEELEALRTAFESGDIPQAASRLRELLANSETTRLEVGVTGESGAGKSSLINALRGLGAEDPGAALTGVVETTMQPSPYPHPQFPDVTLWDLPGAGSPGCSADKY : 123
rat         : MATSRLPAVP-EEETTILMAKEELEALRTAFESGDIPQAASRLRELLATTETTRLEVGVTGESGAGKSSLINALRGVGAEDPGAALTGVVETTMQPSPYPHPQFPDVTLWDLPGAGSPGCSADKY : 124
guineapig*  : ------------------------------------------------------------------------------------------------------------------------- : -
squirrel    : MATSKLPSAPGEETTILMAKEELEALRTAFESGDIPQAASRLRELLAASESTRLEVGVTGESGAGKSSLINALRGLGAEDPRAALTGVVETTMQPSPYPHPQFPDVTLWDLPG----------- : 114
human       : MATSKLPVVPGEENTILMAKERLEALRTAFESGDLPQAASHLQELLASTESIRLEVGVTGESGAGKSSLINALRGLEAEDPGAALTGVMETTMQPSPYPHPQFPDVTLWDLPGAGSPGCPADKY : 125
chimpanzee  : MATSKLPVVPGEENTILMAKERLEALRTAFESGDLPQAASHLQELLASTESIRLEVGVTGESGAGKSSLINALRGLEAEDPGAALTGVMETTMQPSPYPHPQFPDVTLWDLPGAGSPGCPADKY : 125
macaque     : MATSKLPVVPGEETTILMAKERLEALRTAFESGDLPQAASHLQELLASTESTRLEVGVTGESGAGKSSLINALRGLGAEDPGAALTGVVETTMQPSPYPHPQFPDVTLWDLPGAGSPGCPADKY : 125
lemure      : MATSKLPSVPREETTILMAKEELEALRSAFESGDIPQAASRLRELLASSESAGLEVGVTGESGAGKSSLINALRGLGAEDPGAALTGVVETTMQPSPYPHPQFPDVTLWDLPGAGTPGCPADKY : 125
bushbaby*   : MATSKLRSVPREETTILMAKEELEALRTAFESGDIPQAASRLRELLASSDSTRLEVGVTGESGAGKSSLINALRGLGAEDPGAALTGVVETTIQPSPYPHPQFSDVTLWDLPGAGSPGCPADKY : 125
microbat*   : MATSK---CPGEETTILMAKEELEALRTAFESGDIPQAASRLRELLASSESTRLEVGVTGESGAGKSSLINALRGLGAEDPGAALTGVVETTMQPSSYPHPQFPDVTLWDLPGAGCPGCPADKY : 122
shrew       : ------------------------------------------------------------------------------------------QFPDVTL-DLLGAGIPRCPADKY : 22
tenrec*     : MATSRSQAGPGEETTILMAKEELEALRTAFESGDIPQAASRLRELLAASEATRLEVGVTGESGAGKSSLINALRGLGAEDPGAALTGVVETTMQPSPYPHPQFPDVTLWDLPGAGSPGCSADKY : 125
dog         : MATSKLRAVPGEETTILMAKEELEALRSAFESGDIPQAASRLRELLASSQSIRLEVGVTGESGAGKSSLINALRGVGAEDPGAALTGVVETTMQPSPYPHPQFPDVTLWDLPGAGSPGCSADKY : 125
cat         : MATSRLPAVPGEETTILMAKEELEALRTAFESGDIPQAASRLRELLASSDSTRLEVGVTGESGAGKSSLINALRGLGAEDPGAALTGVVETTVQPSPYPHPQLPDVTLWDLPGAGAPGCPADRY : 125
bull        : MATSKLPAVSGEETTILMAKEELEALRTAFESGDIPQAASRLRELLASSDCTRLEVGVTGESGAGKSSLINALRGLGAEDPDAALTGVVETTIEPSPYPHPQFPDVTLWDLPGAGSPGCSADKY : 125
pig         : MATSKLPAVPGEETTILMAKEELEALRTAFESGDIPQAASRLKQLLASSEGGRLEVGVTGESGAGKSSLINALRGLGAEDPGAALTGVVETTMTPSPYPHPQLPDVTLWDLPGAGSPGCSADKY : 125
horse       : MATSKLPAVPREETTILMAKEELEALRTAFESGDIPQAASRLRELLASSESTRLEVGVTGESGAGKSSLINALRGLGAEDPGAALTGVVETTMHPSPYPHPQFPDVTLWDLPGAGSPGCPADKY : 125
elephant    : MATSKSQVPG-EETTILMAKEELEALRTAFESGDLPQAASRLRELLASSECTRLEVGVTGESGAGKSSLINALRGLGAEDPGAALTGVVETTMQPSPYPHPQFPDVTLWDLPGAGSPGCSADKY : 124
oppossum*   : ------------------------------------------------------------------------------------------------------------------------- : -
platypus*   : ------------------------------------------------------------------------------------------------------------------------- : -
                                                                      GxxxxGKS                                             DxxG
                                                                        G1                                                 G2
```

```
                          *        140        *        160        *        180        *        200        *        220        *        240        *
armadillo*  : LKQVDFGRYDFFLLVSPRRCGAVEARLAAEILRQGKKFYFVRTKVDEDLAATRSQRPSGFSEAAVLREIRDHCAEGLRRAGLAEPRIFLVSNLSPARYDFPLLVSTWEHDLPAHRRHAGLLSLPD : 249
mouse       : LKQVDFGRYDFFLLVSPRRCGAVESRLASEILRQGKKFYFVRTKVDEDLAATRSQRPSGFSEAAVLQEIRDHCTERLRVAGVNDPRIFLVSNLSPTRYDFPMLVTTWEHDLPAHRRHAGLLSLPD : 248
rat         : LKEVDFGRYDFFLLVSPRRCGAVETRLASEILRQGKKFYFVRTKVDEDLAATRNQRPSGFSEAAVLQEIRDHCAERLRAAGLSDPRIFLVSNLSPNRYDFPMLVTTWEHDLPAHRRHAGLLSLPD : 249
guineapig*  : ------------------------------------GKKFYFVRTKVDEDLAATRTQRPSGFSEATVLHEIRDHCAERLRAVGVSDPRIFLVSNLSPTRYDFPTLVSTWEHDLPAHRRHAGLLSLPD : 91
squirrel    : ------------------------------------------------------------------------------------------------------------------------- : -
human       : LKQVDFSRYDFFLLVSPRRCGAVETRLAAEILCQGKKFYFVRTKVDEDLAATRTQRPSGFREAAVLQEIRDHCAERLREAGVADPRIFLVSNLSPARYDFPTLVSTWEHDLPSHRRHAGLLSLPD : 250
chimpanzee  : LKQVDFSRYDFFLLVSPRRCGAVETRLAAEILCQGKKFYFVRTKVDEDLAATRTQRPSGFREAAVLQEIRDHCAERLREAGVADPRIFLVSNLSPARYDFPTLVSTWEHDLPSHRRHAGLLSLPD : 250
macaque     : LKQVDFSRYDFFLLVSPRRCGAVETRLAAEILCQGKKFYFVRTKVDEDLAATRSQRPSGFREAAVLQEIRDHCAERLREAGVAEPRIFLVSNLSPARYDFPTLVSTWEHDLPAHRRHAGLLSLPD : 250
lemure      : LKQVDFSRYDFFLLVSPRRCGAIESRLASEILRQGKKFYFVRTKVDEDLAATRSQRPSGYSEVIVQEIRDHCVDRLRAAGVADPRVFLVSNLSPSRYDLPLLMSTWEHDLPAHRRHAGLLSLPD : 250
bushbaby*   : LKQVDFSRYDFFLLVSPRRCGAVESRLATEILRQGKKFYFVRTKVDEDLAATRTQSPSGYSELAVLQEIRDHCA-RLRAAGVSDPRIFLVSNLSPTRYDFPVLVSTWEHDLPAHRRHACLLSLPD : 249
microbat*   : LKQVDFGRYDFFLLVSPRRCGAVEARLASEILRQGKKFYFVRTKVDEDLAATRSQRPSGFSESMVLQEIRDHCTERLRAAGVTDPRIFLVSNLWPVRYDFPLLLSTWEHDLPAHRRHAGLLSLPD : 247
shrew       : LKQVDFSRYDFFLLVSPRRCGAVETRLASEILRQGKKFYFVRTKVDEDLAATRSQRPSVFSEGLVLQEIREHCVERLRAAGVAEPRIFLVSNLSPSRYDFPLLMSTWEHDLPAHRRHAGLLSLPD : 147
tenrec*     : LKQVDFGRYDFFLLVSPRRCGAVESRLAAEILRQGKKFYFVRTKVDEDLAATRSQRPSAFSEAAVLQEIREHCTERLRAAGV--------------------------------------- : 207
dog         : LKQVDFGRYDFFLLVSPRRCGAVETRLASEILRQGKKFYFVRTKVDEDLAATRTQRPSGFSEAAVLQEIRDHCAERLRVAGMTDPRIFLVSNLSPARYDFPLLVSTWEHDLPAHRRHAGLLSLPD : 250
cat         : LKQVDFGRYDFFLLVSARRCGAVETRLASEILGQGKKFYFVRTKVDEDLAATRAQRPSGFSEATVLQEIRDHCAERLRAAGVADPRIFLVSNLSPARYDFPLLVSTWEHDLPAHRRHAGLLSLPD : 250
bull        : LKQVDFGRYDFFLLVSPRRCGAVETRLASEILRQGKKFYFVRTKVDEDLAATRMQRPSGFSEGAVLHEIREHCVERLRGAGVHDPRVFLVSNLSPARYDFPLLMSTWERDLPAHRRHAGLLSLPD : 250
pig         : LKQVDFGRYDFFLLVSPRRCGAVETRLASEILRQGKKFYFVRTKVDEDLAASRTQRPSGFSEAAVLQEIREHCAERLRAAGVSDPRIFLVSNLSPARYDFPLLVSTWEHDLPAHWRHAGLLSLPD : 250
horse       : LKQVDFGRYDFFLLVSPRRCGAVETRLASEILRQGKKFYFVRTKVDEDLAATRTQRPSGFSEAAVLQEIREHCAERLRVAGVTDPRIFLVSNLSPVRYDFPLLVSTWEHDLPAHRRHAGLLSLPD : 250
elephant    : LKQVDFGRYDFFLLVSPRRCGAVESRLASEILRQGKKFYFVRTKVDEDLAATRTQRPSGYSEAAVLQEIRDHCVERLRAAGMSDPRIFLVSNLSPARYDFPLLMSTWEHDLPAHRRHAGLLSLPD : 249
oppossum*   : ------------------------------------------------------------------------------------------------------------------------- : -
platypus*   : ----------------------LAGEVLRQGKRFYFVRTKVDEDLAASRSQRPSGYCEGAVLQEIRDHCSERLRLAGVAEPRVFLVSNLAPARFDFPLLVSTWERELPAHRRHAGLLSLPD : 99
                                                            N/TxxD
                                                              G4
```

```
                260        *        280        *        300        *        320        *        340        *        360        *
armadillo*   : ISLE------------------------------------------------------------------------------------------------------------------ : 253
mouse        : ISLEALQKKKDMLQEQVLKTALVSGVIQALPVPGLAAAYDDALLIRSLRGYHRSFGLDDDSLAKLAEQVGKQAGDLRSVIRSPLANEVSPEIVLRLYSQSSDGAMRVARAFERGIPVFGTLVAGG : 373
rat          : ISLEALQKKKDMLQEQVLKTALVSGVIQALPVPGLAAAYDDALLIRSLRGYHRSFGLDDDSLAKLAEQVGKQAGDLRSVIRSPLANEVSPEIVLRLYSQSSDGAMRVARAFERGIPVFGTLVAGG : 374
guineapig*   : ISLEALQKKKDMLQEQVLKTALVSGVIQALPVPGLAAAYDDALLIRSLRGYHRSFGLDDDSLAKLAEQVGKQAGDLRSVIRSPLANEVSPEIVLRLYSQSSDGAMRVARAFERGIPVFGTLVAGG : 216
squirrel     : ------------------------------------------------------------------------------------------------------------------------ : -
human        : ISLEALQKKKAMLQEQVLKTALVLGVIQALPVPGLAAAYDDALLIHSLRGYHRSFGLDDDSLAKLAEQVGKQAGDLRSVIRSPLANEVSPEIVLRLYSQSSDGAMRVARAFERGIPVFGTLVAGG : 375
chimpanzee   : ISLEALQKKKAMLQEQVLKTALVLGVIQALPVPGLAAAYDDALLIHSLRGYHRSFGLDDDSLAKLAEQVGKQAGDLRSVIRSPLANEVSPEIVLRLYSQSSDGAMRVARAFERGIPVFGTLVAGG : 375
macaque      : ISLEALQKKKAMLQEQVLKTALVLGVIQALPVPGLAAAYDDALLIHSLRGYHRSFGLDEDSLAKLAEQVGKQAGDLRSVIRSPLANEVSPEIVLRLYSQSSDGAMRVARAFERGIPVFGTLVAGG : 375
lemure       : ISLEALQKKKDMLQEQVLKTALVSGVIQALPVPGLAAAYDDALLIRSLRGYHRSFGLDEDSLAKLAEQVGKQAGDLRAVMRSPLANEVSPEAVLRLYSQSSYGAMRVARAFEKGIPVFGTLVAGG : 375
bushbaby*    : ISLEALQKKKDMLQEQVLKTALVSGVIQALPVPGLAAAYDDALLVRSLRGYHRSFGLDDDSLAKLAEQVGKQAGDLRSVIRSLLDNEVSPETVLRLYSQSSYGAMRVARAFEKGIPVFGTLVAGG : 374
microbat*    : ISLEALQRKGDMLQEQVLKTAL-----------------------------------------------------------SPETVLRLYSQSFDGAMRVARAFERGIPVFGTLVAGG : 306
shrew        : ISLEALQKKKDMLQEQVLKTALVSGVIQALPVPGLAAAYDDALLVRSLRGYHRSFGLDDDSLARLAEQVGKQAGDLRSVIRSPLAVEVNPETVLRLYARSSDGAMRVARAFERGVPVFGTLVASG : 272
tenrec*      : ------------------------------------------------------------------------------------------------------------------------ : -
dog          : ISLEALQKKKDMLQEQVLKTALVSGVIQALPVPGLAAAYDDALLIRSLRGYHRSFGLDDDSLAKLAEQVGKQAGDLRSVIRSPLANEVSPETVLRLYSQSSDGAMRVARAFERGIPVFGTLVAGG : 375
cat          : ISLEALQKKKDMLQEQVLKTALVSGVIQALPVPGLAAAYDDALLLRSLRGYHRSFGLDDDSLAKLAEQVGKQAGDLRSVIRSPLANEVSPETVLRLYSQSSDGAMRVARAFERGIPVFGTLVAGG : 375
bull         : ISLEALQKKKDMLQEQVLKTALVSGVIQALPVPGLAAAYDDALLIRSLRGYHRSFGLDDDSLAKLAEQVGKQAGDLRSVIRSPLANEVSPETVLRLYSQSSDGAMRVARAFEKGIPVFGTLVAGG : 375
pig          : ISLEALQKKKDMLQEQVLKTALVSGVIQALPVPGLAAAYDDALLIRSLRGYHRSFGLDDDSLAKLAEQVGKQAGDLRSVIRSPLANEVSPETVLRLYSQSSDGAMRVARAFEKGIPVFGTLVAGG : 375
horse        : ISLEALQKKKDMLQEQVLKTALVSGVIQALPVPGLAAAYDDALLIRSLRGYHRSFGLDDDSLAKLAEQVGKQAGDLRSVIRSPLASELSPETVLRLYSRSSDGAMRVARAFEKGIPVFGTLVAGG : 375
elephant     : ISLEALQKKKDMLQEQVLKTALVSGVIQALPVPGLAAAYDDALLVRSLRGYHRSFGLDDDSLAKLAEQVGKQAGDLRSVIRSPLANEVSPETVLRLYSQSSDGAMRVARAFEKGIPVFGTLVAGG : 374
oppossum*    : --------------------------------------------------------------------------------------GIPVFGDTSGGR : 12
platypus*    : VSLRALQEKKDALQDQVLKAALVSGVIQALPVPGLAAAYDDALLVRSLRGYHRSFGLDDDSLARLAEQVGKPAGDLRAVIRSPLAAEVSSDAVLRLYSQASSGAMRVARAFERGVPVFGTLVAGG : 224


                380        *        400        *        420        *        440        *        460
armadillo*   : ------------------------------------------------------------------------------- : -
mouse        : ISFGTVYTMLQGCLNEMAEDAQRVRIKALEEDEPQGGEVSLEAAGDNLVEKRSTGEGTSEEAPLSTRRKLGLLLKYILDSWKRRDLSEDK : 463
rat          : ISFGTVYTMLQGCLNEMAEDAQRVRIKALEEDET-QGEVSLEAAGDNAVEKRSSGEGTSEEAPLSTRRKLGLLLKYILDSWKRRDLSEDK : 463
guineapig*   : ISFGTVYTMLQGCLNELAEDAQRVRIKALEEDEP-QPEISLEAAGDNSVEKRVTGEAGGEEGQLTTRRKLGLLLKYVLESWKKRDL-EEK : 304
squirrel     : ------------------------------------------------------------------------------- : -
human        : ISFGAVYTMLQGCLNEMAEDAQRVRIKALEDDEP-QPEVSLEVASDNGVEKGGSGEGGGEEAPLSTCRKLGLLLKYILDSWKKHD-SEEK : 463
chimpanzee   : ISFGAVYTMLQGCLNEMAEDAQRVRIKALEDDEP-QPEVSLEVASDNGVEKGGSGEGGGEEAPLSTCRKLGLLLKYILDSWKKHD-SEEK : 463
macaque      : ISFGAVYTMLQGCLNEMAEDAQRVRIKALEEDES-QPEVGLEAAGDNGVEKGGSGEGGSEEAPLSTRRKLGLLLKYILDSWKKHD-SEEK : 463
lemure       : ISFGTVYTMLQGCLNEMAEDAQRVRIKALEEDES-QAEVGLEAAGDGGVEKRGSGEGGGEEAPVSVRRKLGLLLKYILDSWKKRDL-EEK : 463
bushbaby*    : ISFGTVYTMLQGCLNELAEDAQRVRIKAL------------------------------------------------- : 403
microbat*    : ISFGTVYTMLQGCLNEMAEDAQRVRIKALEEAFESQPEVSLDAAGDNGVEKCGVGEGGGEEAPLSTRRKLGLLLKYILDSWKKRDL-EEK : 395
shrew        : ISFGTVYAMLQGCLNEMAEDAQRVRIKALEEDEA-PSEVSLEAGGDVGVEKHGLGESGSEDAPLSTRRKLGLLLKYILD----------- : 350
tenrec*      : ------------------------------------------------------------------------------- : -
dog          : ISFGTVYTMLQGCLNEMAEDAQRVRIKALEEDEP-QSEVSLEAAGDNGVEKRGSGEGGCEEAPLSARRKLGLLLKYILDSWKKRDLSEEK : 464
cat          : ISFGAVYTMLQGCLNEMAEDAQRVRIKALEEDEP-RPSVSLEAAGDNGVEKRVSGEGTCEEAPLSTRRKLGLLLKYILDSWKKRDLLEDK : 464
bull         : ISFGTVYTMLQGCLNEMAEDAQRVRIKALEEDTQPDVSLEAAGDNGVEKRGSGEGSMEEAPLSTRRKLGLLLKYILDSWKKRDLAEDK : 465
pig          : ISFGTVYTMLQGCLNEMAEDAQRVRIKALEEDEP-QPPVSLEAAGDNGVEKRGSREGSCEEAPLSARRKLGLLLKYILDSWKKRDLSEDK : 464
horse        : ISFGTVYTMLQGCLNEMAEDAQRVRIKALEEDEP-QSEVSLEAAGDNGVEKRASGEGVSEEAPLSARRKLGLLLKYILESWKKRDLSEEK : 464
elephant     : ISFGTVYTMLQGCLNEMAEDAQRVRIKALEEDEP-QPQLSLEAAGDSGVEKRGSGEGGSEEAPLSARRKLGLLLKYILDSWKKRDLSEEK : 463
oppossum*    : HLLGTVYTMLQGCLNEMAEDAQRVRIKAM------------------------------------------------- : 41
platypus*    : ISFGTIYTMLQGCLNEMAEDARRVRVKALED------------------------------------------------ : 255
```
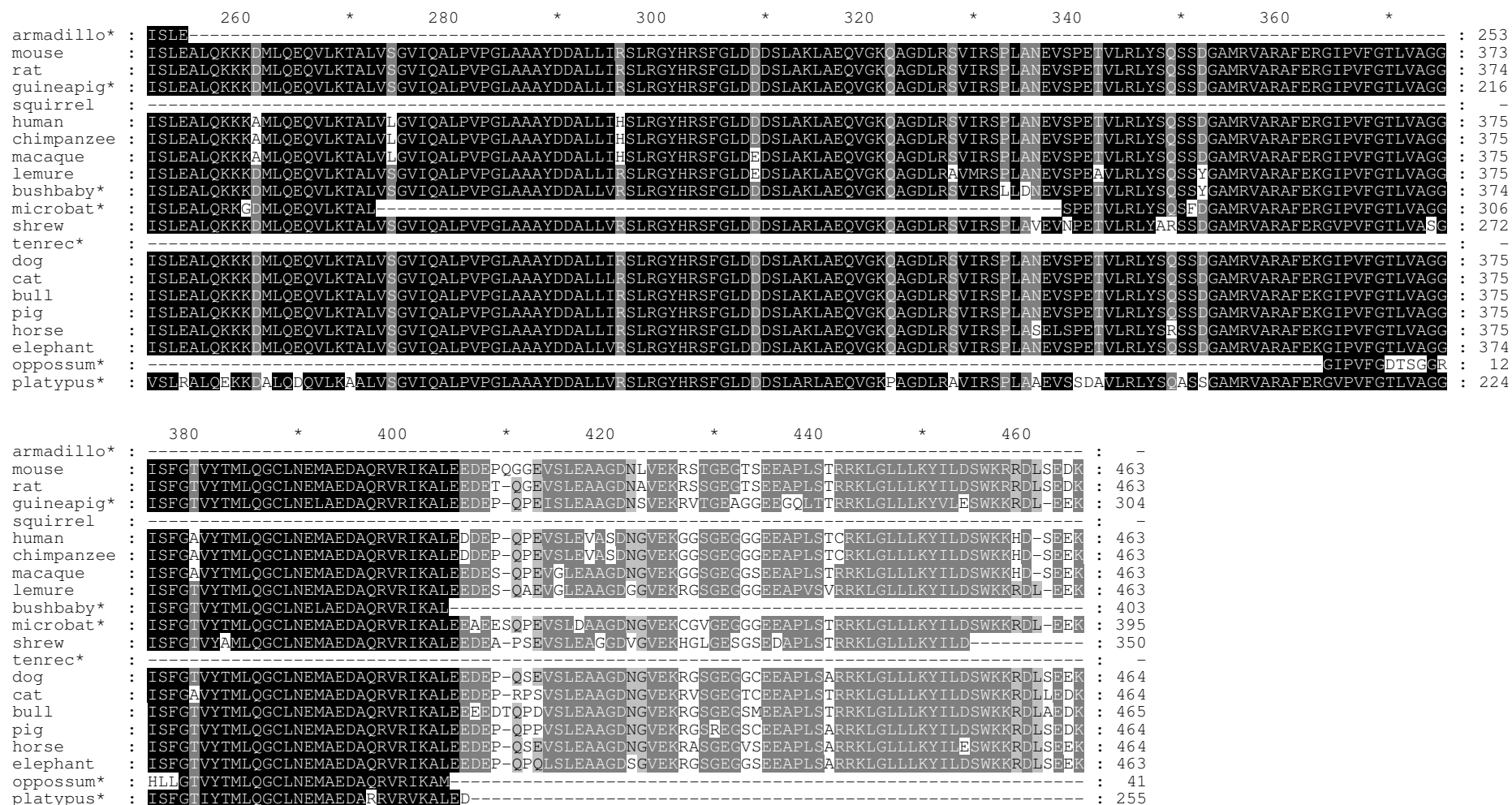
Figure 9. **Alignment of amino acid sequences of all detected Irgc orthologues. .** Amino acid sequences of all 21 Irgc proteins. * indicates incomplete sequences. Conserved canonical GTP-binding motifs G1, G3 and G4 are indicated by red boxes. Shading: black: 75% identity, dark grey: 60%, light grey: 50%. Accession Numbers for all sequences are presented in Table 8

Table 9. **Amino acid identities and similarities between full length Irgc proteins.** Identity and similarity matrix between all full length IRGC sequences was generated by GeneDoc. Each sequence is compared to every other sequence generating three numbers. The upper number represents identical residues, the number in the middle similar residues or conservative substitutions, the lower number residues with gap character. In the white area absolute numbers are given, in the grey shaded area relative values in percent. The diagonal in dark grey shows the sequence length.

	mouse	rat	Human	chimp-anzee	ma-caque	dog	cat	bull	pig	horse	ele-phant
mouse	463	96% 98% 0%	89% 92% 0%	89% 92% 0%	90% 93% 0%	93% 96% 0%	92% 95% 0%	91% 96% 0%	92% 96% 0%	93% 97% 0%	92% 96% 0%
rat	447 455 2	463	89% 93% 0%	89% 93% 0%	91% 94% 0%	93% 96% 0%	92% 96% 0%	91% 96% 0%	93% 96% 0%	93% 97% 0%	92% 96% 0%
human	415 431 4	417 433 2	463	100% 100% 0%	96% 97% 0%	91% 94% 0%	90% 93% 0%	88% 92% 0%	90% 93% 0%	90% 93% 0%	90% 93% 0%
chimpanzee	415 431 4	417 433 2	463 463 0	463	96% 97% 0%	91% 94% 0%	90% 93% 0%	88% 92% 0%	90% 93% 0%	90% 93% 0%	90% 93% 0%
macaque	421 435 4	423 440 2	447 453 0	447 453 0	463	92% 94% 0%	91% 94% 0%	89% 93% 0%	90% 93% 0%	91% 94% 0%	91% 94% 0%
dog	433 449 3	435 450 1	426 439 1	426 439 1	427 440 1	464	93% 96% 0%	93% 95% 0%	95% 97% 0%	96% 98% 0%	95% 97% 0%
cat	431 445 3	431 448 1	420 436 1	420 436 1	424 440 1	434 447 0	464	92% 95% 0%	93% 96% 0%	92% 96% 0%	92% 95% 0%
bull	427 447 2	427 448 2	412 431 2	412 431 2	417 435 2	434 446 1	429 444 1	465	93% 96% 0%	92% 95% 0%	92% 96% 0%
pig	431 447 3	433 449 1	420 434 1	420 434 1	422 436 1	441 453 0	434 448 0	436 447 1	464	94% 96% 0%	94% 97% 0%
horse	435 453 3	434 454 1	421 435 1	421 435 1	425 439 1	446 457 0	431 447 0	432 445 1	440 450 0	464	93% 97% 0%
elephant	431 449 2	430 449 2	420 436 2	420 436 2	424 440 2	442 454 1	427 445 1	432 448 2	437 451 1	435 451 1	463

IRG genes have also been detected in reptiles, amphibians and fish (Bekpen 2005, Julia Hunn personal communication). For the last two classes a homologue of *IRGC* is not clearly recognizable, but a putative *IRGC* orthologue with the preliminary name AC GKS10 is present in the reptile *Anolis carolinensis* (Accession Nr. AAWZ01048015) (Julia Hunn personal communication). The retrieved sequence of AC GKS10 is truncated relative to other IRG proteins, although at the moment it can not be excluded that this truncation is the result of computational error based on too little sequence information. In the phylogenetic analysis it locates close to the IRGC genes. But it was excluded from the tree in Figure 10 because it distorts the overall structure of tree. In order to investigate whether IRGC is indeed the closest relative of AC GKS10 it was aligned with different other IRG proteins and searched for conserved sequence features. The alignment included mouse and human IRGC, IRGC-like proteins from the cat and opossum and mouse Irga6, Irgb6 and Irgd. Some sequence features were conserved only between IRGC and AC GKS10 as indicated in the alignment in Figure 11. Even more features were conserved between IRGC, IRGC-like and AC GKS10. Interestingly, AC GKS10 and IRGC-like proteins have an S in the G4 motif of the G domain,

changing it to SxxD instead of N/TxxD. In a phylogenetic analysis the AC GKS10 locates closer to IRGC than IRGC-like (Figure 12). Thus *AC GKS10* is clearly related to the *IRGC* and *IRGC-like* genes. However, the question whether AC GKS10 is closer related to IRGC or IRGC-like can not be answered. The retrieved sequence of AC GKS10 is truncated relative to the other IRG proteins. This may reflect the reality although it can not be excluded yet that this truncation is the result of a computational error based on too little sequence information.
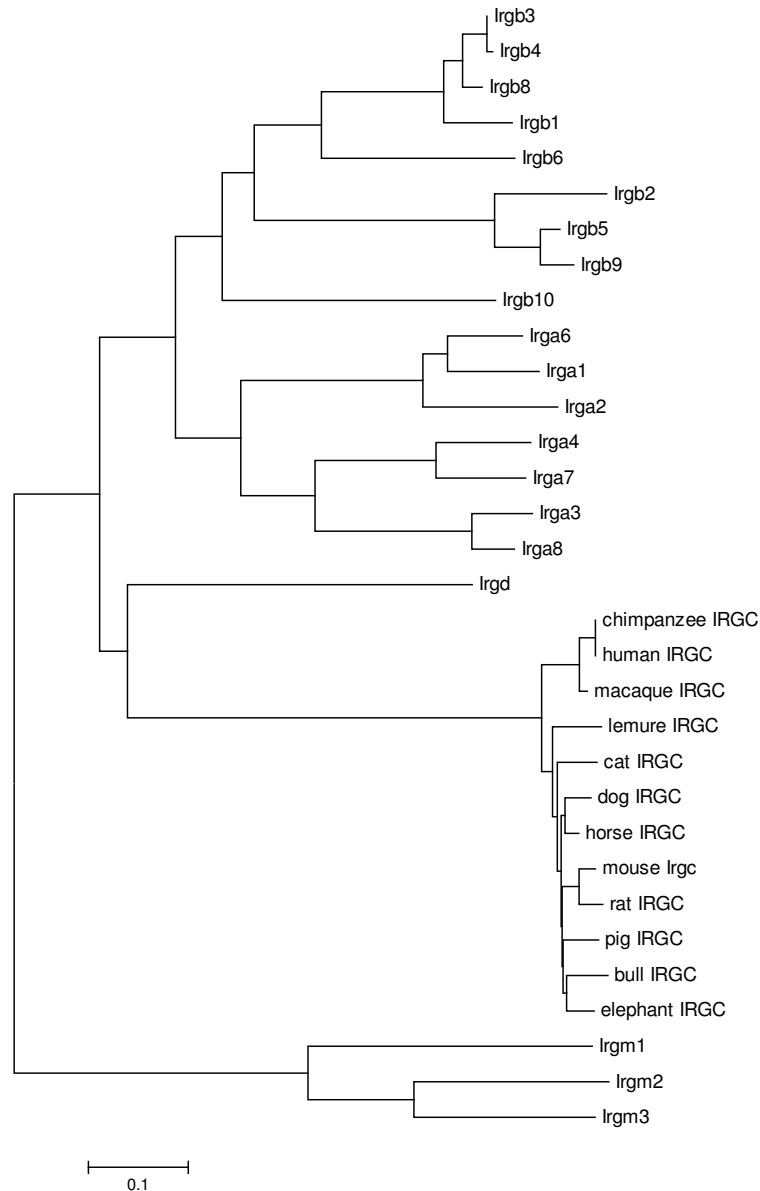
Figure 10. **Phylogenetic relationship between mammalian IRGCs and mouse IRGs.** Phylogenetic tree based on the amino acid sequence of the GTP-binding domain of the indicated proteins. The tree is based on neighbour-joining method with Poisson correction and was conducted with the MEGA 4 software (Tamura 2007).
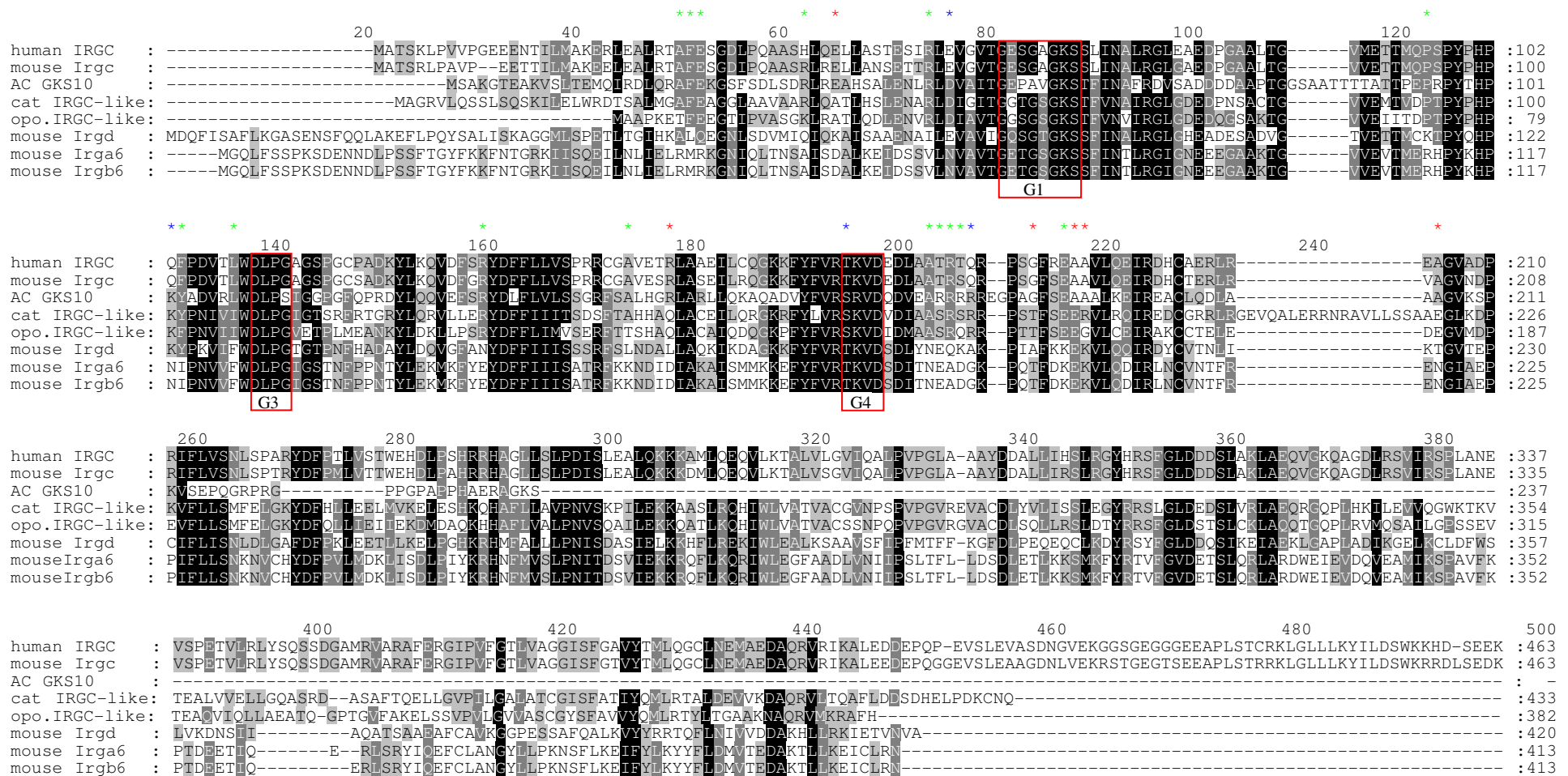
Figure 11. **Alignment of AC GKS10 from *Anolis caroliensis* to diverse other IRG proteins**. Amino acid sequences of IRGC from mouse and human, IRGC-like from cat and opossum (opo.) and mouse Irga6, Irgb6, Irgd. Conserved canonical GTP-binding motifs are indicated by red boxes. * indicates amino acid conserved only between IRGC and AC GKS10, * only between IRGC-like and GKS10 and * between only IRGC, IRGC-like and AC GKS10. Shading: black 85% identity, dark grey: 67%, light grey: 37%
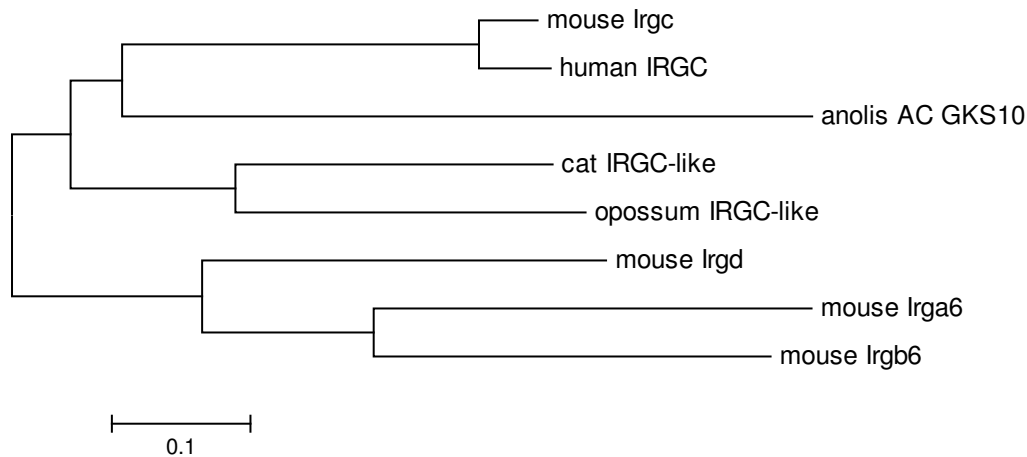
Figure 12. **Phylogenetic relationship between AC GKS10, IRGC and IRGC-like proteins.** Phylogenetic tree based on the amino acid sequence of the GTP-binding domain of the indicated proteins. The tree is based on neighbour-joining method with Poisson correction and was conducted with the MEGA 4 software (Tamura 2007).

3.2 Structure of the Irgc gene

A typical IRG gene consists of a long 3'-exon containing the complete open reading frame and one or more short untranslated 5'-exons (Bekpen 2005). Mouse Irgc is structured in the same pattern.

The 3'-Exon called Exon 2 contains the complete open reading frame with a size of 1392 to 1398 bp. It is flanked by short 5'- and 3'-untranslated regions (UTR). The distance between the stop codon and the start of the poly(A) tail is only 56 bp in the mouse and 62 bp in humans. Very short 3'-UTRs are a common feature of haploid-specific transcripts (Liu 2007). One interesting feature found in primates, rodents, marsupials and monotremates is that the stop codon TAA is part of the poly(A) signal AATAAA. In carnivores, artiodactyls, perissodactyls and proboscideans, that is not the case. Therefore 2 kb downstream of the stop codon was searched for a putative poly(A) signal, but for cat, dog, bull and elephant no signal was detected. Only in the horse the poly(A) signal ATTAAA was detected 1359 bp downstream of the respective stop codon. The consequence of the usage of this site for polyadenylation would be a very long 3'-UTR compared to the other mammals. Therefore it seems unlikely that this site is used, but can not be excluded yet. For the other mammalian orders no sequence information is yet available about the stop codon of IRGC. Which signal is responsible for the polyadenylation of IRGC mRNA in the species without a conserved poly(A) signal is unknown. However, it has to be recognized that in germ cells, and especially in IRGC-expressing round spermatids, approximately 30% of all polyadenylated transcripts lack the consensus sequence AATAAA or ATTAAA (MacDonald 2002, Liu 2007).
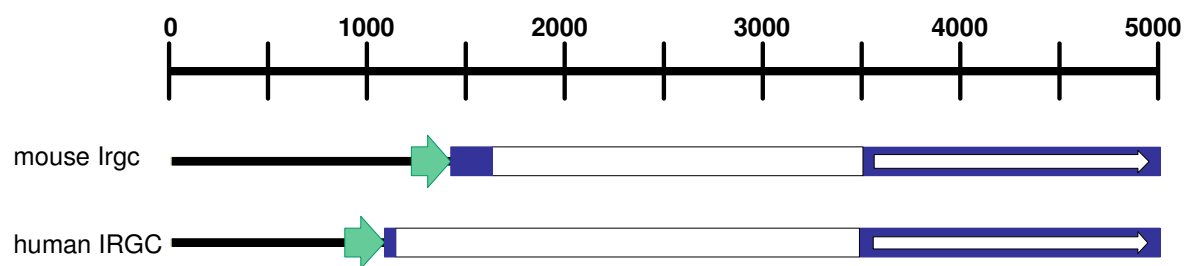
Species	Exon 1	Intron	Exon 2	3'-UTR
mouse	210	1875	1503	56
rat	176	1972	1535	87
cat	41	1494	1499*	no data
dog	44	1488	1498*	no data
bull	80	2316	1551	62
human	57	2350	1520	62
chimpanzee	57	3100	1520	62

Figure 13. **Genomic structure of mouse Irgc and human IRGC.** Exon: blue block, Intron: white block, ORF: white arrow, promoter region: green arrow. The table presents the length in bp of the exons, introns and mRNA of Irgc from different species. The * marks Exon 2 without any information on the 3'-UTR. These exons are most probably longer than the given number. Length of 3'-UTR defined as distance between stop codon and start poly(A) tail. Data derived from ESTs and the Ensembl databases.

The structure of the exon-intron junction of mouse, rat, human, chimpanzee, bull, dog and cat could be resolved. For IRGC from mouse, rat, human, chimpanzee and bull the untranslated 5'-exon, also called Exon 1, could be identified by the alignment of ESTs to the genomic DNA and cDNA clones from the Ensembl databases. Except for chimpanzee the splicing site was verified by RT-PCR on RNA derived from testis of the respective species using primers located in different exons (Figure 25). In Figure 13 the structure of the mouse Irgc and human IRGC gene are shown. From cat and dog no ESTs covering the 5'-exon and the splicing site between the two exons were available. However, the 5'-exon from IRGC of cat and dog were deduced from alignments of Exon 1 of mouse and human to the genomic sequence upstream of the cat or dog Irgc ORF. Interestingly, the same transcription factor binding sites – Sox5, Sox17, NF-Y - as in the other species are located directly upstream of the putative Exon 1 of cat and dog, respectively. That the suggested sequence was indeed part of the 5'-exon of cat and dog, respectively, was verified by RT-PCR on testis RNA from both species (Figure 25). The 5'-exon of mouse and rat differ in size drastically from the other species, as shown in the alignment of the promoter and the 5'-exon in Figure 14. In these two species the exon runs through the splicing site used in the other species and splices 145 bp (mouse) or 147 bp (rat) further downstream, so that the length of the 5'-exon is with 210 bp and 176 bp, respectively,

three to five times longer than in the other species. The starting point of transcription is not defined for all species. In Figure 14 the most 5'-positioned base, which is confirmed to be part of Exon 1, is marked in red. Hence, it is tempting to speculate that the transcription starts at the same base in all species, as the strong conservation of the sequence containing the promoter and the Exon 1 suggests.

The length of the intron varies to some extent with the shortest intron to be found in the dog (1488 bp) and the longest in the chimpanzee (3100 bp), but it is always in the same range of length.
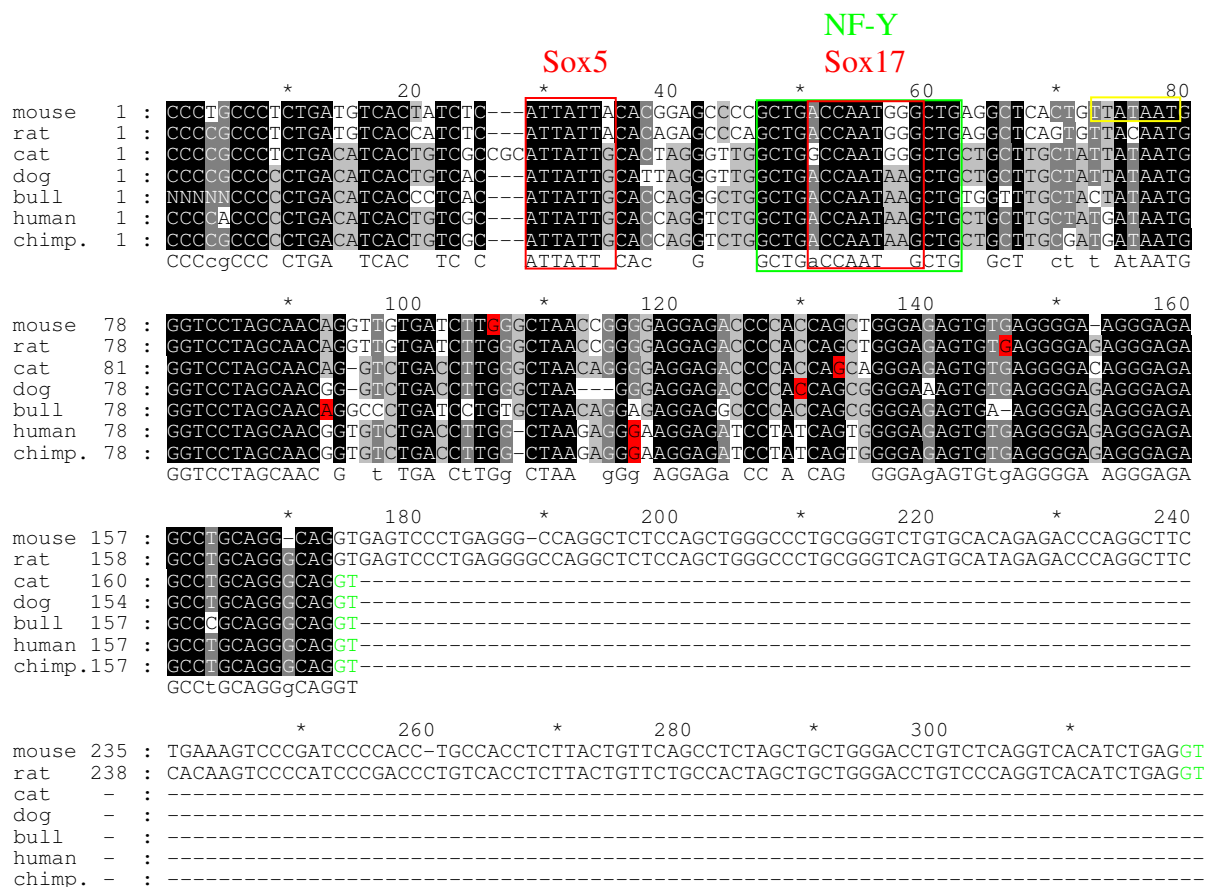
Figure 14. **Alignment of promoter and Exon 1.** Sequences covering the proximal promoter region and Exon 1 from mouse, rat, cat, dog, bull, human and chimp were aligned. Conserved transcription factor binding sites Sox5, Sox17, NF-Y are indicated. Most upstream positioned base verified by ESTs or RT-PCR to be transcribed are marked red. Green coloured bases are the first two bases of the intron. Putative TATA-box in the mouse Irgc promoter reported by Rohde 2003 is indicated by the yellow box.

3.3 Promoter

Induction by interferon-γ is an important functional property of most IRG genes. This induction is mediated by ISRE and GAS sites located in the promoter of these genes (Bekpen 2005). In contrast, the IRGC promoters from mouse, rat, cat, dog, bull, human and chimpanzee do not contain any element responsible for interferon induction. Neither ISRE nor GAS sites were found up to 10 kb 5' of the putative transcription start.

The promoter regions of IRGC from mouse, rat, cat, dog, bull, human and chimpanzee were compared to each other to identify putative conserved transcription-factor binding sites. The analysis was performed with ConSite, a bioinformatics tool searching for conserved binding sites on the basis of phylogenetic footprinting (Lenhard 2003, Sandelin 2004), and the Transcriptional Element Search System TESS (Schug 1997). A region of approximately 100 bp directly upstream of the Exon 1 harbours three conserved binding sites: Nuclear Factor-Y (NF-Y), Sox5 and Sox17 (Figure 14). All three sites are highly conserved between all seven species, although the two Sox sites are not perfect consensus sites for their corresponding transcription factors. The core consensus site for Sox5 is 5'-AACAAT-3' (+ strand) (Denny 1992), but in the IRGC promoter the C at position 3 is replaced by a T. Nevertheless this changed sequence 5'-ATTATT-3' (-) can still be recognized by Sox-5 (Denny 1992). The same can be observed for the Sox17 binding site. Differing from the consensus sequence 5'-C/TATTGT-3' (+) (Kanai 1996) the Sox17 site in the Irgc promoter is 5'-C/TATTGG-3' (-). But also for this altered site binding of Sox17 was demonstrated (Kanai 1996).

Both Sox transcription factors are expressed in haploid spermatids in the testis and seem to play a role in the regulation of spermatogenesis (Denny 1992, Kanai 1996), but they are not testis-specific. L-Sox5, a long form of Sox5, was shown to be involved in the differentiation of chondrocytes that form cartilage (Lefebvre 1998, Smits 2001). Sox17 is essential in early endoderm development (Kanai-Azuma 2002, Tam 2003) and stimulates the differentiation of oligodendrocyte progenitor cells (Sohn 2006) and angiogenesis in liver and kidney (Matsui 2006).

The third transcription factor binding site present in all IRGC promoters is NF-Y. It recognizes the 5'-CCAAT-3' motif (Dorn 1987), which is located in the same position as the Sox17 binding site. In contrast to the two Sox sites NF-Y is a universal transcription factor. The CCAAT-box is present in approximately 30 % of all eukaryotic promoters (Bucher 1990). NF-Y functions always together with at least one other transcription factor. For example interaction of NF-Y with RF-X (Reith 1994), SP-1 (Wright 1995), SREBP1 (Jackson

1998) and Sox7/Sox17 (Niimi 2004) has been demonstrated. In the IRGC promoter an interaction between Sox17 and NF-Y is unlikely, because they bind at the same position.

The putative TATA-box in the murine promoter reported in my Diploma thesis (Rohde 2003) is not well conserved and can be found only in mouse, cat and dog, but is disrupted by different substitutions in rat, bull, human and chimp. Thus, it is questionable if this TATA-box is relevant for the transcriptional regulation of Irgc, because it is known that promoters of testis-specific genes often do not contain a TATA-box (Welch 1995, Somboonthum 2005). The location of the CCAAT-box argues against a functional TATA-box. In TATA-box containing promoters a NF-Y binding CCAAT-box in forward direction is preferentially located between -100 and -80 and never closer than -62 (referring to the first C in the CCAAT) from the transcription start (Montavani 1998), but in the mouse it is located at position -54. This is in agreement with the location of the CCAAT-box in TATA-less promoters, which is between -41 and -80 (Montavani 1998).

3.4 Expression pattern of Irgc

3.4.1 Expressed Sequence Tags (ESTs)

The expression pattern of IRGC was analysed by different methods looking for the RNA message as well as the protein product of the gene.

All public available databases were searched for ESTs of IRGC. In total 213 ESTs from eight different species were detected (Table X). With 151 ESTs (70,9%) the major part of these ESTs originate from the testis, including the ESTs from *Homo sapiens* from the Pool lung-testis-B-cells and germ cell tumors. ESTs from testis were found in all species except *Bos taurus*, where only ESTs from the liver were available. Other organs containing Irgc ESTs are ovary (20 ESTs, 9,4%), brain (14 ESTs, 6,6%), liver (7 ESTs, 3,3%), dendritic cells (6 ESTs, 2,8%), placenta (4 ESTs, 1,9%) and lung (1 EST, 0,5%). A complete list of all ESTs is presented in Appendix II.

Table 10: **List of ESTs from IRGC.** a) ESTs listed by species and organ. Percentage values referring to each species separately. b) ESTs from all species taken together and listed by organ. Values in (…) depending on how the Pool lung, testis, B-cells from human is counted.

a

Species	Tissue	Number of ESTs	Percentage
Mus musculus	testis	25	67,6
	dendritic cells	6	16,2
	pool	5	13,5
	unknown	1	2,7
	total *Mus musculus*	37	
Homo sapiens	pool lung, testis, B-cells	27	37,5
	testis	21	29,2
	germ cell tumors	4	5,6
	epididymis	1	1,4
	brain - medulla	12	16,7
	brain - hippocampus	1	1,4
	brain - glioblastoma	1	1,4
	placenta	4	5,6
	lung	1	1,4
	total *Homo sapiens*	72	
Bos taurus	liver	7	100
Canis familiaris	testis	14	100
Felis catus	testis	1	100
Macaca nemestrina	testis	24	54,5
	ovary	20	45,5
Rattus norvegicus	testis	21	100
Sus scrofa	testis	14	100
Total		213	

b

Tissue	Number of ESTs	Percentage
testis	124 (151)	58,2 (70,9)
ovary	20	9,4
brain	14	6,6
liver	7	3,3
dendritic cells	6	2,8
placenta	4	1,9
lung	1 (28)	0,5 (13,1)
epididymis	1	0,5
B-cells	0 (27)	0,0 (12,6)
pool / unknown	6	2,8
Total	213	

3.4.2 Testis-specific expression of mouse Irgc

In order to find out in which organs Irgc is transcribed and mRNA is produced, a multi-tissue Northern blot was performed using the [α-^{32}P]dATP labelled mouse Irgc-ORF as probe. The only tissue generating a signal was the testis, where a band with a size of approximately 2 kb was detected (Figure 15). The signal corresponds to the length of both Irgc exons (1713 bp) and the poly(A)-tail. In all other tissues Irgc mRNA was not detected. The integrity of the RNA on the blot was demonstrated by using a probe for GAPDH. Bands at the expected size of 1,2 kb with different intensities were detected in all tissues.
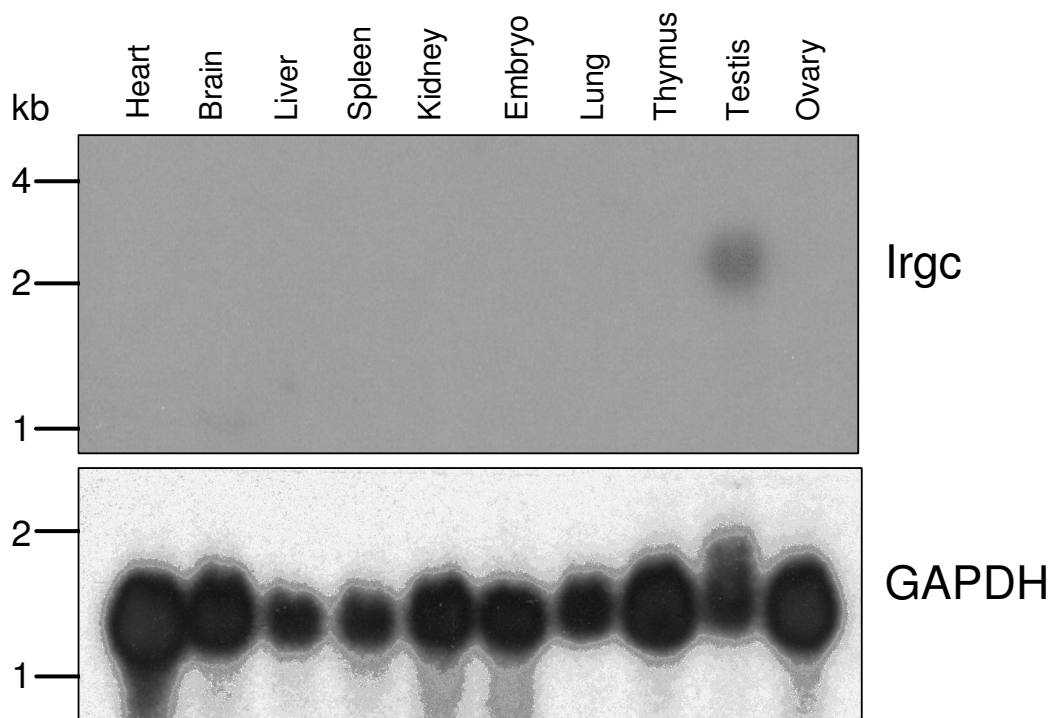
Figure 15. **mRNA of Irgc is detected only in testis.** Using the [α-^{32}P]dATP labelled Irgc ORF as a probe, a multi tissue Northern blot was performed. The autoradiography shows only a signal in the testis with a size of approximately 2 kb. Integrity of mRNA was tested by using a GAPDH specific probe, which generated a signal in all samples.

Whether the mRNA is translated into protein had to be shown by Western blot analysis. Therefore different organs from adult 8 to 12 weeks old C57BL/6J mice were lysed in RIPA buffer and analysed by Western blot with the Irgc-specific antiserum α-CIN 39/3° (Rohde 2003). As in the Northern blot, Irgc could be detected only in the testis (Figure 16). The generated signal runs at a size of approximately 55 kDa, which is bigger than the calculated molecular weight of 50,6 kDa. Additionally the blot was probed with an antibody against the ER-protein Calnexin to demonstrate proper lysis and loading of the sample. The lower Calnexin band seen in kidney, liver, testis and to lesser extent in the epididymis results from a non membrane-bound form of Calnexin, as seen after separation of cytosolic and membrane-bound fraction by ultracentrifugation (Figure 24). The lower Calnexin band stays in the cytosolic fraction in the supernatant after ultracentrifugation, while the upper Calnexin band sediments with the membranous fraction.
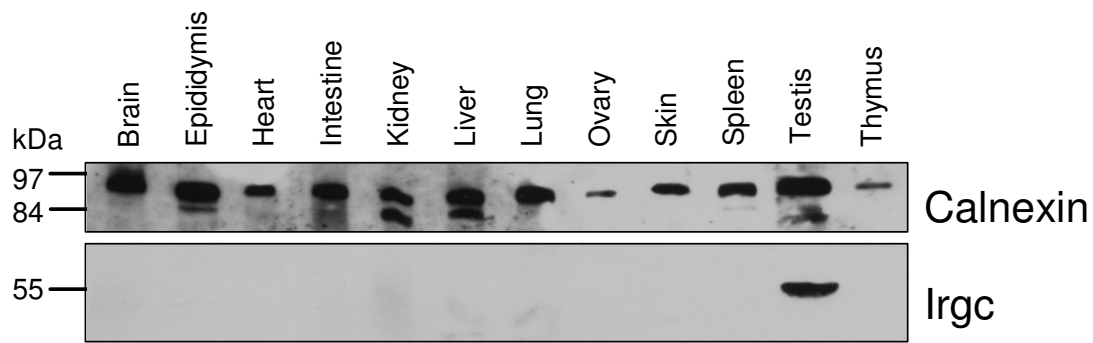
Figure 16. Irgc protein is detected only in testis. Multiple tissues of adult C57BL/6J mice were lysed in RIPA buffer and equal volumes were subjected to Western blotting. Using the Irgc-specific antiserum 39/3°, the protein could be detected only in testis, generating a band corresponding to a size of 55 kDa. The blot was additionally probed with an antibody against Calnexin.

Since ESTs from mouse dendritic cells are present in the databases, Irgc expression in different murine dendritic cell populations was analysed. cDNA from plasmacytoid, double negative, CD4$^+$ and CD8α$^+$ dendritic cells was kindly provided by Oliver Schulz and Caetano Reis e Sousa (Cancer Research UK, London). Irgc expression was analyzed by RT-PCR, but transcripts could not be detected in any of these dendritic cells (Figure 17a). Again GAPDH served as a positive control.

Since IRGC ESTs from ovary (macaque), liver (bull), lung and brain (human) are also present in the databases, cDNA derived from mouse ovaries, liver and lung was analyzed by RT-PCR. Thus as for the dendritic cells, no Irgc expression was detected in any of these organs (Figure 17b and 29). For human IRGC expression was analyzed by RT-PCR in brain, liver
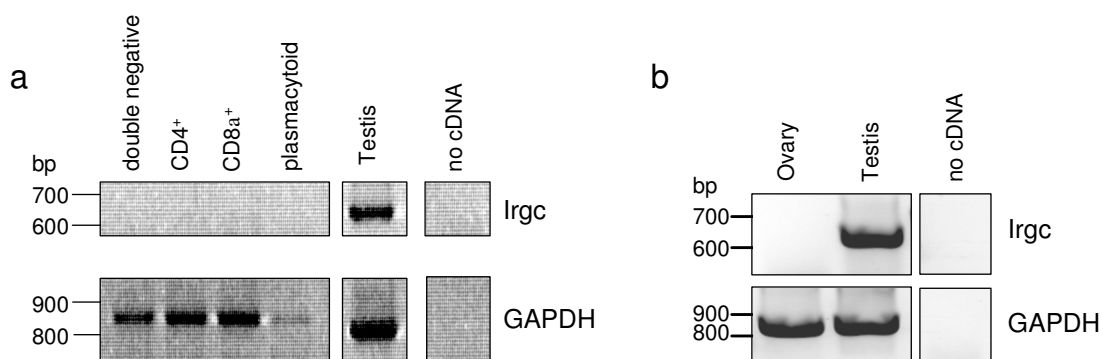
Figure 17. Irgc is not expressed in dendritic cells and the ovary. cDNA from a) dendritic cells of different developmental stages or b) ovaries of adult 2 months old C57BL/6J mice was analyzed by RT-PCR with 50 amplification cycles for expression of Irgc. Testis cDNA was included in both samples to control working PCR conditions. GAPDH was included as control.

and testis. For the first two organs the analysis was negative, in testis IRGC transcripts were detected.

Therefore the detected Irgc mRNA in the testis is also translated into protein. No other organs tested showed any Irgc expression, also including organs like ovary, liver or lung, from which ESTs are present in the databases.

3.4.3   Expression of Irgc is developmentally regulated

After localization of Irgc expression in the mouse testis, the question when it is expressed was addressed. Developing testes from C57BL/6J mice of ages ranging from 7 to 56 days post-natal were screened for Irgc mRNA and protein. RNA derived from the different samples were analysed for Irgc expression by RT-PCR. The first time point where Irgc mRNA could be detected was at the age of 19 days (Figure 18a). At that time the expression was still very weak, but increased drastically in the next two days to reach an expression level at day 21-22 that kept constant with progressing age. The other testis from the same mice were analysed on protein level by Western blot. Irgc protein could not be detected in testis of mice younger than 25 days (Figure 18b). From that age on the pool of Irgc increases with time and a constant level is reached at the age of approximately 35 days at a slower rate compared to the mRNA level.

The time point of the earliest detection of Irgc mRNA coincides with the appearance of abundant round haploid spermatids in the testis (Vergouwen 1993), indicating that the generation of round spermatids and Irgc may be linked to each other.

Although there may be a difference in the sensitivity of the two methods for the detection of Irgc mRNA and protein, there is a delay of up to 6 days between detectable transcription of Irgc and detectable protein. This delay is typical for testis-specific genes and indicates a putative function in spermatogenesis (Braun 2000). The best studied examples of translational repressed genes in spermatogenesis are Protamine 1 and 2 (Balhorn 1984, Kleene 1984), which replace the histones in the nucleus and confer the very tight packaging of the DNA in the spermatozoa, which actually makes further transcription impossible. The repression is conferred by two motifs in the 3'-UTR. The most important motif, which is sufficient for Protamine-like translational repression, is the translational control element (TCE), which is positioned in the 3'-region of the 3'-UTR (Zhong 2001). The protein that binds to the TCE is not identified yet. The second motif located in the 5' region of the 3'-UTR is the Y-box recognition sequence (YRS), which is bound by MSY2 and MSY4 (Fajardo 1997, Giorgini
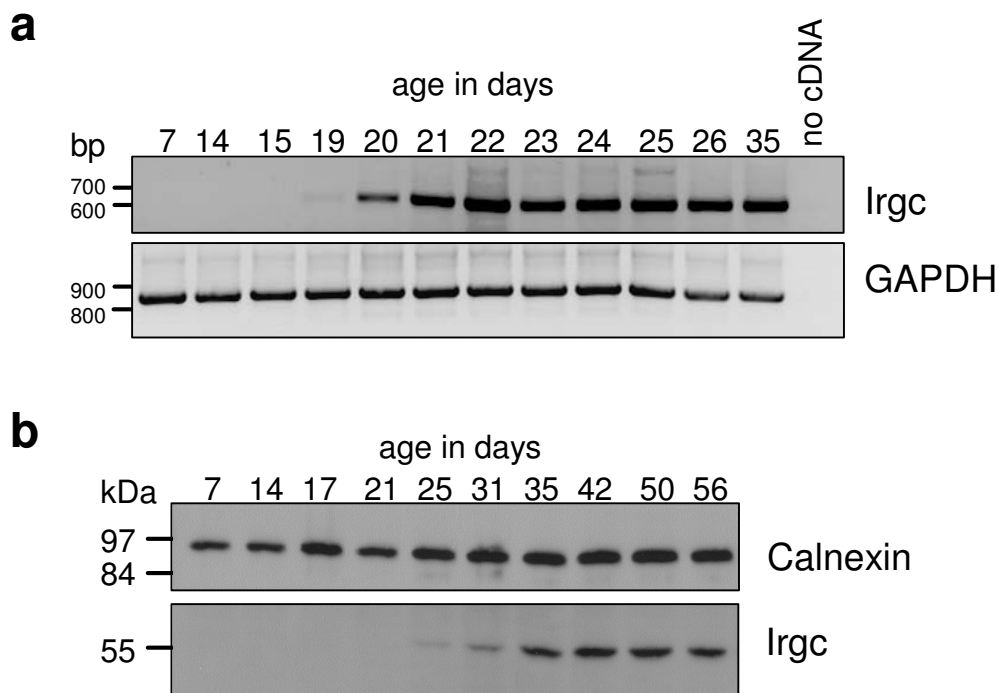
Figure 18. **Expression of Irgc is developmentally regulated in testis.** a) RT-PCR analysis on RNA derived from testis of mice aging 7 to 35 days for the expression of Irgc using 50 amplification cycles. RT-PCR for GAPDH with 30 amplification cycles was performed as control for RNA integrity. b) Western blot analysis from testis of the same mice used in a). Testis were lysed in RIPA buffer and analyzed by Western blot with the Irgc-specific antiserum 39/3°. Integrity of proteins was demonstrated by probing the same Western blot with α-Calnexin antibody.

2001, 2002). Both motifs were not detected in 3'-UTR of Irgc, so the translational repression is mediated by another, so far unknown, mechanism. Since the 3'-UTRs of IRGC genes from different species possess some highly conserved sequence motifs one of these motifs could be responsible for the translational repression of IRGC (Figure 19).
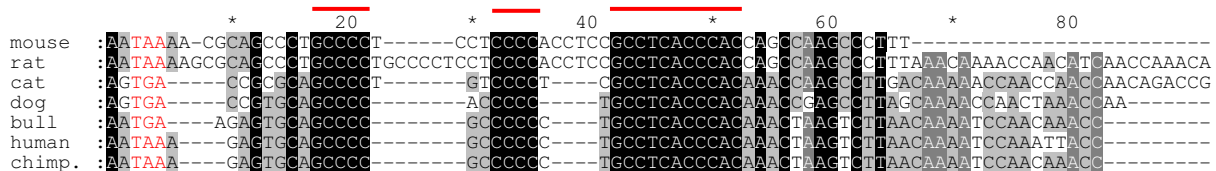
Figure 19**. Alignment of the 3'-UTR of IRGC from different species.** For cat and dog the genomic sequence downstream of stop codon was taken. Red letters indicate the stop codon of the IRGC ORF. Highly conserved motifs marked by red lines.

3.4.4   Irgc is expressed in haploid spermatids

To investigate whether there is a correlation between the appearance of Irgc and round haploid spermatids we performed *in situ* analysis of paraffin embedded sections from testis. By *in situ* hybridization using the N-terminal half of the Irgc ORF as antisense probe, expression of Irgc was shown in the haploid spermatids localized in the inner part of the *tubuli seminiferi* in the testis (Figure 20a, c). The cells on the periphery of the tubules, the spermatogonia and spermatocytes, did not show any expression of Irgc. The specificity of the antisense probe was shown by using a sense probe complementary to the antisense probe, which did not generate any signal (Figure 20b).
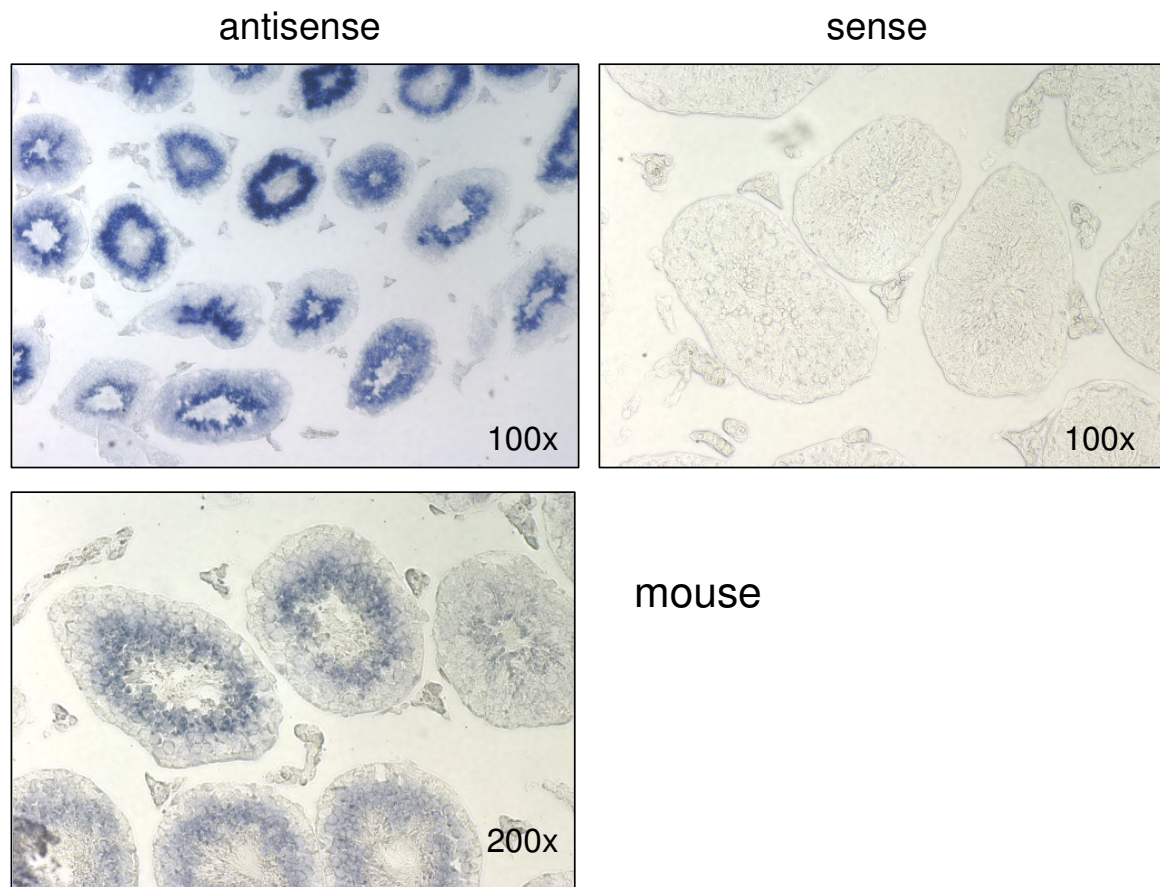
Figure 20**. Irgc is expressed in spermatids in the testis.** The expression of mouse Irgc was analyzed in sections of paraffin embedded mouse testis by *in situ* hybridization. The N-terminal antisense probe from mouse Irgc was used to detect the Irgc mRNA (a, c), the specificity of the antisense probe was demonstrated by using the complementary sense probe of mouse Irgc (b). Substrate: BM purple.

Immunocytochemical stainings were performed on testis sections to show the protein distribution in the testis. By using the Irgc-specific antiserum 39/3° the Irgc protein was shown to be synthesized in late round and elongated spermatids in the inner part of the *tubuli*

seminiferi, thus confirming the results of the *in situ* hybridization (Figure 21). The staining using the colour substrate HistoGreen shows a sharp boundary between the Irgc-expressing haploid spermatids and the non-expressing pachytene spermatocytes, which are still diploid (Figure 21d). No Irgc was detected in the myoid cells and basement membrane surrounding the seminiferous tubules and the cells in the intertubular region, like Leydig cells and macrophages. The specificity of the antiserum was demonstrated by using testis sections of Irgc deficient mice. These sections do not show any green staining using the same protocol, confirming the specific binding of the antiserum to Irgc.
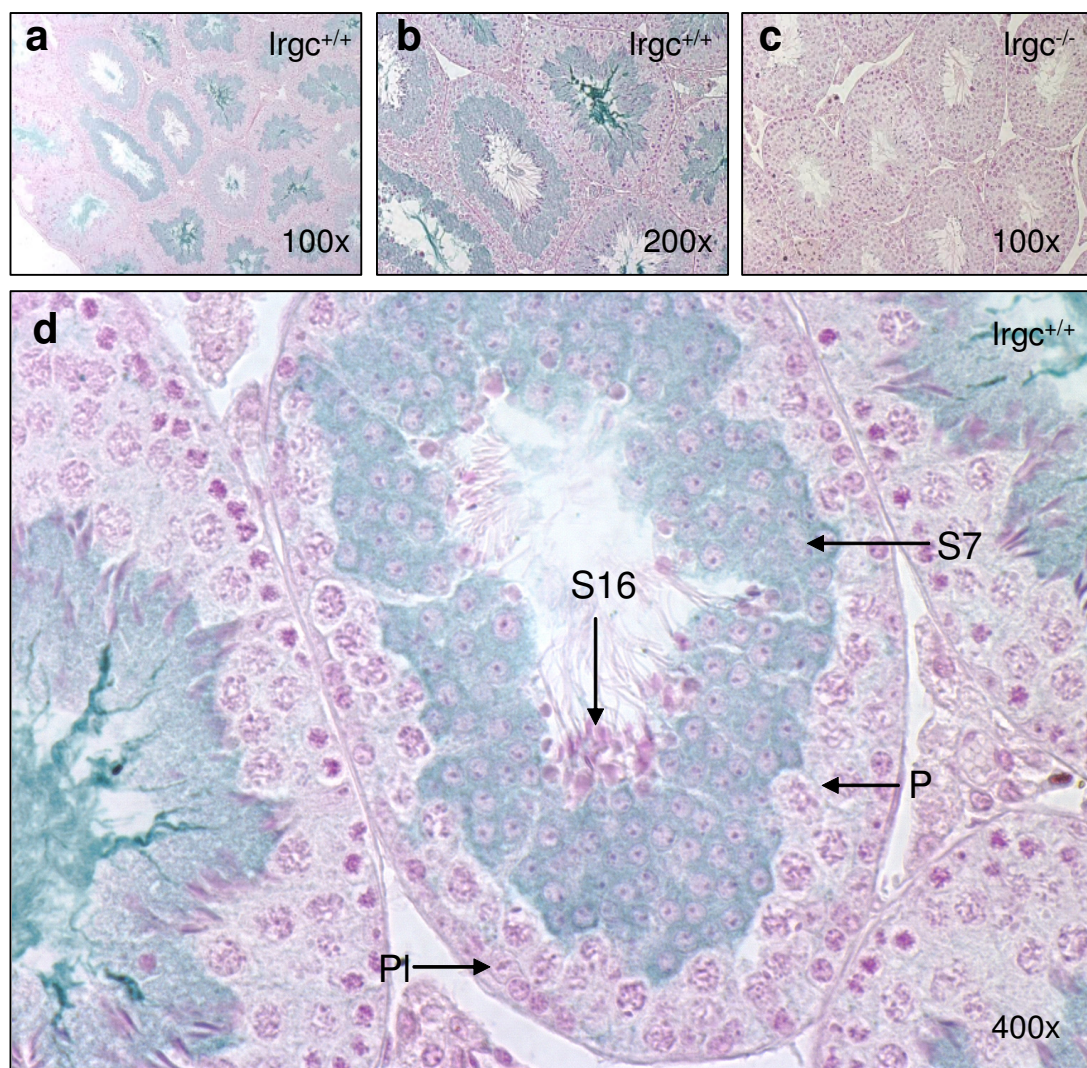
Figure 21. **Expression of Irgc in haploid spermatids.** Immunocytochemical analysis of sections of paraffin embedded testis. Sections from wt (a, b, d) and Irgc$^{-/-}$-mice (c) were probed with the Irgc-specific antiserum 39/3°. Absence of any green staining in testis of Irgc$^{-/-}$-mice (c) demonstrates specificity of the antiserum. Substrate: HistoGreen. Counterstaining of nuclei: Nuclear Fast Red. P: pachytene spermatocytes, Pl: preleptotene spermatocytes, S7: step 7 spermatids, S16: step 16 spermatids

Irgc protein was not detected in the epididymis (Figure 16), where the mature spermatozoa are stored, suggesting that mature spermatozoa do not contain any Irgc. Hence, spermatozoa isolated from the caput of the epididymis, were stained with the Irgc-specific antiserum 39/3°, but Irgc could not be detected (Figure 22). Thus, the conclusion that Irgc is absent from mature spermatozoa was verified.
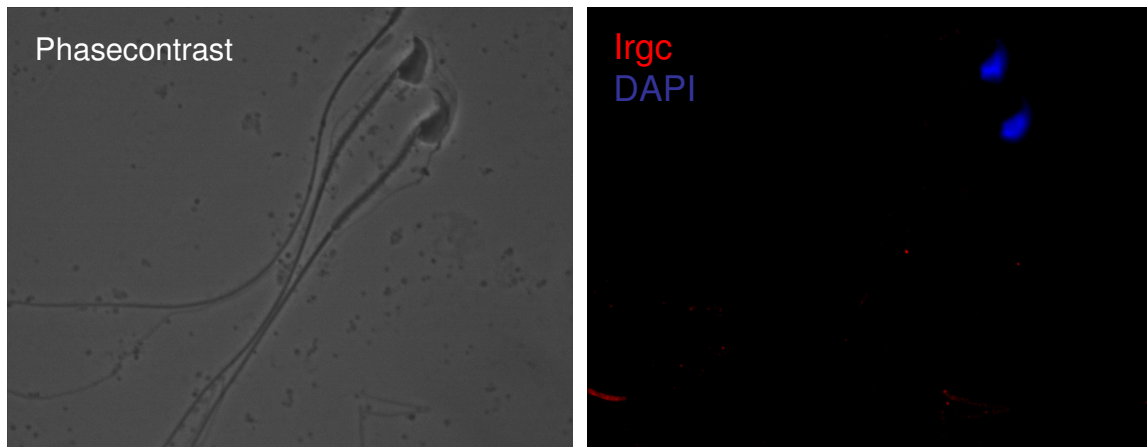
Figure 22. **Mature spermatozoa do not contain any Irgc.** Spermatozoa isolated from the epididymis were fixed in 4% paraformaldehyde in PBS and stained with the Irgc-specific antiserum 39/3°. Secondary antibody: goat-anti rabbit IgG Alexa 546, DNA stained with DAPI. Magnification: 1000x.

To get further information about the intracellular localization of Irgc, squash preparations of cells from *tubuli seminiferi* were performed and the fixed cells stained for Irgc. Late round and elongated spermatids contain Irgc (Figure 23). The Irgc is mainly localized in the cytosol and is excluded from the nucleus. The spermatocytes and the Sertoli cells positioned between and around the spermatids and the spermatocytes did not show any Irgc expression. In addition to the round and elongated spermatids another kind of Irgc containing structures without evident nuclei were detected, whose character and origin is not exactly clear (Figure 23 yellow arrows). However, there are two explanations for these structures. They could be spermatids, whose nucleus is for some reason not visible or got lost through the preparation of the cells, meaning they are a preparation artefact. The other possibility would be that they are residual bodies containing the cytoplasm, which gets excluded from the spermatids during late spermiogenesis. This would also explain how the mature spermatozoa remove their Irgc.
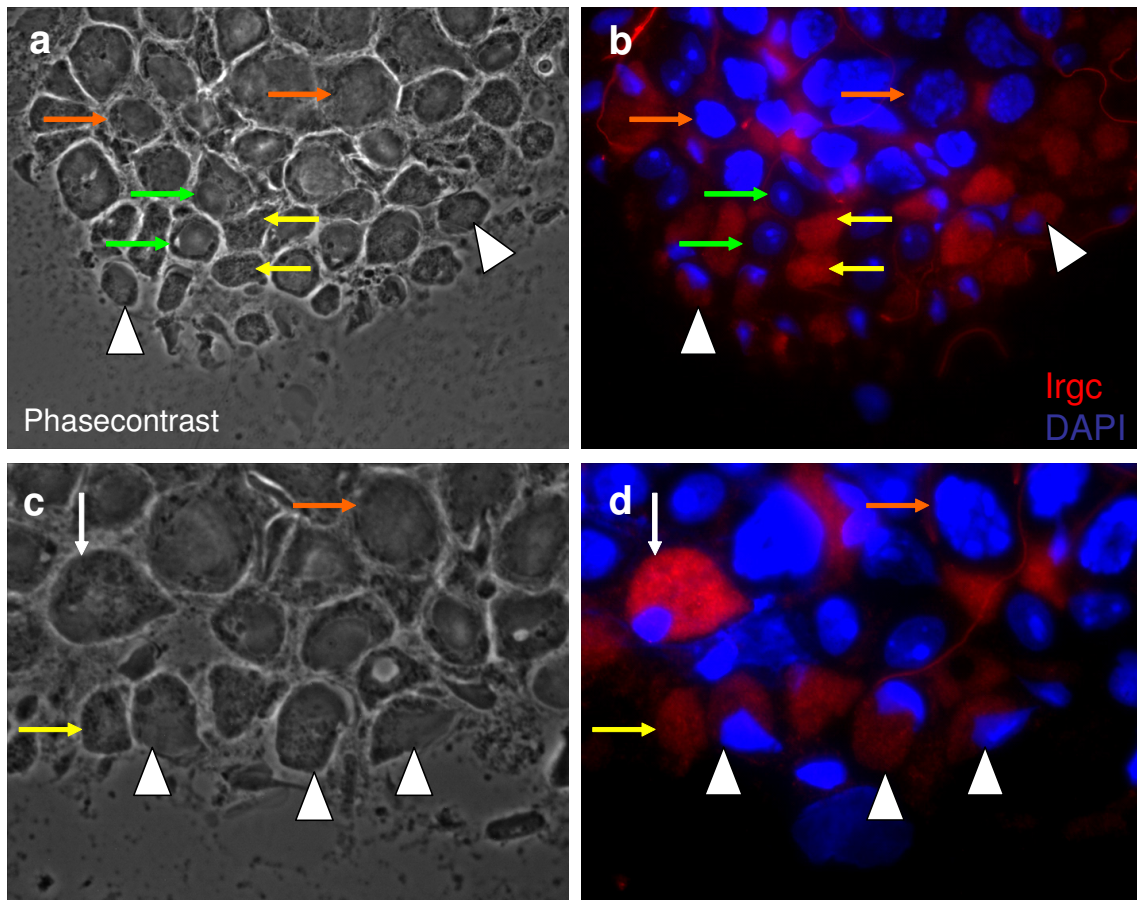
Figure 23. **Irgc is expressed in late round and elongated spermatids.** Squash preparations of cells from seminiferous tubules, fixed with 4 % PFA in PBS and stained with the Irgc-specific antiserum 39/3°. Secondary antibody: goat-anti-rabbit IgG Alexa546, DNA stained with DAPI. Irgc is expressed in late round (white arrow) and elongated spermatids (white arrowhead), but not in Sertoli cells (green arrow) and spermatocytes (orange arrow). Irgc-containing structures without defined origin (yellow arrow). Magnification: a, b: 630x, c, d: 1000x.

3.5 Membrane binding behaviour of Irgc

To test whether there is also a membrane bound fraction of Irgc, as seen for most other IRGs (Martens 2004), hypotonic lysates of seminiferous tubules were prepared. After lysis approximately half of the Irgc protein gets removed from the lysate by a short low-speed centrifugation step (5 min at 1.000g), which is performed to clear the lysate from nuclei, cellular debris and unlysed cells. In this pre-cleared lysate the cytoplasmic and membrane-bound fraction were separated by a 100.000g centrifugation step. The major part of the Irgc was found in the supernatant and was therefore localized in the cytoplasm. Thus there was also a minor part of Irgc that was membrane-bound and pelleted (Figure 24).

To test under which conditions the Irgc pelleted in the pre-clearance step could be solubilised again, the pellet was resuspended in different buffers and centrifuged at 100.000 g for 30 min to separate soluble Irgc from the bound form. While using PBS and 1 M sodium chloride did

not have any effect on the Irgc, 100 mM sodium carbonate (pH 11,75) and low urea concentrations (2 M) could solubilise Irgc partially. High urea concentrations (4 M, 6 M) and the detergent Triton X-100 (1 % in PBS) shifted Irgc completely to the soluble fraction (Figure 24).

The membrane-binding behaviour of Irgc is consistent with other members of the GKS-subfamily of IRG proteins, which are mainly cytosolic (Irgd) or evenly distributed between cytosol and membranes (Irga6, Irgb6) (Martens 2004). The members of the GMS-subfamily, the Irgm proteins are, in contrast, predominantly membrane associated (Martens 2004).
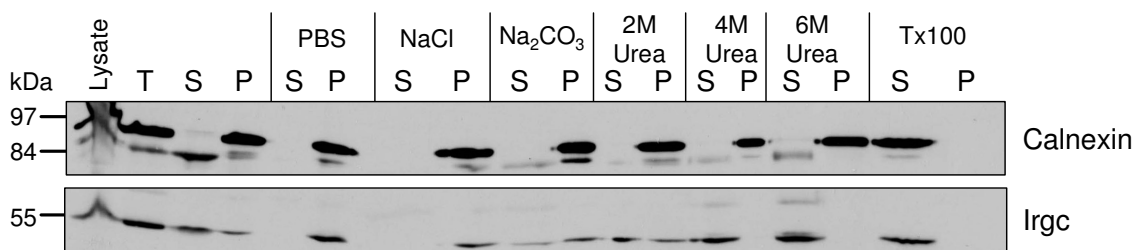
Figure 24. **Hypotonic lysates of tubuli seminiferi reveal membrane-bound fraction of Irgc.** Hypotonic lysates of tubuli seminiferi were briefly centrifuged to remove nuclei, unlysed cells and cell debris. Pellet was resuspended (T) in PBS 0,5% SDS. Remaining lysate was centrifuged for 30 min at 100.000 g to separate membrane-bound components, which go to the pellet (P), from cytosolic components, which stay in the supernatant (S). Fraction T was resuspended in the indicated buffers and centrifuged again. Pellets were resuspended in PBS 0,5% SDS. Equal volumes of S and P fractions were subjected to Western blot analysis.

3.6 The expression pattern of IRGC in testis is conserved

After defining the Irgc expression pattern in the testis of mice the question arose, whether this pattern is conserved in humans and other mammals, as in general suggested from the EST distribution in other species.

Human IRGC expression was detected by RT-PCR in testis, but not in brain and liver (Figure 25a). Expression of IRGC in testis was also shown by RT-PCR in dog, cat, rat and bull (Figure 25b). Subsequently sections of paraffin embedded testis of human, dog, cat, cow and rat were analysed by *in situ* hybridization. In all species IRGC is expressed in the same pattern in testis. Transcription starts in haploid spermatids and the mRNA message is detected in the respective cells (Figure 26 and 27). The spermatogonia and spermatocytes at the periphery of the *tubuli seminiferi* and the cells in the intertubular space do not express IRGC, analogous to the situation in the mouse. Thus, the pattern of transcription in testis is conserved in all species that were analysed and it is very likely that it is generally conserved

in all mammals. Interestingly the expression is independent of the number of IRG genes possessed by each species. Hence, it is tempting to speculate, that IRGC mediates a conserved function in the spermiogenesis of all mammals.
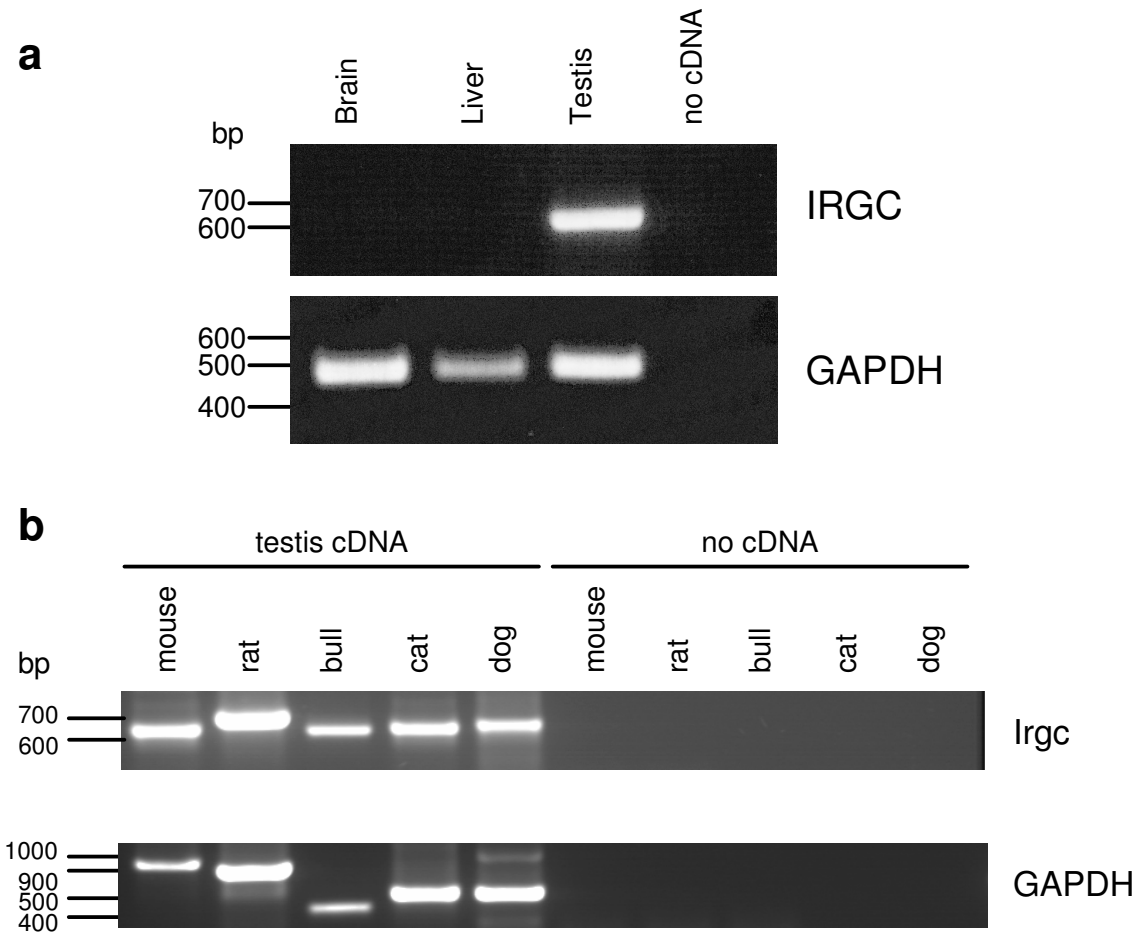

Figure 25. **Expression of IRGC in testis is conserved between mammals.** a) RNA from human brain, liver and testis were analyzed for the expression of IRGC by RT-PCR with 50 amplification cycles. GAPDH was used as control. b) RNA from the testis of the species indicated were analyzed for the expression of Irgc by RT-PCR with 50 amplification cycles. GAPDH was used as control, except for rat where GAPDHS was used.

antisense   sense
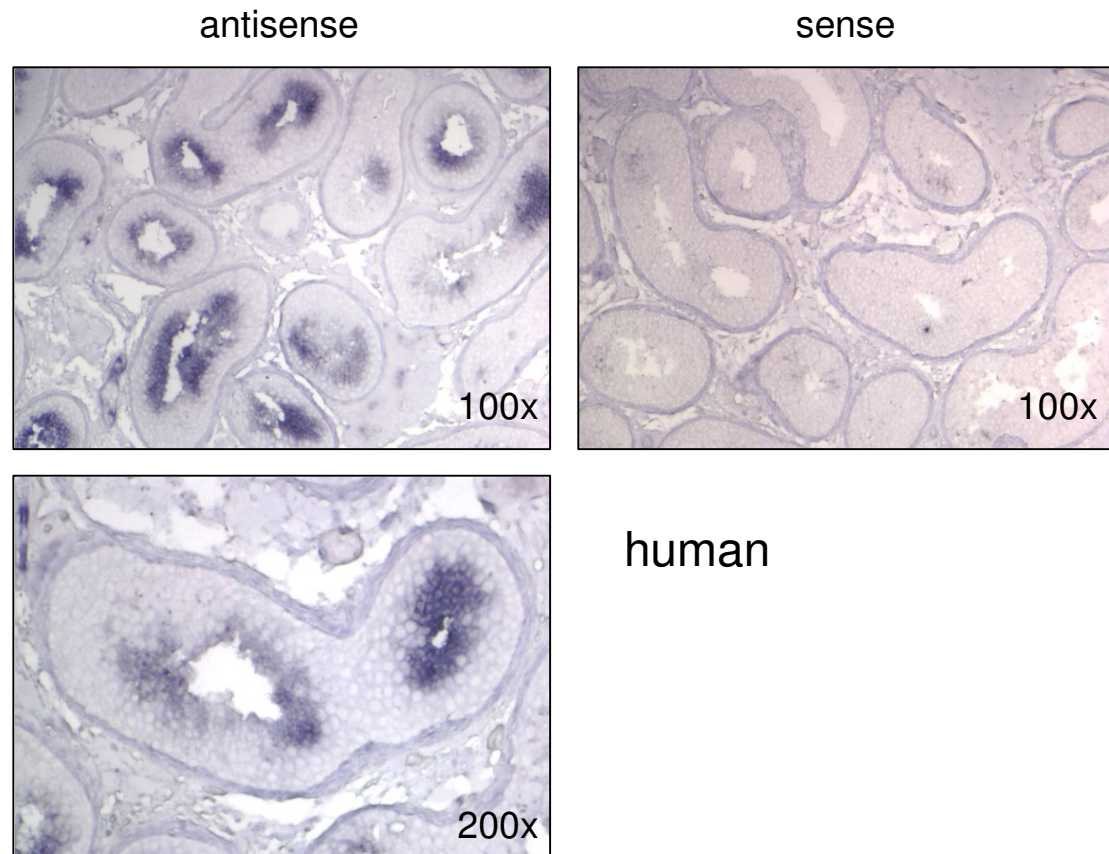
human

Figure 26. **Expression of human IRGC is conserved in testis.** The expression of human IRGC was analyzed in sections of paraffin embedded human testis by *in situ* hybridization. The antisense sense probe with a length of 852 bp covers 90 bp of the 5'-UTR and 762 bp of the ORF of human IRGC and generates a signal in the haploid spermatids in the seminiferous tubules. The complementary sense probe does not generate any signal inside the tubules showing the specificity of the antisense probe. Substrate: BM purple.

3.7 Irgc is not inducible by interferon *in vitro* or by infection *in vivo*

Most *IRG* genes were shown to be induced by stimulation with IFN-γ (Gilly 1992, Boehm 1998, Bekpen 2005). The induction by interferons is mediated by interferon-stimulated response elements (ISRE) and γ-activated sequence (GAS) sites located in the promoter. As stated before, the Irgc promoter is lacking these elements. However, we tested if Irgc is interferon-inducible in L929 fibroblasts. After stimulation with IFN-β or IFN–γ no RT-PCR signal of Irgc could be detected (Figure 28), as in uninduced L929 cells. The cDNA was additionally analysed for the expression of Irga2, which is known to be interferon-inducible and served as a positive control (Bekpen 2005). After stimulation with IFN-β or IFN–γ Irga2 is strongly induced, while without interferon induction the expression is absent.
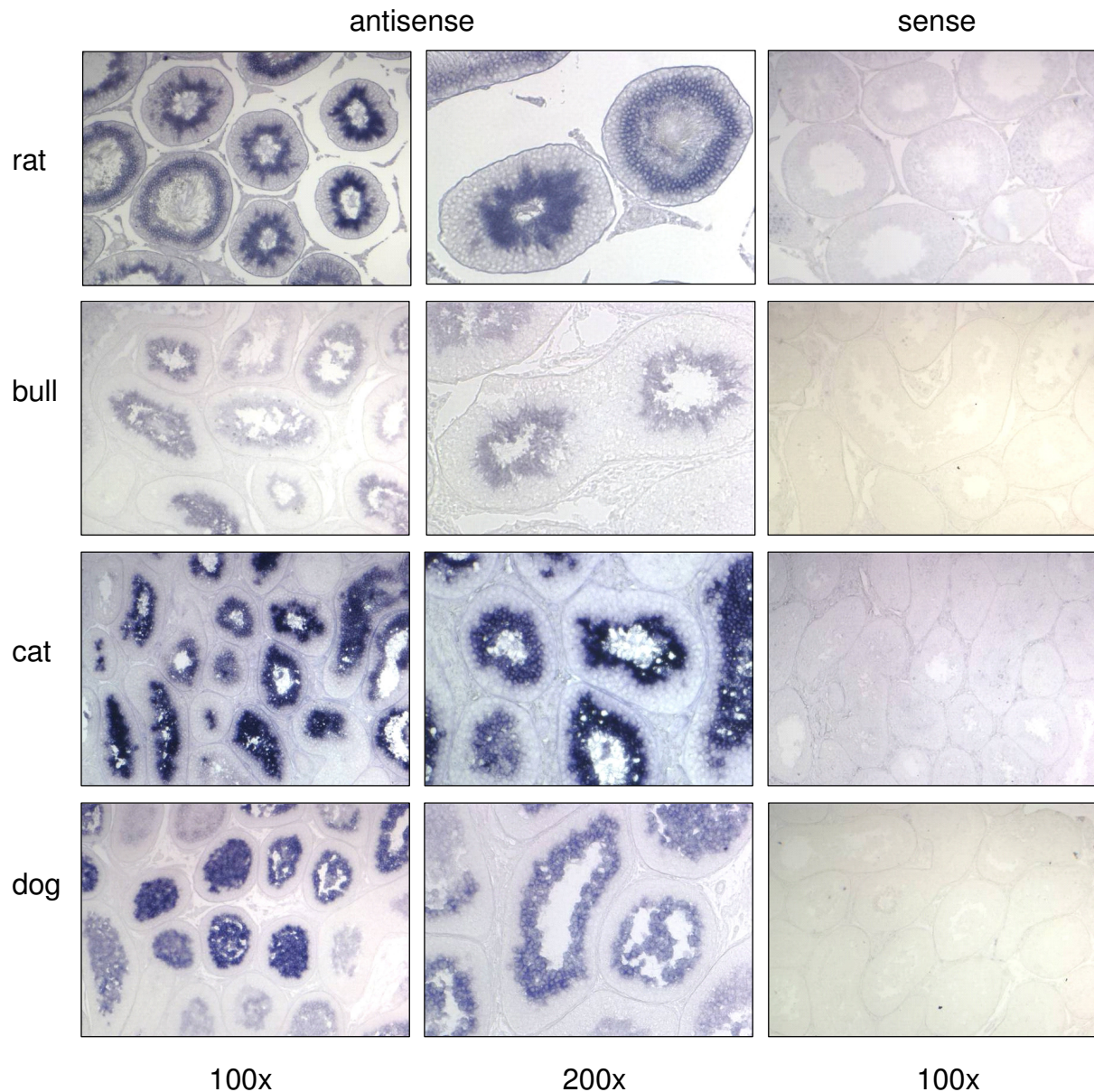
antisense   sense

Figure 27. **Irgc expression pattern in mammalian testis is conserved.** The expression of Irgc was analyzed in sections of paraffin embedded testis from rat, bull, cat and dog by *in situ* hybridization. The N-terminal antisense probe from mouse Irgc was used to detect the Irgc mRNA (left and middle row). The specificity of the antisense probe was demonstrated by using the complementary sense probe of mouse Irgc (right row). Substrate: BM purple.

In a second experiment induction of Irgc by infection was investigated. C57BL/6J mice were infected with *Listeria monocytogenes in vivo*. After 24 hours liver, lung and spleen of *Listeria* infected and non infected animals were taken and expression of Irgc and Irga2 was analysed by RT-PCR. While the Irga2 expression level was elevated in all three tested organs after infection compared to the expression levels in non-infected mice, Irgc expression could not
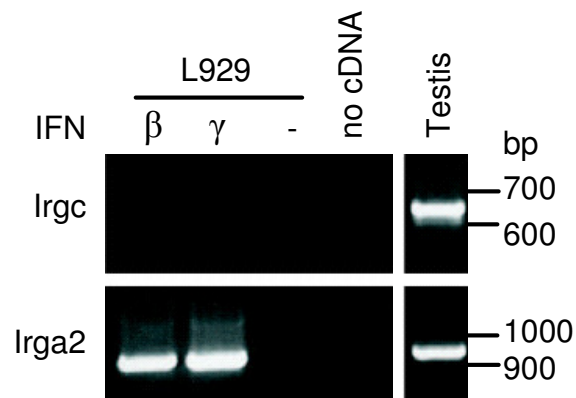
Figure 28. **Irgc is not induced by IFN-β or IFN-γ in mouse L929 fibroblasts.** L929 fibroblasts were induced for 24 hours with IFN-β or IFN-γ or left uninduced (-). Even after 50 amplification cycles Irgc expression could not be detected by RT-PCR, whereas Irga2 showed a strong response to the induction by both interferons. cDNA from mouse testis served as positive control.

Be detected in any of these three organs, whether the mice were infected or not, even after a PCR with 50 amplification cycles (Figure 29). Hence, infection with *L. monocytogenes* does not have any effect on Irgc expression. These results lead to the conclusion that Irgc, in contrast to most other members of the IRG family, is not a resistance factor.

The situation in humans was also analyzed. Since IRGC is the only full-length IRG protein in humans, it may have additional functions compared to mouse Irgc, which are fulfilled by other, interferon-inducible IRG proteins in the mouse. The promoter of *IRGC* is conserved
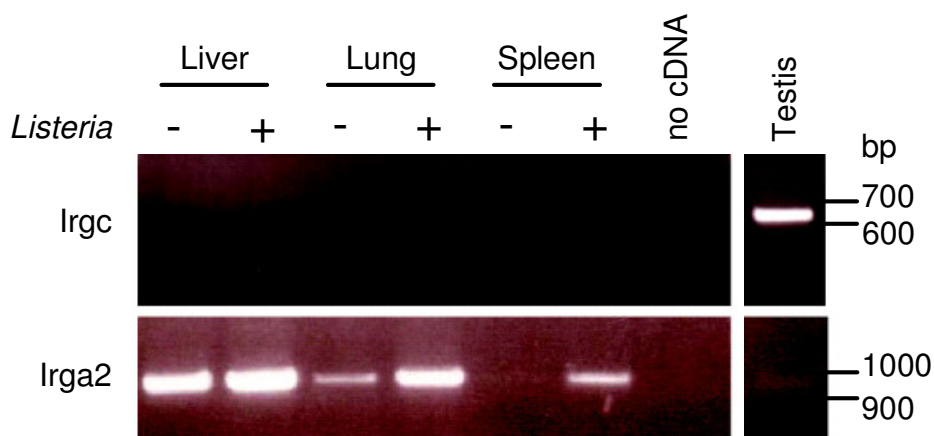
Figure 29. **Irgc is not induced by infection with *Listeria monocytogenes*.** RT-PCR on RNA from tissues of uninfected mice (-) or mice infected 24 hours previously with *Listeria monocytogenes* (+). For Irgc 50 amplification cycles were used, for Irga2 only 30. Irga2 was induced in all tissues tested, while Irgc was not induced in any.

relative to the mouse and is also lacking any interferon response elements. Primary fibroblasts and six different cell lines were induced by IFN-β and IFN-γ, respectively. IRGC was not induced in any of them (Figure 30). To control proper induction by IFN-β and IFN-γ, the cells were also tested for the induction of GBP-1, which is known to be interferon-inducible (Cheng 1983, Cheng 1985). GBP-1 was induced to various degrees by IFN-γ in all tested celllines except HepG2, while stimulation by IFN-β did not have any big effect on the GBP-1 expression level. Only in T2 cells and primary fibroblasts an induction of GBP-1 by IFN-β was recognizeable, but it was weaker than the IFN-γ effect.
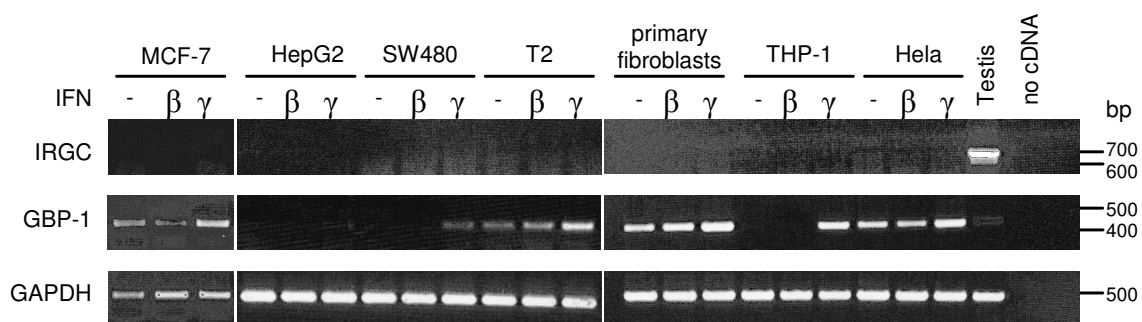
Figure 30. **Human IRGC is not induced by interferons *in vitro*.** Human cell lines or primary cells were induced with IFN-β or IFN-γ for 24 hours or left uninduced (-). IRGC expression was analysed by RT-PCR with 50 amplification cycles, but expression was only detected in testis. Induction of GBP-1 was assayed as positive control and is constitutively expressed only in human testis. GAPDH was assayed as control for cDNA integrity.

Thus, a role of IRGC in resistance is unlikely. In context of the conserved testis-specific expression pattern, it seems likely that the function of human IRGC is the same as that of mouse Irgc, although IRGC is the only complete *IRG* gene in humans. Thus the resistance mediated by the interferon inducible *IRG* genes in the mouse has to be performed by other mechanisms and pathways in humans.

3.8 Irgc deficient mice were generated

To get further information about the function of Irgc, mice lacking Irgc were generated. The ORF of Irgc located on Exon 2 was removed and replaced by the ORF of the reporter gene EGFP (enhanced green fluorescent protein). Thus, EGFP is expressed under the control of the Irgc promoter.

A detailed description about the generation of the Irgc$^{-/-}$-mice is presented in Material and Methods 2.4. The homozygous Irgc$^{-/-}$-mice were viable and did not show any obvious anomaly in morphology or behaviour.
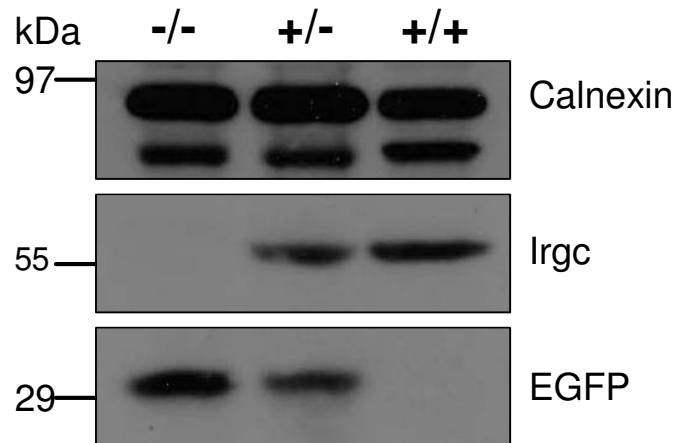

Figure 31. **Irgc and EGFP expression in testis from Irgc$^{-/-}$-, Irgc$^{+/-}$- and Irgc$^{+/+}$-mice.** Testis from adult mice of the indicated genotype were lysed with RIPA-buffer and equal volumes subjected to Western blotting and probed for Calnexin, Irgc and EGFP.

The testis from adult wildtype Irgc$^{+/+}$-, heterozygote Irgc$^{+/-}$- and homozygote knock out Irgc$^{-/-}$-mice were analysed for the expression of Irgc and EGFP by Western blot. The Irgc$^{+/+}$-mice showed expression of Irgc, but not EGFP, while the Irgc$^{-/-}$-mice expressed only EGFP and no Irgc (Figure 31). The heterozygote Irgc$^{+/-}$-mice expressed both proteins, but at lower levels than respective homozygote mice. Hence, the expression of Irgc and EGFP is manipulated in the way desired in the knock out strategy.

To investigate the EGFP expression *in situ*, paraffin embedded sections of testis from Irgc$^{-/-}$-mice were stained with an antiserum recognizing EGFP. EGFP was detected in the spermatids in the center of the seminiferous tubules (Figure 32), like Irgc in testis of wt mice (Figure 21). However, there is a clear difference in the staining pattern. While Irgc is detected in late round and elongated spermatids, EGFP is detectable only in late elongated spermatids. In late round spermatids EGFP was, in contrast to Irgc, not detected. There are different possible explanations for this delay of EGFP detection. The putative poly(A)-signal from Irgc, which includes the stop codon of the ORF, is disrupted after the integration of EGFP (Figure 32d). Therefore the EGFP mRNA may be inefficiently polyadenylated, leading to a decreased mRNA stability and/or decreased translation late. The consequence would be that it takes longer to produce an EGFP pool, which is detectable by the antiserum. Other possible

explanations for the late detection of EGFP are a lower specificity of the antiserum and differences in the protein synthesis rate and stability of EGFP compared to Irgc.
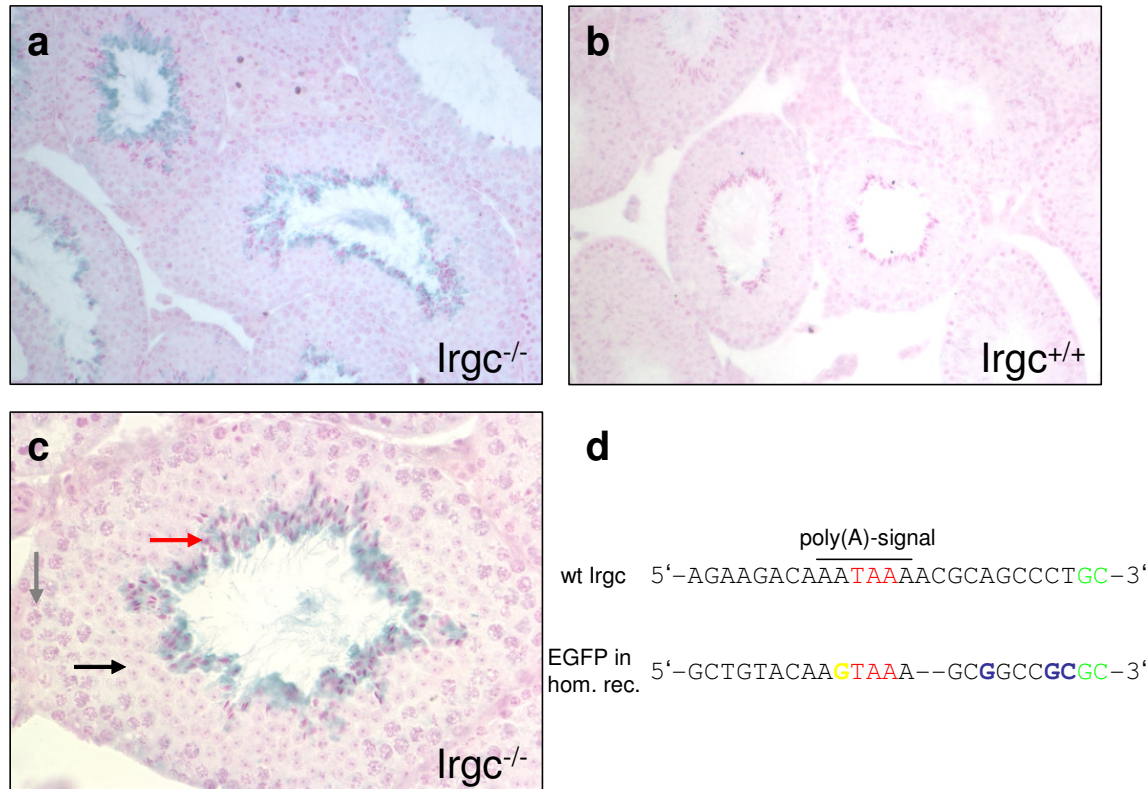

Figure 32. **Expression of EGFP in the testis of Irgc$^{-/-}$-mice.** Immunocytochemical staining of 6 µm thick sections of paraffin embedded testis from Irgc$^{-/-}$-mice with the EGFP-specific BD Living Colors A. v. Peptide Antibody (a, c). EGFP is detected in late elongated spermatids (red arrow), but in contrast to Irgc (Figure 21) not in late round spermatids (black arrow). No EGFP staining is detected in diploid spermatocytes and spermatogonia (grey arrow). Specificity of the antiserum was demonstrated by staining sections from Irgc$^{+/+}$-mice (b). Substrate: HistoGreen. Counterstaining of nuclei: Nuclear Fast Red. Magnification: a, b: 200x, c: 400x. d) Sequence around the stop codon for wt Irgc and after homologous recombination (hom. rec.) for EGFP. The G (yellow) disrupts the putative poly(A)-signal present in wt Irgc. Other substitutions for the introduction of a *Not*I restriction site are indicated in blue. Green letters indicate from which point the sequence in wt and recombinant is the same.

3.8.1   The testis and sperm morphology of Irgc$^{-/-}$-mice is normal

As demonstrated, Irgc is expressed exclusively in the haploid spermatids in the testis. Thus, the morphology of the testis was analysed in Irgc$^{-/-}$-mice in order to see, whether the deficiency of Irgc disturbs the formation of spermatozoa and leads to defects or alterations in spermatogenesis like spermatogenic arrests or generation of deformed spermatozoa.

Sections of paraffin embedded testis from Irgc$^{-/-}$-mice were stained by haematoxylin and eosin and analysed. The testis did not show any differences compared to testis from wildtype mice (Figure 33). Spermatogenic arrests at a certain stage of spermatogenesis, increased apoptosis
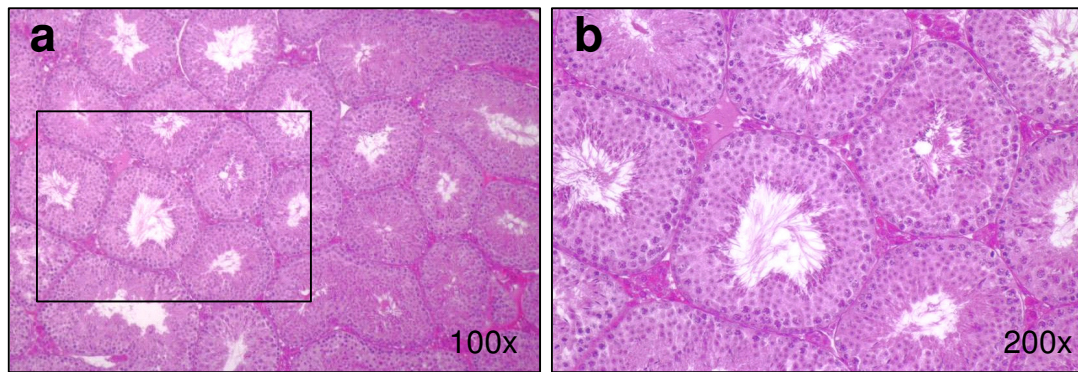
Figure 33. **Morphology of *tubuli seminiferi* of testis from Irgc⁻/⁻-mice is normal.** Sections of paraffin embedded testis from Irgc⁻/⁻-mice were stained with haematoxylin and eosin. Boxed area in a) is shown in higher magnification in b).

or generation of deformed spermatozoa, as seen for null mutants of other haploid expressed genes, were not observed (Matzuk 2002, de Rooij 2003).

The morphology of the epididymis from knock out Irgc⁻/⁻- and wildtype Irgc⁺/⁺-mice was also analysed, but no difference could be observed. In both genotypes the tubules of the epididymis was filled with mature spermatozoa (Figure 34). These mature spermatozoa from
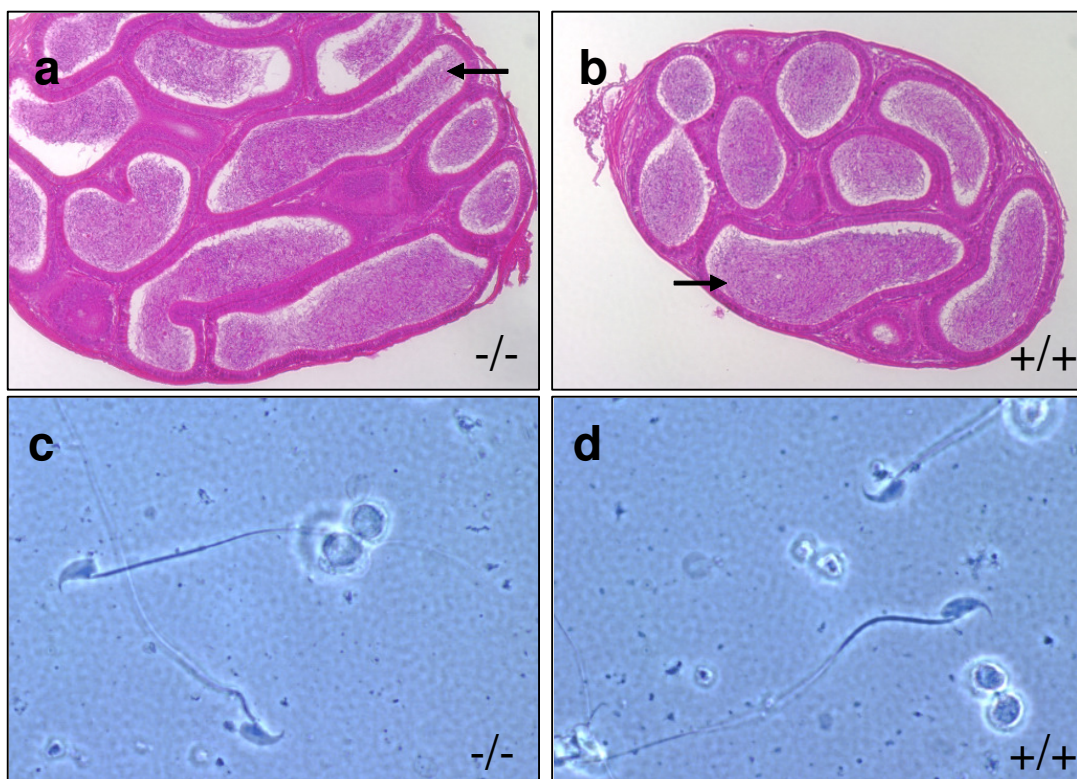
Figure 34. **Morphology of spermatozoa from Irgc⁻/⁻-mice is normal.** Sections of paraffin embedded epididymis were stained with haematoxylin and eosin. The morphology of the epididymis from Irgc⁻/⁻-mice (a) is normal compared to Irgc⁺/⁺-mice (b). In both genotypes the tubules are filled with mature spermatozoa (black arrow). Spermatozoa isolated from the epididymis of Irgc⁻/⁻-mice (c) do not show any morphological differences compared to spermatozoa from Irgc⁺/⁺-mice (d). Magnification: a, b: 100x, c, d: 1000x.

Irgc$^{-/-}$- and Irgc$^{+/+}$-mice were isolated from the caput of the epididymis and compared to each other. The spermatozoa from Irgc$^{-/-}$-mice are morphological normal and do not show any deformations (Figure 34).

3.8.2 Testis morphology of Irgc$^{-/-}$-mice stays normal with increasing age

A specific phenotype may develop in an age-dependent manner in the testis of Irgc$^{-/-}$-mice. Hence, the testis morphology of adult Irgc deficient mice up to an age of 22 months was studied and compared to that of wildtype litter mates of the same age. Mice of the following ages were analysed: 76, 105, 118, 157, 232, 265, 420, 456, 500, 642, 683, 708 days. In Figure 35 haematoxylin and eosin stained testis sections of Irgc$^{+/+}$- and Irgc$^{-/-}$-mice with an age of
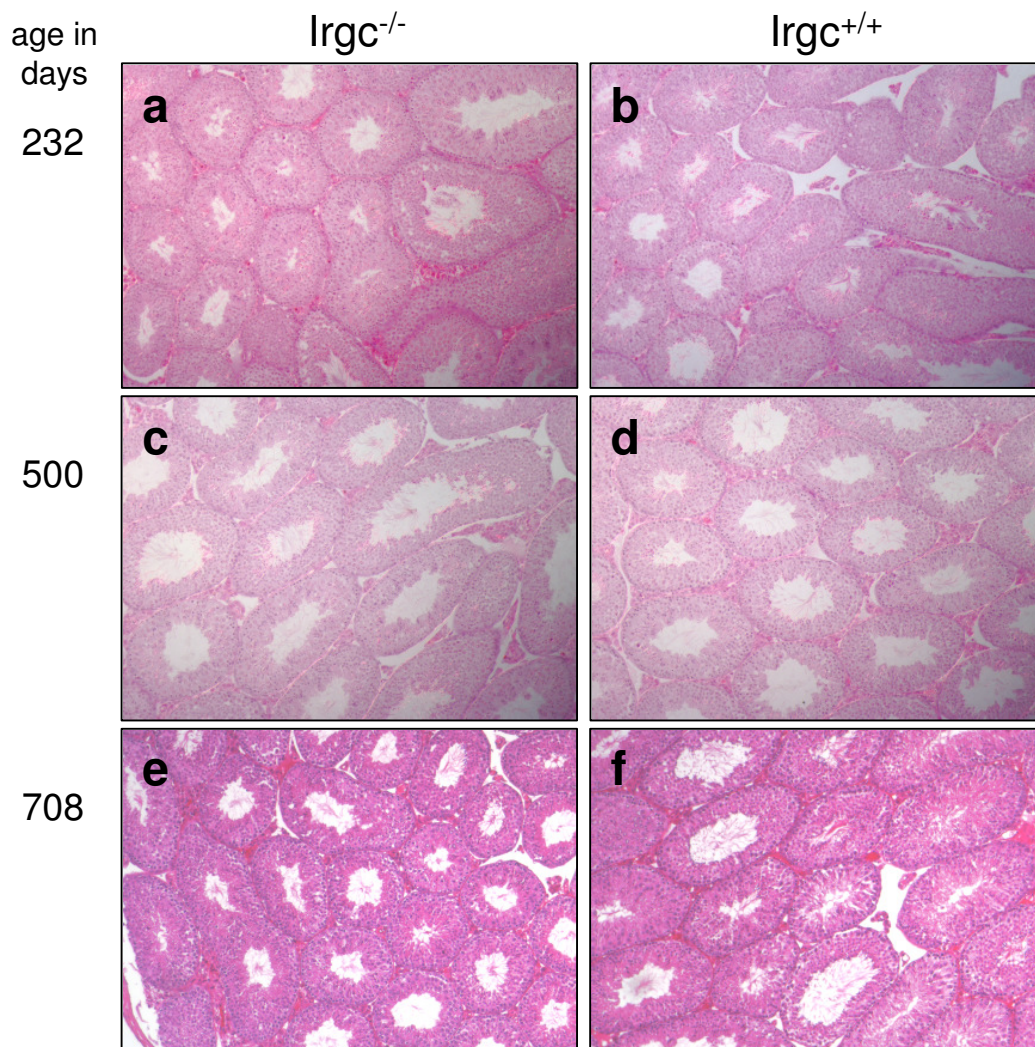

Figure 35. **Morphology of testis from Irgc$^{-/-}$ stays normal with increasing age.** Sections of paraffin embedded testis from Irgc$^{-/-}$- (a, c, e) and Irgc$^{+/+}$-mice (b, d, f) of the same age and litter were stained with haematoxylin and eosin. Magnification: 100x.

232, 500 and 708 days are shown. Independent of the age no differences in the morphology between wildtype and Irgc^{-/-}-mice were detected. Tubules covering all stages of spermatogenesis were present in all analysed testes. The results of this analysis suggest that Irgc deficiency does not cause an age dependent phenotype in testis. This is in agreement with the fact that also old Irgc^{-/-}-mice are capable of producing offspring. The oldest Irgc^{-/-}-male (#575) to produce offspring was 296 days old when it fertilized the female. Then the breeding was stopped. At the age of 9 to 10 months on average the breeding efficency of typical laboratory mice drops drastically (Lambert 2007). So it can be concluded, that Irgc^{-/-}-mice have a normal reproductive life span.

3.8.3   Irgc^{-/-}-mice are fertile

As demonstrated, the testis and spermatozoa of Irgc^{-/-}-mice did not show any morphological differences compared to wildtype mice. However, these morphological observations do not exclude an effect on the fertility of these mice.

By setting up breedings of male and female Irgc^{-/-}-mice it was tested, whether the Irgc^{-/-}- mice are still fertile and capable of producing offspring. The fertility of the Irgc^{-/-}-mice was immediately proven by the birth of the first offspring, excluding the possibility that Irgc deficiency leads to infertility. Nevertheless, there could be a reduced fertility as a consequence of the Irgc deficiency, resulting in smaller litter sizes compared to wildtype mice. Although the seminiferous tubules and spermatozoa do not show any morphological disorders, the spermatozoa could have a reduced ability to fertilize oocytes based on defects associated with swimming, sensing the egg, penetrating the *zona pellucida* or acrosome
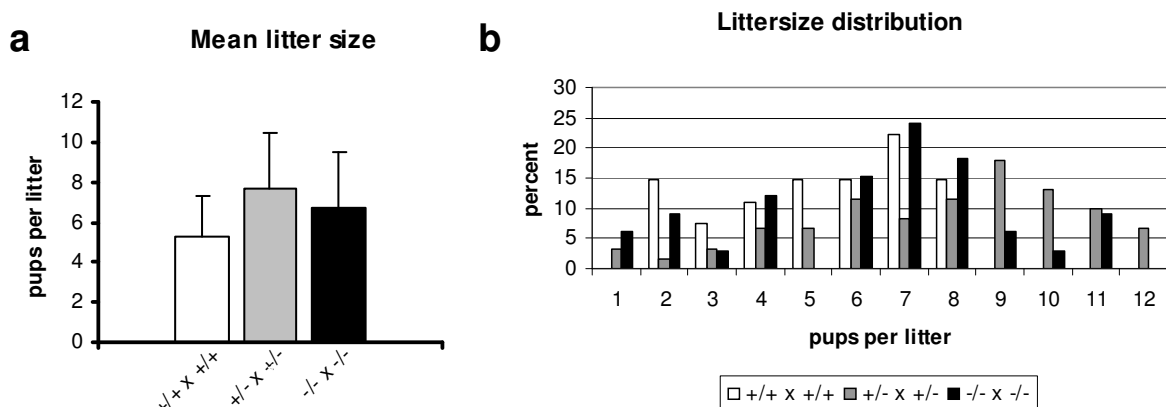

Figure 36. **Irgc deficiency has no negative effect on fertility.** a) Mean litter size of breedings between Irgc^{+/+}-, Irgc^{+/-}- or Irgc^{-/-}-mice. b) Distribution of litter size according to the Irgc genotypes. Data based on 5 breedings between Irgc^{+/+}-mice (27 litters), 8 between Irgc^{+/-}-mice (61 litters) and 8 Irgc^{-/-}-mice (33 litters).

reaction. To test this, 8 interbreedings of Irgc$^{-/-}$-, 8 of Irgc$^{+/-}$- and 5 of Irgc$^{+/+}$- mice were set up and the generated offspring compared. The mean litter size of Irgc$^{-/-}$-mice was with 6,7 (± 2,79) pups per litter actually bigger than the 5,3 (± 2,04) for Irgc$^{+/+}$-mice (Figure 36a). The mean litter size of Irgc$^{+/+}$-mice is in agreement with the values expected for breedings of wildtype C57BL/6J mice, which produce on average 4,9 pups per litter (Lambert 2007). The highest fertility was obtained from the breedings of heterozygote mice with a mean litter size of 7,7 (± 2,76). Therefore a negative effect of Irgc deficiency on fertility can be excluded.

In this context it is noteworthy and highly significant (p<0,0015 by student's *t*-test), that large litters of nine or more pups were only generated in breedings of Irgc$^{+/-}$-mice and to a lesser extent of Irgc$^{-/-}$-mice. In breedings of Irgc$^{+/+}$-mice litters with more than eight pups were not observed (Figure 36b). If these differences are due to the effect of the knockout, must be analysed further. The suggestion is that breedings involving the Irgc^{-}-chromosome are more fertile than those without. In this analysis the roles of male and female breeding partner cannot be resolved. Though the differences in the litter sizes may be accompanied by an uneven segregation of the Irgc wildtype and ko allele leading to a segregation distortion phenotype.

In order to distinguish the roles of the Irgc^{-}-chromosome in the male and female breeding partner, heterozygote males were crossed to homozygote wt females and homozygote males were crossed to heterozygote females. The generated offspring was analyzed for their respective Irgc genotype. Preferential transmission of the Irgc^{-}-chromosome from one breeding partner and deviations from the mendelian segregation ratio could be detected by this experimental setup. In total 401 mice were genotyped, 259 derived from heterozygote males and 142 derived from heterozygote females (Table 11). In 51,4% the Irgc$^{+/-}$-males passed the Irgc^{-}-chromosome to their offspring. This value is close to the 50% expected for a mendelian segregation. However heterozygote females passed their Irgc^{-}-chromosome only to 44,4% of their offspring. Therefore the difference between males and females in the transmission of the Irgc^{-} allele constitutes 7%. Although these numbers indicate statistical significance (p<0,05 by χ² test) the relevance of these data needs further investigations.

Table 11. **Offspring derived from crossings of heterozygote Irgc$^{+/-}$- and homozygote Irgc$^{+/+}$-mice.**

	breeding pairs	litters	offspring	genotype offspring		ratio ♂/♀
				+/-	+/+	
♂ heterozygote x ♀ homozygote	10	32	259	70♂/63♀	76♂/50♀	146♂/113♀
			Ø8,1	133 (51,4%)	126 (48,6%)	56,3%/43,7%
♂ homozygote x ♀ heterozygote	4	21	142	28♂/35♀	37♂/42♀	65♂/77♀
			Ø6,8	63 (44,4%)	79 (55,6%)	45,8%/54,2%

The distribution of the littersize was also analyzed in this cohort of breedings (Figure 37). The mean litter size was bigger for Irgc$^{+/-}$-males 8,1 (± 2,68) compared to 6,8 (± 2,57) for Irgc$^{+/+}$-males (Table 11). However, litters with a size of nine or more pups were also produced by Irgc$^{+/+}$-males in contrast to the first cohort of breedings (Figure 36). It has to be recognized that the females have different Irgc genotypes in these two breedings.
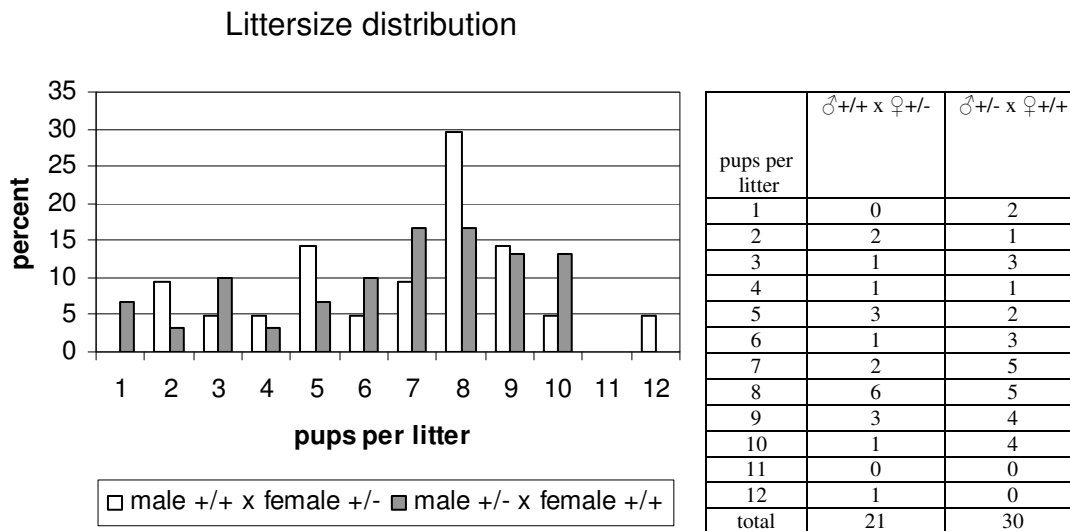
Littersize distribution

pups per litter	♂+/+ x ♀+/-	♂+/- x ♀+/+
1	0	2
2	2	1
3	1	3
4	1	1
5	3	2
6	1	3
7	2	5
8	6	5
9	3	4
10	1	4
11	0	0
12	1	0
total	21	30

Figure 37. **Littersize distribution derived from crossings of heterozygote Irgc$^{+/-}$- and homozygote Irgc$^{+/+}$-mice.** The diagram presents the distribution of litter sizes in percent values. The table gives the absolute numbers.

Besides the small variations in the segregation of the Irgc$^-$ allele there is also a difference in the sex ratio. Irgc$^{+/-}$-males produced 56,3% male offspring, which is slightly above the expected value for C57BL/6 mice of 52,3% (Weir 1960). For Irgc$^{+/+}$-males the ratio of male offspring was 10,5% lower and added up to only 45,8%. The results are also statistical significant (p<0,01 by χ² test). These data will also need further investigation to verify this sex ratio distortion, especially because the data is based on only four breedings of homozygote males and heterozygote females.

3.9   Yeast Two-Hybrid screen for interaction partners

Because the Irgc$^{-/-}$-mouse could so far give no information about the function of Irgc, a yeast two-hybrid screen was performed to detect putative interaction partners of Irgc. A cDNA library from testis was chosen to be screened for such partners. The testis library cloned into the vector pACT2 and transformed into the MATα yeast strain Y187 was obtained from BD

biosciences. These yeasts were mated with AH109 MATa containing pGBD-Irgc as bait. Following 22 hours incubation at 30°C the cells were spread on selective SD-Leu/-Trp/-His/-Ade plates.

After selection two candidates turned out to be true positives in the yeast two-hybrid, which were identified as eRF1 (eukaryotic release factor 1) and GORASP2 (Golgi reassembly and stacking protein 2), also called GRASP55. They both interacted with the vector pGBD-Irgc, containing the Irgc cloned to the Gal4 DNA binding domain, leading to growth of yeast under selective conditions on SD-Leu/-Trp/-His/-Ade plates (Figure 38). To control the specificity of the interaction, yeast containing the eRF1 and GORASP2 constructs were mated to yeast containing the empty vector pGBD-C1, which expresses only the Gal4 DNA binding domain. These yeasts did not grow under selective conditions, indicating that the Gal4 DNA binding domain by itself does not interact with eRF1 and GORASP2, respectively. By introduction of mutations in the highly conserved G1 motif of Irgc the interaction could be altered. The exchange of the K at position 65 to an A (K65A) should prevent hydrolysis of GTP to GDP and P_i, but not the binding of GTP. The second mutation was the change of the S at position 66 to N (S66N). This exchange should abolish the ability of Irgc to bind GTP. Both mutations were chosen in analogy to Irga6, where the desired effect had been demonstrated (Julia Hunn, personal communication). The interaction of eRF1 and GORASP2 to the Irgc K65A mutant was much weaker than to Irgc wildtype, as seen in the clearly reduced growing of yeast in the yeast two-hybrid (Figure 38b,d,e,g). In case of the Irgc S66N mutant the effect was even more drastic. The interaction between Irgc S66N and eRF1 or GORASP2, respectively was completely abolished, resulting in a total inhibition of yeast growth under selective conditions. These effects indicate that the interaction between Irgc and the putative interaction partners is dependent on the binding and hydrolysis of GTP by Irgc.

The IRGs are well conserved to each other and interaction between different IRGs has been demonstrated (Julia Hunn personnel communication). Hence the interaction between the two candidates eRF1 and GORASP2, respectively, and other IRG proteins was analysed in the yeast two-hybrid assay. Yeast transformed with the vector pGBD-C1 containing the ORF of Irga6, Irgb6, Irgd and Irgm1-3 were mated to yeast transformed with pACT1-eRF1 and pACT1-GORASP2, respectively and cultured under selective conditions. eRF1 did not interact with any of the other IRG proteins, but GORASP2 did. It interacted strongly with Irga6 and very weakly with Irgb6. The interaction of GORASP2 and Irga6 in yeast two-hybrid was only slightly weaker than between GORASP2 and Irgc, as seen in a small delay in
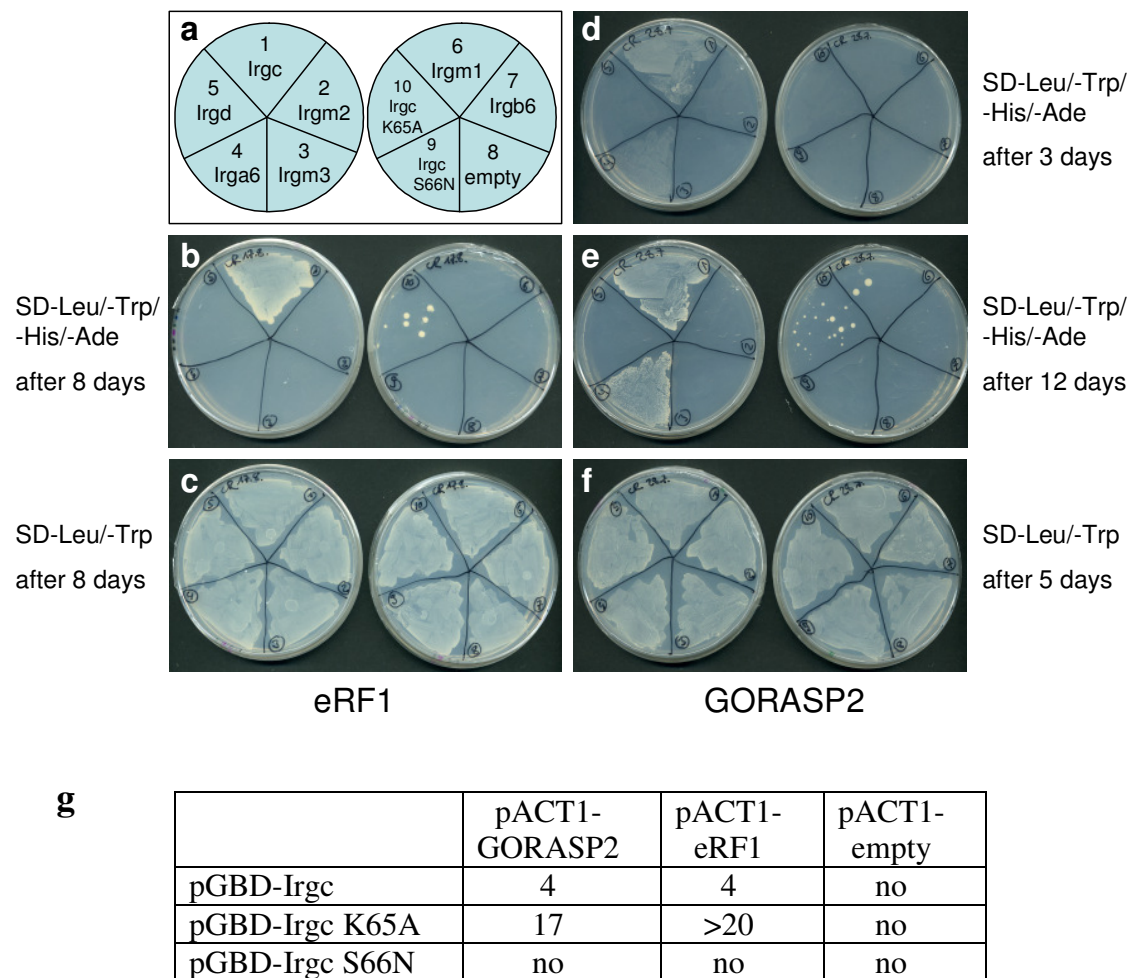
Figure 38. **Interaction of eRF1 and GORASP2 with different IRGs in a yeast two-hybrid assay.** a) Scheme how the different combinations are arranged on the SD-plates. Interaction of pACT-eRF1 and pACT1-GORASP2 with pGBD-…1) Irgc, 2) Irgm2, 3) Irgm3, 4) Irga6, 5) Irgd, 6) Irgm1, 7) Irgb6, 8) empty, 9) Irgc S66N, 10) Irgc K65S. Interaction of IRGs with pACT1-eRF1. After 8 days of selection on SD-Leu/-Trp/-His/-Ade plate (b) or SD-Leu/-Trp plate (c). Interaction of IRGs with pACT1-GORASP2 (clone 17). After 3 days (d) and 12 days (e) of selection on SD-Leu/-Trp/-His/-Ade plates or after 5 days of selection on SD-Leu/-Trp plate. g) Table showing the duration in days until maximal confluency is reached under selective conditions on SD-Leu/-Trp/-Ade plates.

the growing of yeast under selective conditions (Figure 38d). Interestingly, Irga6 and Irgc also interact directly in yeast two-hybrid (Julia Hunn personal communication). The interaction of Irgb6 and GORASP2 is very weak, resulting in the growth of only very few colonies.

In the testis library screen three independent clones of GORASP2 (clone 17, 44, 50) were detected. They all had in common that the protein was C-terminally truncated compared to the full-length GORASP2 ORF. Shorter and co-workers described a testis-specific splice variant of GORASP2 in the rat with a size of approximately 1,4 kb, which is roughly 1 kb shorter than the ubiquitiously expressed GORASP2 mRNA (Shorter 1999). In the full length murine

GORASP2 mRNA the 1355 bp long intron between the Exons 9 and 10 is spliced out, generating an ORF of 1356 bp. 326 bp of the ORF are located on Exon 10. The testis-specific splice variant of GORASP2 was termed tsv GORASP2 (tsv = testis-specific splice variant). In tsv GORASP2 the first 9 exons are shared with the full length form, representing the first 1033 bp of the ORF. But after Exon 9 the transcript runs for 55 bp into the intron 9-10 before the transcription is terminated (Figure 39). The ORF of tsv GORASP2 ends after 26 bp in the intron and has a total size of 1059 bp. The 3'-UTR of tsv is only 29 bp long and contains a poly(A) signal.

In the rat there is also a putative stop codon located in the intron between Exon 9 and 10 after 26 bp and 9 bp downstream of this stop codon there is a poly(A) signal. A putative rat tsv GORASP2 would be 1,1 kb long plus the poly(A) tail, which is roughly 1 kb shorter than the 2,1 kb long normal rat GORASP2 transcript. This fits to the size of 1,4 kb observed by Shorter and co-workers. Thus, it is very likely, that the testis specific variant of rat GORASP2 described by Sorter and co-workers is generated in the same way as in the mouse.
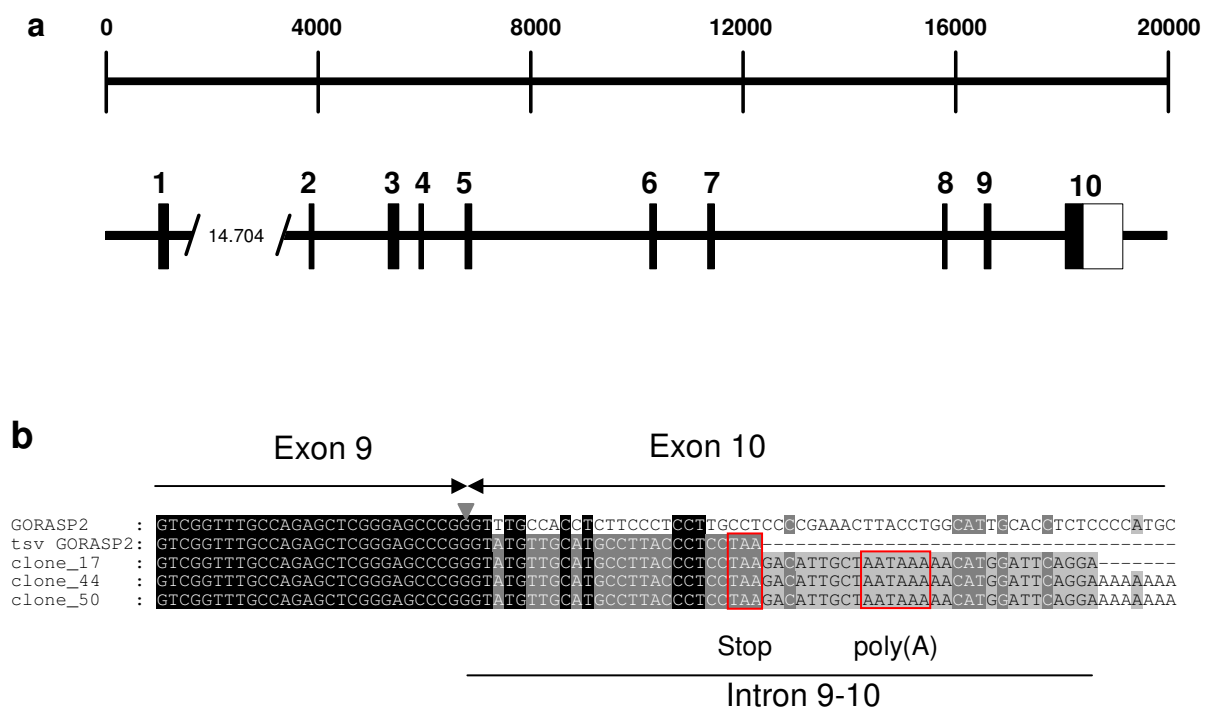

Figure 39. **Scheme of splicing pattern of the tsv (testis-specific splice variant) GORASP2.** a) Scheme of the genomic localization of the 10 exons of GORASP2. Black boxes represent coding exons, white boxes non-coding parts of exons. b) The alignment of the GORASP2 ORF and the GORASP2 clones (17, 44, 50) identified in the yeast two-hybrid screen revealed the structure of tsv GORASP2. Last base of Exon 9 at position 1033 of the ORF is indicated by the grey arrowhead. Sequence of GORASP2 continues with Exon 10, tsv GORASP2 with Intron 9-10, leading to a truncated version of the protein lacking the complete Exon 10. Stop-codon and poly(A) signal of tsv GORASP2 are indicated by red boxes.

The expression pattern of tsv GORASP2 in the testis was examined with an RT-PCR approach discriminating between normal and tsv GORASP2. The developmental regulation of both forms was analyzed in developing postnatal testis from mice of different ages. The normal form of GORASP2 was expressed on a constant level in the testis independent of the age (Figure 40). In contrast to that tsv GORASP2 is expressed in low levels in very young, 2 days old mice, but the expression was strongly upregulated starting from around day 19, which is the time when the first haploid spermatids are generated in the testis (Vergouwen 1993), implicating that tsv GORASP2 is strongly expressed in spermatids.
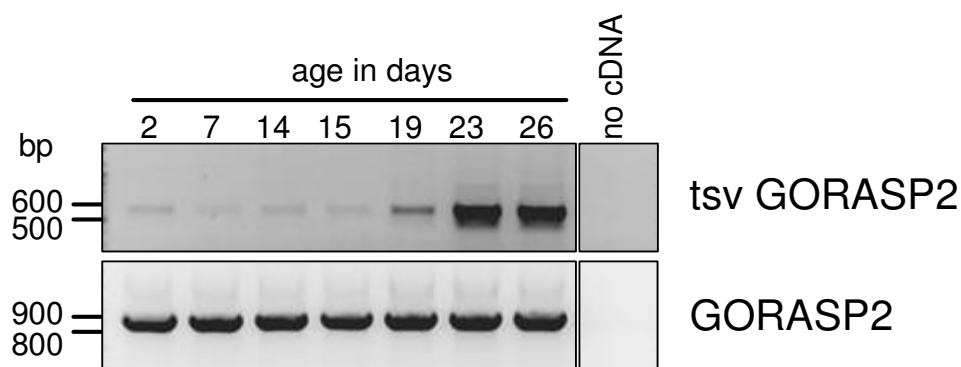

Figure 40. **Comparism of GORASP2 and tsv GORASP2 expression in mouse testis.** RNA from testis of mice with an age of 2 to 26 days was analysed by RT-PCR for the expression of tsv GORASP2 and GORASP2.

To test this assumption, the tsv GORASP2 expression levels in different parts of the testis were compared. The seminiferous tubules were divided into two regions. The outer region contains the diploid spermatogonia and spermatocytes and the inner region, the center of the tubules, containing the haploid spermatids and spermatozoa. These regions were cut by laser microdissection (LMD) from Nuclear Fast Red stained cryosections of mouse testis (Figure 41). Pools of roughly 100 sections from each region were generated. Additionally a pool of 50 sections from whole *tubuli seminiferi* was generated. Then the RNA was isolated from these pools and followed by RT-PCR looking for GORASP2, tsv GORASP2, Irgc and GAPDH transcripts. The expression level of GORASP2 and GAPDH were quite similar in the inner and outer region (Figure 42). tsv GORASP2 was also expressed in both regions, but the expression in the inner region was stronger. The differences between inner and outer region were most significant for Irgc. While it was strongly expressed in the haploid cells of the inner region, it was hardly detectable in the outer region. Hence, these results confirm the conclusion that GORASP2 is upregulated in haploid spermatids and consequently is most

abundant in the population of spermatogenic cells which also express Irgc. The question if spermatogenic cells express both forms of GORASP2 or switch from the normal form to tsv at some point in spermatogenesis can not be answered with this experimental approach, because the samples from the inner region also contain Sertoli cells, which are located from the basis to the center of the *tubuli seminiferi*. Therefore the pool from the inner region also contains Sertoli cells and does not consist of a pure haploid population of cells. Additionally a contamination of the cell pools can not be excluded. Hence, the very low signal for Irgc expression in the outer region is most likely the result of few spermatids contaminating the pool of sections. Also it has to be taken in account, that tsv is expressed in low levels in the testis in very young mice, which do not possess any haploid cells yet. Hence, 100% haploid specific expression of tsv GORASP2 can be excluded.
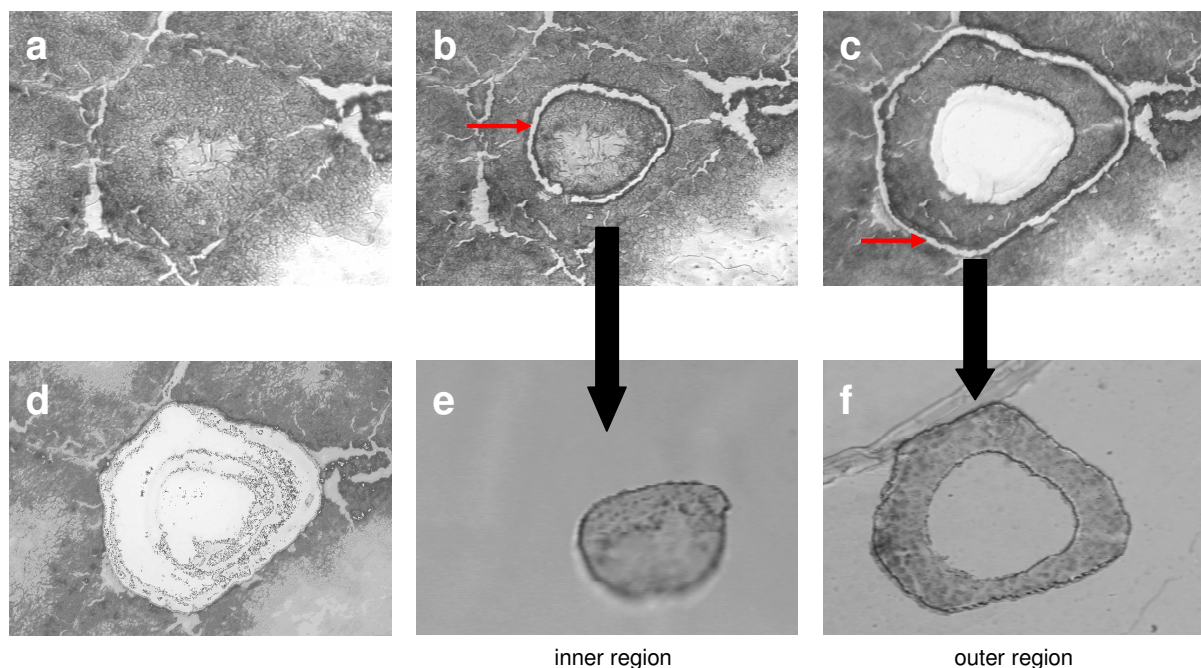

Figure 41. **Samples cut from testis sections by laser microdissection.** a) Shows a Nuclear Fast Red stained seminiferous tubule of 10 µm thick cryosection on membrane-covered slide. b) The inner region of the tubule containing the haploid spermatids and spermatozoa is cut with the laser. The red arrow marks the section made with the laser. The sample transferred with a laser beam onto a drop of mineral oil in a cap above the slide (e). c) After the inner region has been removed the outer region is (red arrow) and also transferred onto a separate cap (f). d) Section after the sequentially removal of the seminiferous tubule.
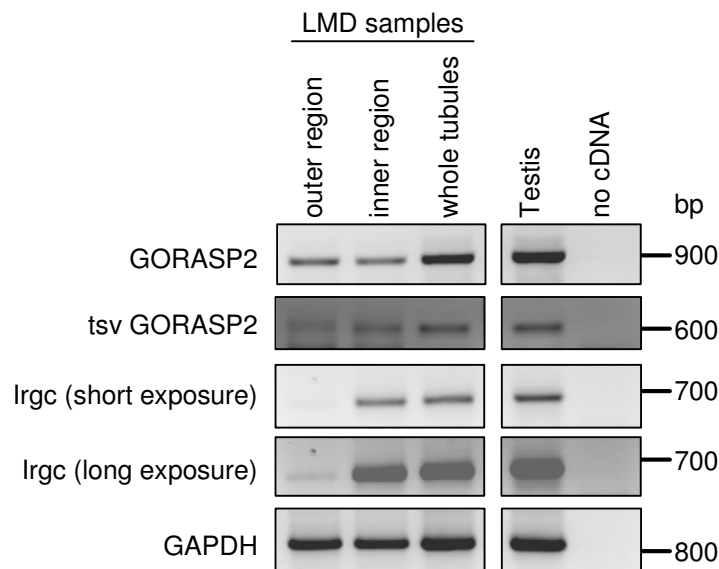
Figure 42. **RT-PCR on laser microdissection samples of seminiferous tubules.** Cells were cut by laser microdissection (LMD) from seminiferous tubules in testis section. Outer region contains cells on the basis of seminiferous tubules (spermatogonia, spermatocytes), inner region cells from the inner part of the tubules (spermatids, spermatozoa). RNA was isolated from sections and analysed by RT-PCR with 50 amplification cycles for the expression of GORASP2, tsv GORASP2, Irgc and GAPDH. RNA from whole tubules and cDNA from whole testis were taken as controls.

3.10 Irgc does not interact with Hook1

The first protein described to interact with an IRG protein was the microtubule binding protein Hook3 (Kaiser 2004), which interacts with Irga6 in bone marrow-derived macrophages. The family of Hook proteins consists of three members. Interestingly, Hook1 shows an expression pattern in testis similar to Irgc, meaning it is transcribed predominantly in haploid spermatids. A natural occurring mutation in the Hook1 protein was shown to be responsible for the abnormal spermatozoon head shape (azh) mutant mouse (Mendoza-Lujambio 2002). The non-functional Hook1[azh] leads to a dysmorphic structure of the manchette, a structure made out of microtubules responsible for shaping the nucleus and the spermhead. This results in an abnormal shape of the sperm head (Meistrich 1990). Other features of this mutation are tailless sperms and arrests of spermatogenesis in some *tubuli seminiferi*.

Since interaction between Hook and IRG proteins had been demonstrated and Hook1 and Irgc have the same expression pattern, interaction between these two proteins was tested. Yeast transformed with the vectors pGBK-Hook1 or pGAD-Hook1 were mated with yeast containing pGAD-Irgc or pGBD-Irgc, respectively, to test if these two proteins interact in the yeast two-hybrid system. Under selective conditions on SD-Leu/-Trp/-Ade no growth of yeast
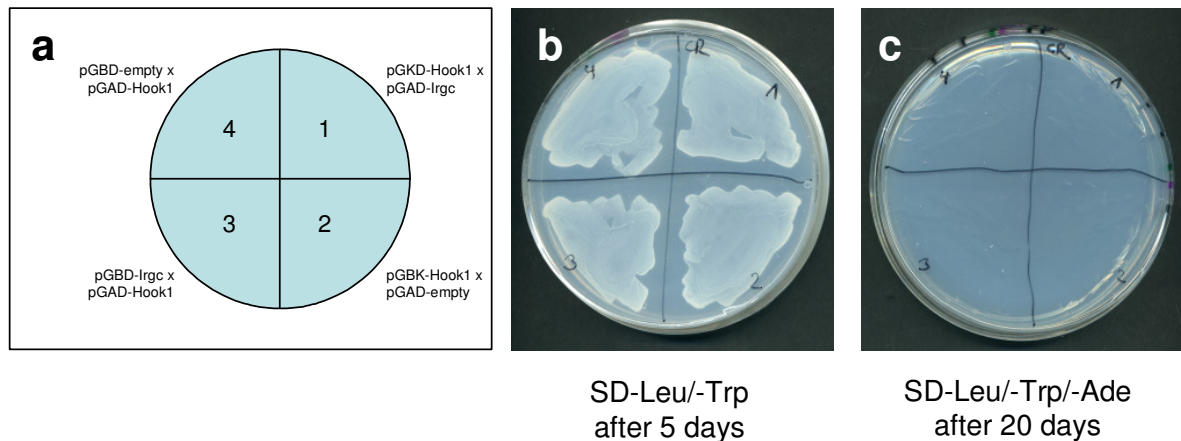
Figure 43. **Irgc and Hook1 do not interact in a yeast two-hybrid assay.** a) Scheme how the different combinations are arranged on the SD-plates. Growth of yeast on SD-Leu/-Trp plates after 5 days (b) and on SD-Leu/-Trp/-Ade plates after 20 days.

was detected (Figure 43), meaning that Hook1 and Irgc did not interact in this experimentel setup.

Irgc$^{-/-}$ mice do not show any phenotype, Hook1$^{azh/azh}$ mice show the abnormal spermatozoan headshape leading to a drastically decreased fertility of Hook1$^{azh/azh}$ males. If Irgc and Hook1 interact directly or in some common pathway, the deficiency of both proteins might result in a more severe phenotype in spermatogenesis. Thus, female Hook1$^{azh/azh}$-mice were bred to male Irgc$^{-/-}$-mice. The resulting offspring was screened for Hook1$^{+/azh}$/ Irgc$^{+/-}$ mice, which were interbred to generated homozygous double knock out mice. Testis from Hook1$^{+/+}$/ Irgc$^{+/+}$-, Hook1$^{azh/azh}$/ Irgc$^{+/+}$- and Hook1$^{azh/azh}$/ Irgc$^{-/-}$-mice were embedded in paraffin and haematoxylin and eosin stained sections were prepared to compare the testis morphology in these three genotypes. The Hook1$^{azh/azh}$/ Irgc$^{+/+}$-mouse showed the characteristic previously described deformed sperm heads (Figure 44e, g, i). Most of the *tubuli seminiferi* displayed normal spermatogenesis (Figure 44b). The Sertoli-cell-only syndrome reported by Mendoza-Lujambio and co-workers in few seminiferous tubules could not be observed (Mendoza-Lujambio 2002). The additional Irgc deficiency did not lead to a more severe phenotype in Hook1$^{azh/azh}$/ Irgc$^{-/-}$-mice (Figure 44c, f, h, j) compared to Hook1$^{azh/azh}$/ Irgc$^{+/+}$-mice. The same defects in sperm head morphology were observed and single and double knockout were indistinguishable from each other. However, additionally the fertility of Hook1$^{azh/azh}$/ Irgc$^{+/+}$- and Hook1$^{azh/azh}$/ Irgc$^{-/-}$mice should be compared, since the effect of the double knockout may be morphological invisible. The *azh* mutation leads to a drastically reduced fecundity between 4% and 9% of wildtype mice, but not to a complete sterility (Meistrich 1994). If the number of offspring produced by Hook1$^{azh/azh}$/ Irgc$^{+/+}$-males would be significantly different from that
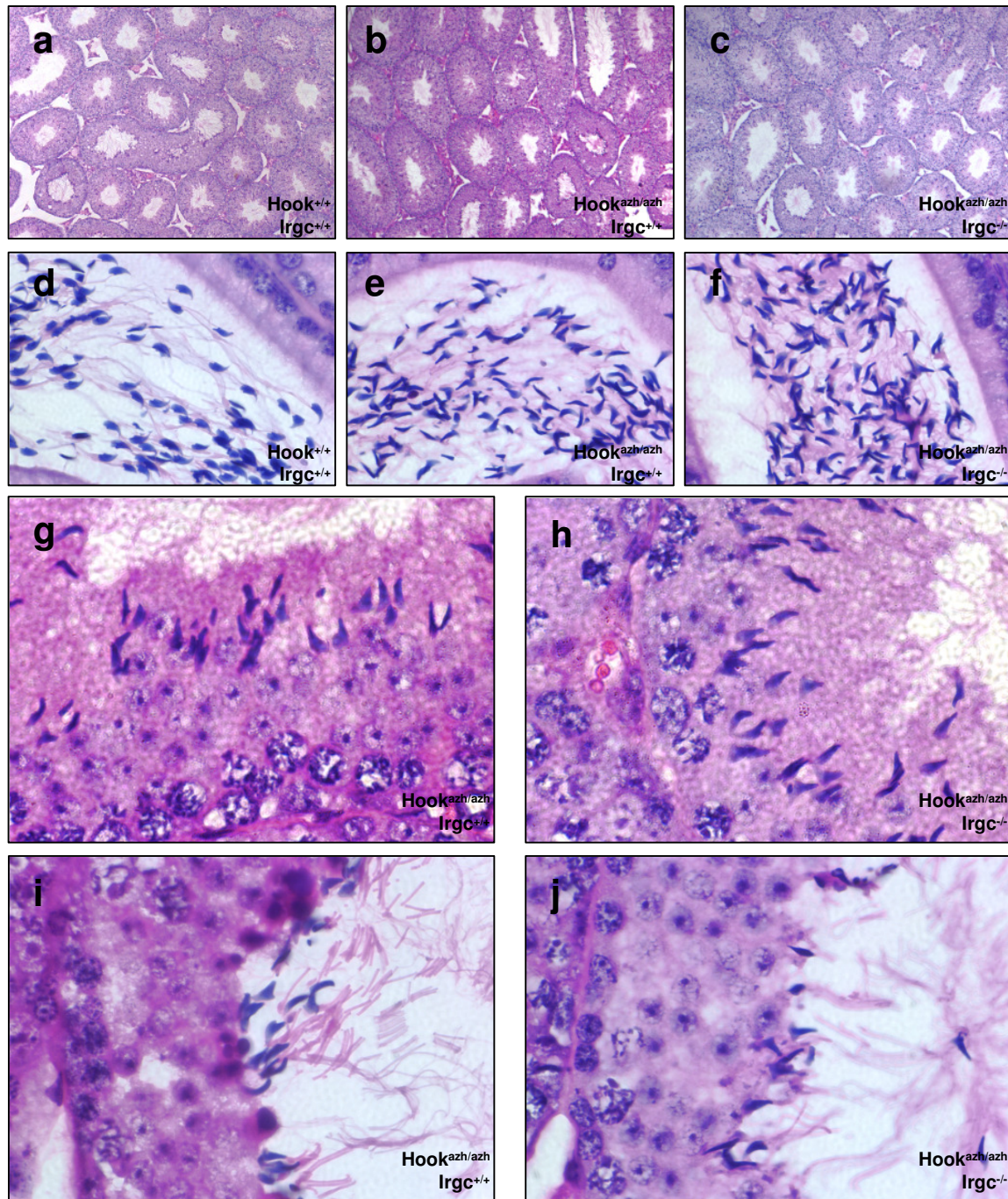
Figure 44. **Phenotype of Hook1$^{azh/azh}$/ Irgc$^{+/+}$- and Hook1$^{azh/azh}$/ Irgc$^{-/-}$-males in testis is the same.** Comparison of testis morphology in Hook1$^{+/+}$/ Irgc$^{+/+}$-, Hook1$^{azh/azh}$/ Irgc$^{+/+}$- and Hook1$^{azh/azh}$/ Irgc$^{-/-}$-mice on haematoxylin and eosin stained paraffin sections. Overview on the morphology of the seminiferous tubules in wt (a), Hook1$^{azh/azh}$/ Irgc$^{+/+}$- (b) and Hook1$^{azh/azh}$/ Irgc$^{-/-}$-mice (c). Normal spermatozoa in the epididymis of wt mice (d) and deformed spermatozoa of Hook1$^{azh/azh}$/ Irgc$^{+/+}$- (e) and Hook1$^{azh/azh}$/ Irgc$^{-/-}$-mice (f) with the characteristic azh headshape. Defective sperm development in Hook1$^{azh/azh}$/ Irgc$^{+/+}$- (g, i) and Hook1$^{azh/azh}$/ Irgc$^{-/-}$-mice (h, j) leading to the abnormal spermatozoan headshape. Magnification: a-c: 100x, d-j: 1000x.

of Hook1$^{azh/azh}$/ Irgc$^{-/-}$-males the lack of both proteins would have an additional phenotype. Unfortunately, neither the 2 Hook1$^{azh/azh}$/ Irgc$^{+/+}$-males nor the 2 Hook1$^{azh/azh}$/ Irgc$^{-/-}$-males tested were able to produce any offspring, meaning that all these males were infertile.

Taken together, the performed experiments do not support the assumption that Hook1 and Irgc interact in any way with each other.

3.11 Irgc does not interact with Irgq in yeast two-hybrid

In all mammalian species that possess the quasi-GTPase *IRGQ* it is closely linked to *IRGC* (Bekpen 2005, Julia Hunn personal communication). This linkage is very well conserved and it is tempting to speculate that these two genes are linked to each other because they interact in some way with each other.

In a yeast two-hybrid approach the interaction of mouse Irgc and Irgq was tested. The whole Irgq ORF and the 406 amino acids encoded on the long Exon 4 (IrgqE4) were cloned into the yeast two-hybrid vectors pGAD-C1 and pGBD-C1 and then transformed into yeast with the proper mating type. These yeasts were mated with yeast containing pGAD-Irgc and pGBD-Irgc respectively and then cultured, but under selective conditions on SD-Leu/-Trp/-Ade plates no growth of yeast was observed (Figure 45). Hence, Irgc and Irgq did not interact in this assay.
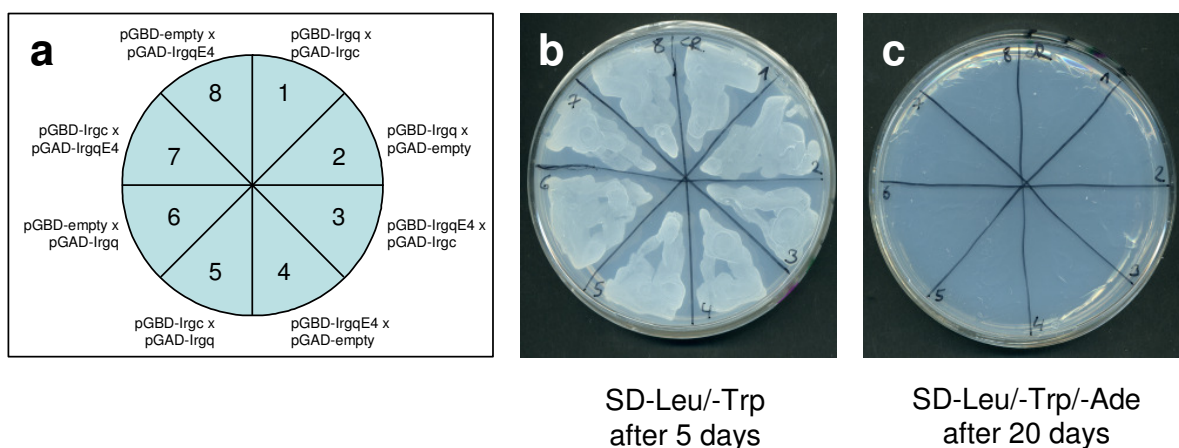

Figure 45. **Irgc and Irgq do not interact in a yeast two-hybrid assay.** a) Scheme how the different combinations are arranged on the SD-plates. Growth of yeast on SD-Leu/-Trp plates after 5 days (b) and on SD-Leu/-Trp/-Ade plates after 20 days.
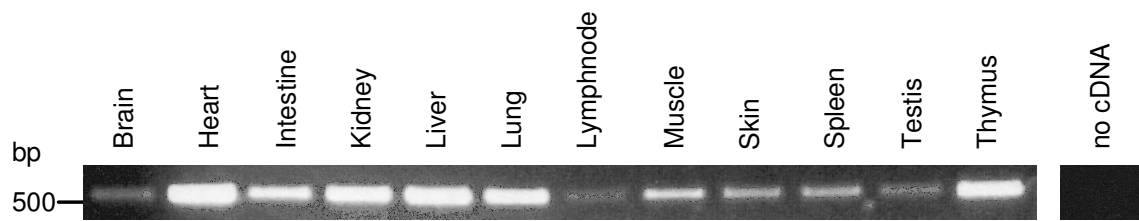
Figure 46. **Irgq is ubiquitously expressed.** Expression of Irgq was analysed in the indicated mouse tissues by RT-PCR with 50 amplification cycles.

Next we analyzed the expression pattern of Irgq in mice by RT-PCR. The transcript of Irgq was detected in all tissues analyzed suggesting that it is expressed ubiquitously (Figure 46). Thus, the expression pattern of Irgq is strinkingly different from that of Irgc, which is only expressed in haploid spermatids.

Despite the conserved linkage of Irgc and Irgq, no experimental data suggesting an interaction between these two proteins could be obtained.

4.   Discussion

The Immunity-related GTPases (IRGs), also known as p47 GTPases, have been discovered as a prominent part of the cellular response to the stimulation with interferon-γ (Gilly 1992). Subsequently their role as important resistance factors in the mouse was established. The group of intracellular pathogens identified to be affected by the actions of IRG proteins is growing (Taylor 2007).

One member of the GTPases in the mouse is different in many aspects. *Irgc* is not included in the clusters on chromosome 11 and 18 harbouring all the other *IRG* genes but has a unique chromosomal localization on chromosome 7. Interestingly, *Irgc* is the only *IRG* gene with an unambiguous orthologue in humans. Therefore it is essential to study *Irgc* in the mouse in order to get insights into the role of *IRG* genes in humans.

4.1   *IRGC* is highly conserved among mammals

IRGC was previously identified in the mouse, human, rat, dog, cat and rat, but the sequence of the complete ORF was available only for mouse and human (Rohde 2003). Since then the genome sequencing projects of many species have made huge progress. As a result of this development the number of *IRGC* genes identified by BLAST searches in different species grew from six to 21. In 12 species the complete ORF was identified, in another nine fragments of varying sizes. All these *IRGC* orthologues were derived from mammals and included all three mammalian subclasses; the *Monotremata*, the *Marsupialia* and the *Eutheria*. This implies that *IRGC* is the only *IRG* gene that is conserved in all mammals, since higher primates have lost all other *IRG* genes except *IRGC*, the truncated *IRGM* fragment and a highly anomalous, IRG-related sequence previously named IRGQ.

The IRGC protein is highly conserved with amino acid identities of at least 88% between the available full-length sequences. Although for the two evolutionary most distant species, the monotreme platypus and the marsupial opossum, only fragments of IRGC were discovered, these fragments already suggest that the amino acid identity compared to the other orthologues will still be very high (Figure 9). The high degree of similarity between the IRGC proteins was also demonstrated by a phylogenetic analysis. In comparison between all mouse IRG proteins and a subset of IRGC proteins it was revealed, that mouse Irgc is much closer related to all other IRGCs than to any other mouse IRG (Figure 10). The divergence within

the different clades of mouse IRG proteins, the Irgas, Irgbs, Irgds or Irgms, is much bigger than among the IRGC proteins from different mammals. This strong conservation suggests a conserved function throughout the mammals, most likely in a conserved mechanism. It contrasts with the rapid evolution and expansion seen in the other *IRG* genes (Bekpen 2005), that was also reported for other multigene families involved in pathogen resistance like the 2'-5' olidoadenylate synthetase gene family (Kumar 2000) or the CD33-related subfamily of Siglecs (Angata 2006).

Outside the mammals a clear orthologue of *IRGC* is missing, although *IRG* genes were detected in all classes of vertebrates except birds, and also in the cephalochordate *Branchiostoma floridae* which has 16 IRG homologues (Bekpen 2005, Julia Hunn personal communication). Recently a putative *IRGC* orthologue was discovered in the reptile *Anolis carolinensis* (AAWZ01048015), which got the provisional name AC GKS10 (Julia Hunn personal communication). In phylogenetic analysis it locates close to the IRGC clade, suggesting that it is IRGC-related (Figure 12). Alignments of this *Anolis* sequence with diverse other IRG proteins were conducted in order to identify conserved features in addition to the canonical GTP-binding motifs (Figure 11). AC GKS10 shares a list of sequence features with both IRGC and IRGC-like proteins, respectively, and is clearly IRGC-related. Based on the sequence data available it is not possible to decide whether AC GKS10 is closer related the IRGC or IRGC-like clade. Anyway it seems very likely that AC GKS10 is derived from the same ancestral gene as *IRGC* and *IRGC-like* genes, respectively.

Interferon-induction of *IRG* genes has also been shown outside the mammals in the zebrafish (Dirk Sieger, Cornelia Stein personal communication). Since *Anolis carolinensis* possesses a repertoire of 10 different *IRG* genes belonging to different clades (Julia Hunn personal communication) it is likely that at least some of them are interferon-inducible and involved in immunity. Therefore it would be very interesting to analyze the expression profile and interferon-inducibility of AC GKS10. Constitutive expression in the testis would strongly indicate that the function may be conserved relative to mammalian IRGC proteins.

Taken together it can be concluded that the *IRGC* genes are highly conserved in mammals and form a distinct clade in the family of *IRG* genes. The finding of the AC GKS10 sequence in reptiles indicates that *IRGC* may be present also outside the mammals.

In addition to the sequence of the protein the structure of the gene is also conserved. The gene structure from seven *IRGC* orthologues, mouse, rat, cat, dog, bull, chimpanzee and human,

could be resolved (Figure 13). As is characteristic in general for *IRG* genes, the complete ORF is encoded on a single long exon, which is preceded by a short untranslated exon. This untranslated 5'-exon is strongly conserved between all seven *IRGC* genes, although the start point of the 5'-exon is not exactly defined yet. The most 5' positioned base verified by ESTs or RT-PCR experiments to be transcribed varies between the seven analyzed species (Figure 14). The strong conservation of the region including the 5' exon and the promoter makes it tempting to speculate that the transcription of all *IRGC* genes starts at the same position.

Nevertheless, there is striking difference between mouse and rat on the one side and all other species on the other side. In mouse and rat the downstream splice site of the 5' exon is different, leading to a 5' exon that is more than 140 bp longer than in the other species (Figure 14). The splice site used in the other species is still present in mouse and rat. The cause for the preference of a different splicing site has not been revealed.

Interestingly the stop codon TAA is part of the putative poly(A) signal in many *IRGC* genes, although this feature is not generally conserved (Table 8). For the classes lacking the AATAAA, namely the carnivores, artiodactyls, perissodactyls and proboscideans, no other common poly(A) signal (AATAAA/ATTAAA) was detected in the putative 3'-UTR, which is most likely shorter than 100 bp (Figure 13, 19). Since especially in haploid spermatogenic cells the use of alternative poly(A) signals is common and up to 30% of the polyadenylated transcripts lack the common poly(A) signals AATAAA and ATTAAA (MacDonald 2002, Liu 2007), the use of another signal seems very likely for *IRGC* in those species where an AATAAA or ATTAAA is not present. Since IRGC mRNA from cat, dog and bull, which do not have a common poly(A) signal (Table 8, Figure 19), could be reverse transcribed into cDNA by oligo-dT priming, these transcripts also have to be polyadenylated (Figure 25).

4.2   Highly conserved elements in the promoter of *IRGC*

The promoter of IRGC is well conserved among mammals. Three transcription factor binding sites are conserved in all seven analyzed orthologues (Figure 14). These are the Sox5, Sox17 and NF-Y binding sites.

The family of Sox (SRY-related high-mobility-group box) transcription factors consists in mouse and human of 20 genes divided into ten separate groups and are regulators of diverse developmental processes (Bowles 2000). They contain the HMG domain previously identified in SRY (sex determining region Y gene), which is responsible for DNA binding. The

recognition sequences of all Sox proteins are very similar, but they have distinct expression patterns and molecular properties (Wilson 2002).

Sox5 was discovered as transcription factor that is massively expressed in haploid spermatids (Denny 1992). Besides its testicular expression an essential role of Sox5 in chondrogenesis has been discovered (Lefebvre 1998, Smits 2001). So far one target of Sox5 in testis was identified, which is *IκBβ* (Budde 2002). Indeed *IκBβ* and *IRGC* show the same expression pattern in the testis (Figure 47). Both are expressed in haploid spermatids, where Sox5 is also present in high amounts. These data are highly suggestive for an activating effect of Sox5 on *IRGC* transcription. Although binding of Sox5 to the altered Sox5 site 5'-ATTATT-3' present in all studied *IRGC* promoters has been shown (Denny 1992), direct binding of Sox5 to the *IRGC* promoter has to be demonstrated to support the assumption that Sox5 is involved in the transcriptional regulation of *IRGC*.
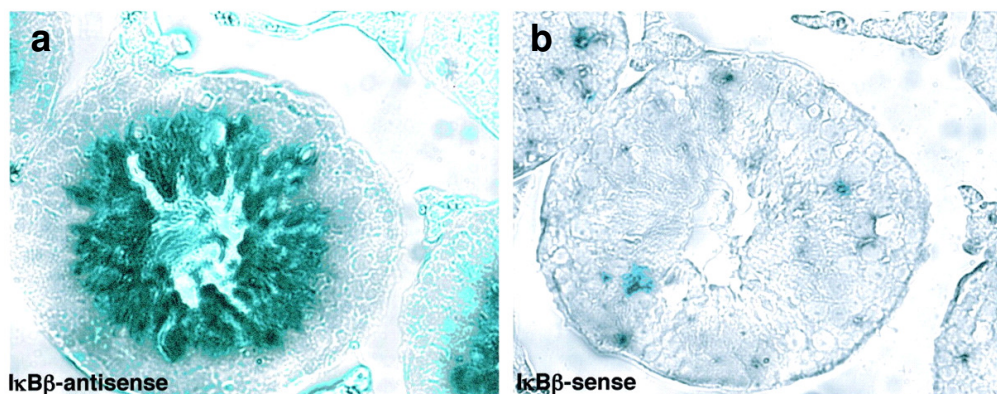
Figure 47. **Expression of IκBβ mRNA in mouse testes in haploid spermatids (from Budde 2002).** *In situ* hybridization of sections from mouse testes. a) With the antisense IκBβ probe mRNA was detected in haploid spermatids. b) Specificity of the probe was demonstrated by using the IκBβ-sense probe, which did not generate any specific signal.

The role of Sox17 in spermatogenesis is complex. The expression of a truncated isoform of Sox17 that can neither relocate into the nucleus nor bind the recognition sequence was shown in postmeiotic cells (Kanai 1996). In contrast, in premeiotic cells the full-length Sox17 was expressed. This lead to the conclusion, that Sox17 loses its activity through this switch to the truncated isoform (Kanai 1996). Nevertheless, Sox17 has been implicated in the activation of transcription of SPAG6, PF6 and PF20 in the mouse, which are essential components of the central apparatus of the axoneme in the spermtail (Horowitz 2005). Expression of these genes is upregulated in the testis from day 16 postpartum (p.p.), which suggests initiation of

transcription during meiosis. Mouse Irgc expression is detectable from day 19 p.p. on in the testis. Taken into account that the Sox17 site detected in the promoter of *IRGC* differs from the main consensus sequence of the Sox17 recognition site and that the assumptions of Horowitz and co-workers are based on *in silico* promoter analysis and are not supported by direct experimental data, an activating effect of Sox17 on *IRGC* transcription seems unlikely.

The Nuclear factor-Y (NF-Y) is a universal transcription factor recognizing the CCAAT-box (Montavani 1998). Hence it is unlikely to be the main regulator of *IRGC* expression in haploid spermatids. NF-Y was shown to interact with other transcription factors und thus stimulate their activity. Among these factors were also Sox7 and Sox17 (Niimi 2004). An interaction with Sox17, however, is unlikely in the case of *IRGC*. Firstly, there are some arguments against a role of Sox17 in the regulation of *IRGC* as discussed above. Secondly, NF-Y and Sox17 would bind exactly at the same position in the *IRGC* promoter and thus binding of both transcription factors at the same time is not possible. However, since interaction of NF-Y with Sox proteins has been shown, Sox5 may interact with NF-Y to initiate *IRGC* transcription.

4.3   *Irgc* is expressed only in haploid spermatids

The expression pattern of mouse *Irgc* was analyzed in detail with a wide variety of methods and *Irgc* expression could be localized in haploid spermatids, suggesting a function of Irgc in spermatogenesis (Figure 15, 16, 20, 21).

The protein is present only in haploid spermatids, as was demonstrated by immunocytochemical stainings (Figure 21). A sharp boundary between Irgc expressing spermatids and non-expressing spermatocytes was evident. This indicates the tight regulation of Irgc transcription and translation. Irgc is located mainly in the cytosol, but there is also a membrane-bound fraction of Irgc as was demonstrated by hypotonic lysis of *tubuli seminiferi* (Figure 24). Hence the membrane-binding behaviour is consistent with that of other GKS-IRG proteins.

The absence of Irgc from the mature spermatozoa, which are released into the lumen of the seminiferous tubules after spermiogenesis, was demonstrated (Figure 22). This implicates that Irgc is involved only in the formation of the sperm, but does not mediate a function in the mature sperm itself, like other testis-specific proteins (Table 1). Two possible explanations for the absence of Irgc from sperm are imaginable. The cellular pool of Irgc could be degenerated by the time of spermiation. Though there would not be any detectable protein left. The half

life of Irgc protein is unknown, but for Irga6 it is approximately 16 hours (Tobias Steinfeldt personal communication). Most likely the half life of Irgc is even longer, because it takes at least 6 days from the first detectable appearance of Irgc in the testis at day 25 p.p until a constant Irgc level is reached sometime between day 31 and 35 p.p (Figure 18). Since Irgc is still detectable in late elongated spermatids (Figure 21, 23) it seems unlikely that the complete Irgc pool degenerates within the last day of spermiogenesis. This leads to the other possible mechanism, that Irgc gets excluded with the removal of the cellular cytoplasm. The squash preparations of the *tubuli seminiferi* suggest that Irgc gets excluded from the spermatozoa with the residual body (Figure 23). An interesting question in this context is whether Irgc gets eliminated passively with other cellular components, which are not needed anymore or takes over an active role in the formation of the residual body. Little is known about the exact molecular mechanisms leading to the formation of the residual body. The residual body shares some features associated with apoptosis. Their membrane binds to Annexin V, the cytoplasm is condensed and the levels of CASPASE-1 and the BCL2 family-member BAK are elevated (Krajewski 1996, Blanco-Rodriguez 1999). Like apoptotic germ cells the residual bodies are phagocytosed by Sertoli cells (Chemes 1986, Shiratsuchi 1997). Hence local actions of caspase-cascades have been suggested to promote the elimination of cytoplasm as has been shown in *Drosophila* (Huh 2004). However IRG proteins have not been implicated in the activation of apoptosis yet.

The enrichment of acid phosphatase activity attributable to endogenous lysosomes led Chemes to the conclusion that autophagy is involved in the early phase of residual body formation (Chemes 1986). Other data supporting this indication is missing and also nothing is known about the expression of autophagy markers like Atg5 (Klionsky 2003) or LC3 (Kabeya 2000) in elongated spermatids. Since Irgm1 was shown to be an inducer of autophagy in macrophages in defense against *M. tuberculosis* (Gutierrez 2004) it is tempting to speculate that Irgc is involved in the induction of autophagy as a mechanism to start elimination of residual cytoplasm in elongated spermatids.

IRGC is the only full length *IRG* gene in higher primates. Thus the IRGC proteins in these species have to mediate their function independent of any other IRG protein. The expression pattern of *IRGC* in the testis is conserved among different mammals (Figure 26, 27). This conserved expression profile in haploid spermatids strongly implicates a conserved function in sperm development in mammals, independent of the number of *IRG* genes which the respective species possesses. Interestingly, the anti-microbial function of interferon-inducible

IRG proteins seems to require complex interactions between different family members (Julia Hunn, Steffi Könen-Waisman, Sascha Martens, Nina Schröder personal communication). Since higher primates have only one IRG protein left it has to mediate its function alone or together with other non-IRG proteins. Therefore it is likely that IRGC proteins outside the higher primates mediate their function also independent of other IRG proteins.

As demonstrated, Irgc is transcribed up to 6 days earlier than translated, indicating translational repression of the mRNA (Figure 18). This is common in spermatogenic cells (Kleene 2003). Because the nucleus becomes compacted and therefore transcriptional inactive, all necessary mRNAs have to be synthesised before this stage of development is reached. Thus the appearance of a protein in haploid spermatids is mainly regulated through repression and activation of translation and not transcription. The mechanisms of translational repression in spermatogenic cells are not universally understood yet. The best characterized examples are the protamines. Their translation is regulated upon at least two motifs located in the 3'-UTR, the translational control element (TCE) (Zhong 2001) and the Y-box recognition sequence (YRS) (Fajardo 1997, Giorgini 2000, 2001). Since protamines have an expression profile similar to Irgc a similar repression mechanism was considered, but both motifs are absent from the 3'-UTR of Irgc. Otherwise the mechanisms of translational repression in postmeiotic cells remain largely unknown. Recently the 5'-UTR and 3'-UTR of the sperm mitochondrial cysteine-rich protein (SMCP) has been implicated in translational repression, but the sequence motifs responsible for the translational inhibition have not been identified yet (Hawthorne 2006). Regulation of the length of the poly(A) tail in the cytoplasma by the testis-specific cytoplasmic poly(A) polymerase (TPAP) is also involved in translational activation, but the motifs or factors regulating the activity of TPAP are still unknown (Tay 2001, Kashiwabara 2002). Thus the mechanism regulating the translational repression and activation of IRGC remains unknown. The highly conserved sequence motifs detected in the 3'-UTR of IRGC (Figure 19) are promising candidates for further investigations of the translational control of IRGC.

Although the majority of IRGC ESTs from the databases were derived from the testis, ESTs from other tissues were also present (Table 10). Besides the 24 ESTs from the testis, from the macaque also 20 ESTs derived from ovaries are present in the database. Since ovary and testis are the only two organs to produce haploid cells this could indicate, that the function of IRGC would be haploid specific rather than spermatid specific and may be related to meiosis,

although the expression pattern of IRGC argues against that. The IRGC ESTs derived from the macaque ovary in the database were derived from a young adult female animal. Therefore young adult mice (8 weeks old) were chosen to investigate the Irgc expression in mouse ovaries, but no transcripts or protein could be detected. Although it has to be considered that most oocytes in the ovary are arrested in the prophase I of meiosis and less than 100 are at different stages of follicle development in mouse and rat and even less in primates (Hirshfield 1991). Thus the number of haploid cells is much lower in the ovary than in the testis, which could make detection of haploid-specific transcript more difficult in females. In this context it should be mentioned that all ESTs from macaque are derived from a single set of experiments and only one animal.

However, in mouse expression of Irgc in any other organ than testis could not be detected (Figure 15, 16). The same was true for human, where IRGC transcripts were detected in the testis, but not in brain and liver (Figure 25). Results obtained during my diploma thesis, which showed in a single experiment expression of Irgc in Purkinje cells in the brain detected by immunocytochemistry could not be repeated (Rohde 2003). Differences in the expression pattern between different mammalian species are unlikely, because the promoter is highly conserved. For example, in the IRGC promoter of the bull no liver-specific promoter elements were detected, although seven ESTs from the liver are present in the database.

4.4   IRGC is not a resistance factor

As mentioned before, the *IRG* genes were discovered as a major part of the cellular response to stimulation with IFN-γ (Gilly 1992, Boehm 1998). The role of different IRG proteins as resistance factors has been demonstrated. These are two functional characteristics of *IRG* genes in general, which are both not true for *IRGC*.

The interferon-inducibility of *IRG* genes is mediated by multiple ISRE and GAS sites in the promoter region of the respective genes and their inducibility has been demonstrated (Gilly 1992, Boehm 1998, Bekpen 2005). The *IRGC* promoter is lacking any interferon related promoter elements. As a result neither the stimulation with type I interferon nor type II interferon have any inducing effect on IRGC expression (Figure 28, 30). This was tested for mouse and human cell lines. Also *in vivo* infection of mice with *L. monocytogenes* did not have any effect on the expression of Irgc (Figure 29). Therefore *IRGC* is lacking this functional characteristic feature, inducibility by interferon-γ, common for most other *IRG* genes.

The fact that *IRGC* has a conserved expression pattern in the testis in all mammals analyzed and possesses a promoter without any interferon response elements, strongly suggests, that IRGC is, in contrast to the other IRG proteins, not a resistance factor. In the light of this conclusion, the differences in the arsenal of *IRG* genes between higher primates and all the other mammals become increasingly interesting. Especially the comparison between human and mouse deserves special attention, because the mouse is used as a model for human infectious disease. At least 14 of the mouse *IRG* genes are inducible by interferon-γ, while none of the human *IRG* genes are (Bekpen 2005).

Although recently human *IRGM* has been implicated in resistance against *M. tuberculosis* (Singh 2006) the data are not conclusive and do not explain the fact that *IRGM* is not interferon-inducible but constitutively expressed under the control of the LTR of the endogenous retrovirus, ERV9 (Bekpen 2005). Whether IRGM is a functional GTPase has not been demonstrated and the C-terminal truncation argues against it. Thus the higher primates seem to have lost the entire IRG resistance system. The loss or absence of a highly effective antimicrobial system implies that the possession of such a system carries a significant cost outweighing the benefits. Since higher primates are nevertheless able to resist infections by pathogens that require the action of IRG proteins in the mouse, other resistance systems are deployed to handle the infection. These significant differences have to be considered when experimental results from infection studies in the mouse model are transferred to the human.

Although all the data obtained argue against Irgc as a resistance factor, Irgc expressed under the control of a mifepristone inducible promoter in 3T3 cells localizes to the parasitophorous vacuole upon infection with *Toxoplasma gondii* (Figure 48) (Julia Hunn personal communication). The localization to the vacuole is dependent on interferon-γ stimulation of the cell or the transfection of six other mouse IRG proteins (Irga6, Irgb6, Irgd, Irgm1-3). Therefore Irgc needs similar conditions to relocalize to the parasitophorous vacuole as other GKS-IRGs (Irga6, Irgb6, Irgd) in this experimentel setup. Since Irgc was shown to interact with Irga6 and Irgm3 in a yeast two-hybrid experiment (Julia Hunn personal communication), an interaction between these proteins at the parasitophorous vacuole seems also possible. There are further indications that Irgc and Irga6 share some structural properties important for protein interactions. Irga6 interacts like Irgc with tsv GORASP2 in a yeast two-hybrid assay.

Therefore the question arises, whether the relocalization of Irgc to the parasitophorous vacuole is of any functional relevance. Some functional features of the *IRG* genes argue against that. The members of the IRG family are well conserved to each other. The possibility of hetero-oligomers consisting of different IRG proteins was discussed recently (Martens

2006), though one could imagine that Irgc is included into such oligomeric structures consisting of different IRG proteins, because it shares some common, yet unidentified motifs with the other IRG proteins.

It also has to be taken in account that the experimental conditions do not reflect the *in vivo* situation. *In vivo* Irgc is expressed only in haploid spermatids in the testis, while it is absent in any fibroblasts, independent of infection or interferon-stimulation. Hence, an anti-*Toxoplasma* effect of Irgc is unlikely. In order to support the conclusion that the relocalization of Irgc to
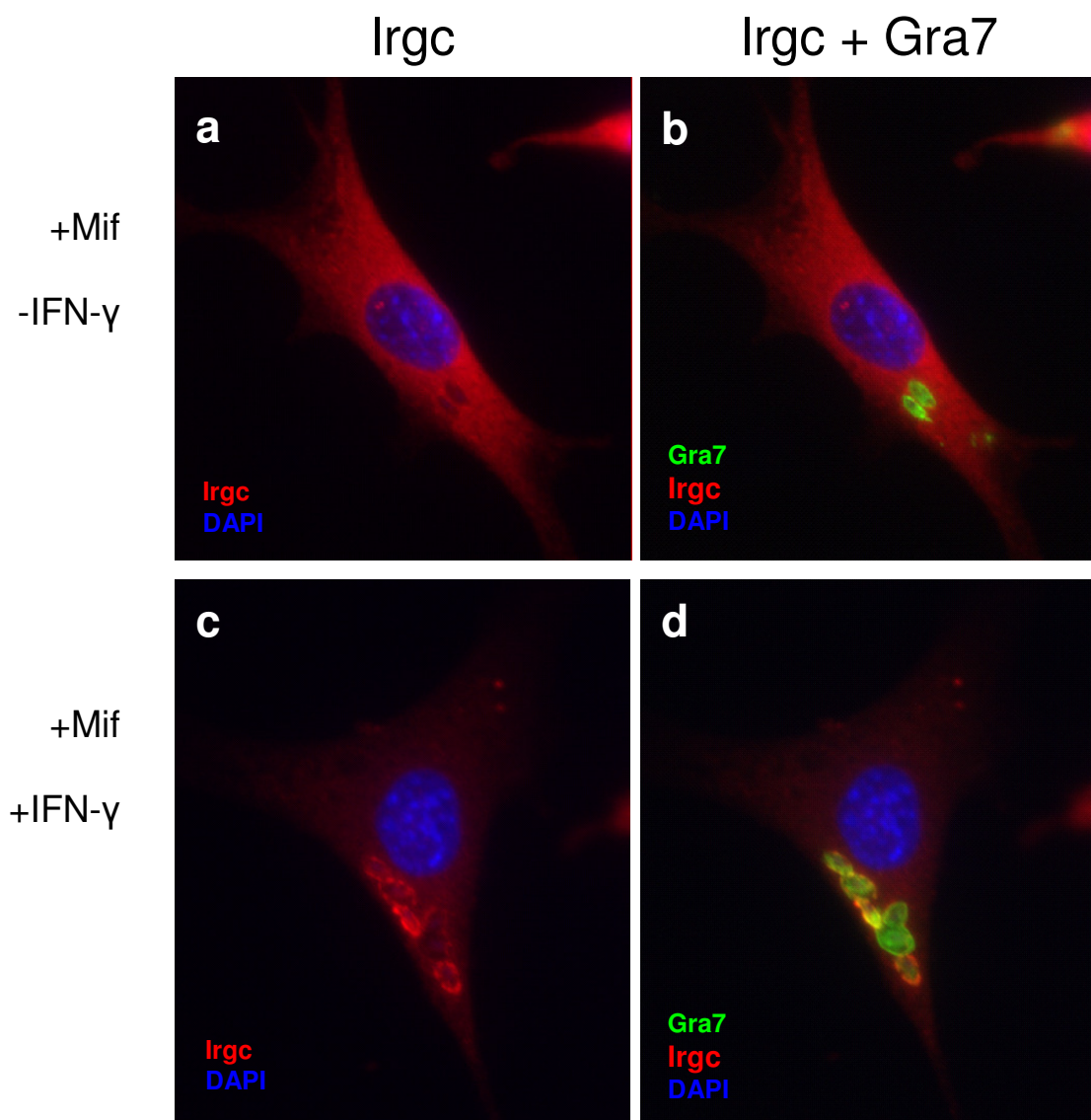
Figure 48**. IFN-γ dependent relocalization of Irgc to the parasitophorous vacuole in 3T3 cells.** 3T3 cell line expressing Irgc under the control of a mifeprestone (Mif) inducible promoter. Irgc relocalizes to the *T. gondii* containing parasitophorous vacuole only in IFN-γ stimulated cells (c, d). Without interferon stimulation Irgc does not relocalize to the vacuole (a, b). Irgc stained with α-CIN 39/3°, T. gondii stained with α-Gra7, nuclei stained with DAPI (pictures kindly provided by Julia Hunn)

the parasitophorous vacuole is without functional relevance, it would be interesting to know, whether Irgc deficient mice show an increased susceptibility to *T. gondii* infection. However, it has to be considered that Irga6-deficient mice do not show an increased susceptibility to *T. gondii* infection, although *in vitro* experiments showed Irga6 is an important factor in resistance against *T. gondii* in at least some cell types (Martens 2005, Parvanova 2005).

4.5   Irgc deficient mice are fertile and show no distortions in spermatogenesis

In order to get insights on the function of Irgc, mice deficient for Irgc were generated. Irgc has a conserved expression profile in the testis with expression only detectable in haploid spermatids (Figure 16, 21). Therefore a distortion or arrest of spermatogenesis could be the consequence of the lack of such a conserved protein. For a wide variety of testis-specific genes the effects of targeted deletions have been studied. The observed phenotypes vary, making it impossible to predict the effect of a targeted deletion of a spermatogenic cell-specific gene. The strongest effect observed is an arrest of spermatogenesis at well defined stages in spermatogenesis (Matzuk 2002, de Rooij 2003). A list of genes essential for spermatogenesis and the point when their action is required is presented in Figure 49. The function mediated by the missing or mutated gene is essential for the further progress of spermatogenesis and can not be mediated by any other gene.

For some genes that are specifically expressed in spermatogenic cells targeted deletion does not have any obvious effect on spermatogenesis. Examples for these genes are the endopeptidase acrosin (Baba 1994), the testis-specific linker histone H1t (Lin 2000) or the Testicular haploid expressed gene (Theg) (Mannan 2003). One explanation for this observation is that the function mediated by these proteins is redundant and can be taken over by other proteins. It is also possible, that the function is not necessary for sperm development and functional sperm can be formed without this protein.

Besides these two extremes, no effect and arrest of spermatogenesis with infertility, targeted deletions of the genes involved in sperm development can also cause intermediate effects. Deletions can affect sperm number, shape or motility with the consequence of reduced fertility. Examples are the transition protein 2 (Zhao 2001) or the activator of CREM in testis (ACT) (Kotaja 2004).
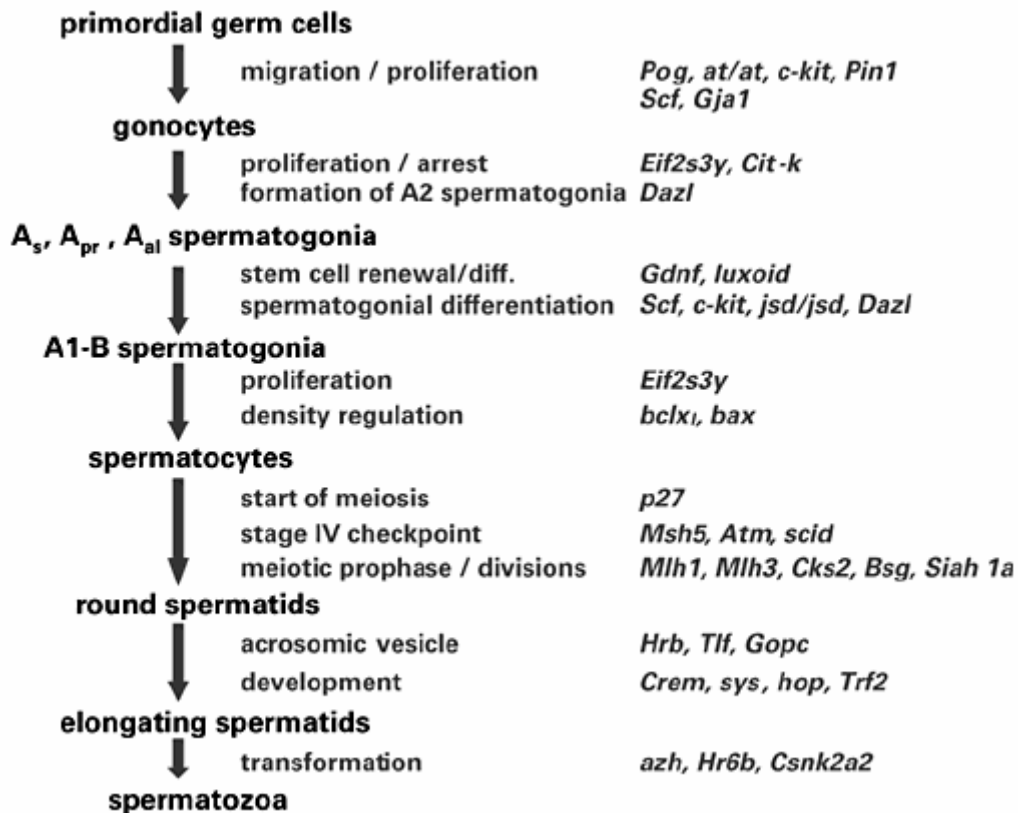
Figure 49. **Genes critically important at specific steps in the spermatogenic process (from de Rooij 2003).**

However, the deficiency of Irgc does not lead to any morphological abnormalities in spermatogenic cells and spermatogenesis seems not to be affected by the targeted deletion of Irgc (Figure 33). The possibility was considered, that the Irgc deficiency may lead to a phenotype in spermatogenesis that would become obvious only with a certain age. However, the morphology of the testis of Irgc$^{-/-}$-males up to an age of 700 days was indistinguishable from that of littermate wildtype males (Figure 35) and 10 months old Irgc$^{-/-}$-males still produced offspring. Thus age does not have any effect on Irgc deficiency in mice.

Is the function of Irgc in spermatogenesis redundant and could this redundancy explain the lack of an obvious phenotype? There is one strong argument against this assumption. IRGC is highly conserved throughout all mammals. If other proteins could mediate the function of IRGC, the conservative or purifying selection on IRGC would not be as high as it obviously is. The consequence would be a weaker conservation of the *IRGC* gene during the course of evolution. However, there is the possibility that a prominent phenotype is suppressed by the controlled laboratory conditions the mice live in. Factors like social ranking of the males or limited food resources, which are essential for the reproductive success of males in natural

conditions, do not play any role in the experimental conditions used in this study. Therfore a phenotype of Irgc$^{-/-}$-mice may present, but could not be identified yet. On the other hand it might be that the function mediated by IRGC during spermatogenesis is not as important as assumed based on the high degree of conservation of the protein. The correlation between high degrees of conservation between different species and the importance of the function may be not as tight as was thought. A recent study by Ahituv and co-workers demonstrated that the deletion of ultraconserved regulatory elements with a length of 221 to 731 bp did not cause any obvious phenotype in the respective mice (Ahituv 2007).

The obtained data for the Irgc$^{-/-}$-mice showed that a negative effect of Irgc deficiency on fertility can be excluded. Actually the data suggest a slight positive effect of Irgc deficiency on fertility (Figure 36). Especially the appearance of large litters only in context with at least one Irgc$^-$ allele is peculiar and suggests the possibility of a distorted segregation. This question was approached by breedings of Irgc$^{+/-}$-males to wt females and wt males to Irgc$^{+/-}$-females. If the Irgc$^-$ allele had no effect on segregation the expected ratio between the Irgc$^{+/+}$- and Irgc$^{+/-}$-genotype would be 1:1 assuming mendelian segregation. The observed ratio differed slightly from the expected value (Table 11). Irgc$^{+/-}$-males passed the Irgc$^-$ allele to 51,4% of all offspring, Irgc$^{+/-}$-females only to 44,4%. The resulting difference was statistically significant (p<0,05 by χ^2 test). Whether it also has functional relevance has to be investigated further. Therefore it is essential to increase the number of analyzed breedings and litters. Since the observed segregation differences are small, three explanations are possible. Firstly, the variations occurred randomly and are not connected to the Irgc genotype. Secondly, the EGFP protein expressed in the haploid spermatids has a disturbing effect. Tavaeau and co-workers reported that a transmission ratio distortion observed in their Calpain3 deficient mice was caused by the transcriptional activity from the *Pgk1* promoter of a neomycin-cassette (Tavaeau 2004). Although the neomycin-cassette was deleted in the Irgc deficient mice created for this study an effect of the EGFP transcripts or protein on the transmission ratio can not be excluded. Thirdly, the variations indeed represent a segregation distortion phenotype caused by the Irgc$^-$ allele. Low variations in segregation lead to the identification of two t-complex distorters (Tcd). The t haplotype in mice, occupying the proximal third of chromosome 17, leads to severe transmission ratio distortions. Males heterozygous for this locus (t/+) transmit in up to 99% of all cases the t allele to their offspring (Lyon 2003). This is astonishing, especially because homozygosity for the t allele causes sterility and is often lethal. Recombination of the t haplotype is suppressed by four large inversions, inhibiting

disruption of the t-complex. The rare recombinants with partial t haplotypes were essential tools to reveal the mechanism causing the segregation distortion. Five loci are responsible for this phenomenon, the t-complex responder (Tcr), which is encoded by the sperm motility kinase (*Smok*) (Herrmann 1999) and four t-complex distorters (Tcd). Two of these Tcds were identified recently, *Tagap1* (t complex-encoded GTPase-activating protein 1) (Bauer 2005) and *Fgd2*, a Rho guanine exchange factor (Bauer 2007). The experiments verifying the Tcd-function of these two genes were based on segregation distortions of partial haplotypes. The partial t haplotype t^6 is lacking *Tagap1* and transmitted to 80% of the offspring. Additional expression of Tagap1 increased the ratio by 8% to 88% (Bauer 2005). In a similar experimental setup the transmission of the t allele was reduced from 47% to 35% by the deletion of one Fgd2 allele (Bauer 2007). These two examples illustrate that also the observed differences in the segregation of the $Irgc^-$ allele may be a genetic phenotype.

The statistically significant sex ratio distortion observed in the same breedings is actually bigger than the variation in the segregation of the $Irgc^-$ allele (Table 11). $Irgc^{+/-}$-males produced with 56,3% male offspring more than the expected 52,3% for C57BL/6 mice (Weir 1960), while in breedings of $Irgc^{+/+}$-males and $Irgc^{+/-}$-females only 45,8% of the offspring was male. The cause for sex ratio distortions can be diverse. They include diet and nutrition (Trivers 1973, Alexenko 2007), infections with pathogens (Ehman 2002, Kankova 2007) and environmental stress (Lichtenfels 2007). If such an external factor would have caused the observed deviation in the sex ratio, these factors should have the same effect on the breedings independent from the genotype of the breeding partners. Although it can not be excluded that the $Irgc^{+/-}$- and $Irgc^{+/+}$-males react in a different way to an external factor. Since only four breedings of $Irgc^{+/+}$-males with $Irgc^{+/-}$-females were included in this experiment it is crucial to include more breeding pairs to put the results on a wider statistical basis and minimize variations based on the individual mice used.

4.6   Putative interaction partner of Irgc

In the yeast two-hybrid screen of a testis derived cDNA library two proteins were identified as putative interaction partners for Irgc. One is the eukaryotic release factor 1 (eRF1), the other the Golgi reassembly and stacking protein 2 (GORASP2) (Figure 38).

The family of GORASP proteins consists of the two members GORASP1 and GORASP2, also called GRASP65 and GRASP55, respectively. They are characterized by the N-terminal GRASP domain, which consists out of two PDZ-domains and is highly conserved (Barr 1998,

Shorter 1999). The GRASP domain is followed by a GM130 binding domain. The C-terminal region is the most divergent region of the protein. Both GORASP proteins are phosphorylated during mitosis and dephosphorylated at the end of mitosis when the Golgi is reassembled in the daughter cells (Jesch 2001, Wang 2003). Mitosis-dependent phosphorylation leads to the disruption of GORASP1 oligomers, which reassemble after dephosphorylation and mediate cisternal stacking of the Golgi (Wang 2003).

Interestingly, the three independent GORASP2 clones identified in the screen were all C-terminally truncated. Therefore the possibility of a testis-specific splice variant was considered. Shorter and co-workers reported a testis-specific transcript for GORASP2 in rat testis (Shorter 1999). Alignments of the identified clones with the GORASP2 ORF suggested that the variant termed tsv GORASP2 is generated by alternative splicing (Figure 39). After Exon 9 the transcript runs into the intron instead of Exon 10, which is excluded from the variant. The resulting tsv GORASP2 ORF has a length of 1059 bp and is therefore 323 bp shorter than the full-length GORASP2. Expression of tsv GORASP2 was demonstrated in testis by RT-PCR with primers discriminating between the normal and tsv GORASP2 (Figure 40). A truncated testis-specific transcript was also described for GORASP1 (Barr 1997), which may be generated in the same way tsv GORASP2.

Although tsv GORASP2 is expressed in low levels in the testis of very young mice, expression is upregulated at the same age as the first haploid cells are generated, and therefore at the same time when Irgc is transcribed for the first time in testis (Figure 40). This fact suggested that Irgc and tsv GORASP2 are co-expressed in haploid spermatids. Laser microdissection (LMD) and RT-PCR were chosen to analyse the expression profiles of GORASP2, tsv GORASP2 and Irgc in the fractions of diploid and haploid cells in the seminiferous tubules (Figure 41). The results indicated that GORASP2 is expressed ubiquitously in the testis, while tsv GORASP2 expression is stronger in haploid spermatids than diploid spermatogonia and spermatocytes (Figure 42). However the difference in expression levels between haploid and diploid cells was much smaller for tsv GORASP2 than for Irgc. Irgc transcripts were mainly detected in haploid cells. The significance of the very weak Irgc signal detected in diploid cells is questionable, because all the other techniques applied to investigate Irgc expression argue for expression in haploid cells. Also contaminations of the pool of diploid cells cut by LMD with small amounts of haploid cells can not be excluded. Very few haploid cells may be sufficient to generate the weak Irgc signal detected in the pool of diploid cells.

The function of tsv GORASP2 in testis is unknown. The C-terminal SPR (serine/proline rich) domain of GORASP1 is necessary for the cell-cycle related regulation of oligomerization (Wang 2003). In the absence of the SPR domain GORASP1 oligomers are more stable and do not break down during mitosis. Thus the testis-specific GORASP variants may have a stabilizing effect on GORASP oligomers and thereby stabilize Golgi stacks. However, the part of the SPR domain still present in tsv GORASP was shown to be sufficient for cell-cycle related regulation of GORASP1 (Wang 2003). Especially the functional role of the part of the protein missing in the tsv GORASP2 is not understood yet. Another yet unresolved aspect is the cellular localization of tsv GORASP2. While full-length GORASP2 localizes to the Golgi, it has to be demonstrated if tsv GORASP2 behaves in the same way. Since Irgc did not show any Golgi localization, interaction of Irgc and GORASP2 may take place in the cytosol. However, a more detailed analysis is required to resolve this issue.

Although the detailed analysis was concentrated on GORASP2, the interaction of Irgc and eRF1 may be important. Indeed this issue deserves further analysis, which could not be performed during this study.

Hook1 was thought to be a candidate for interaction with Irgc. Two facts suggested this interaction. Firstly, the reported interaction of Hook3 and Irga6 in bone marrow derived macrophages (Kaiser 2004). Therefore the interaction of other members of the Hook- and IRG-family seemed possible. Secondly, the expression pattern of *Hook1* and *Irgc* are very similar. As *Irgc*, *Hook1* is mainly expressed in haploid spermatids, although these are not the only cells where *Hook1* is expressed (Mendoza-Lujambio 2002). Hook1 is a microtubule-binding protein and essential for the formation of the manchette. This structure is crucial for the proper shaping of the spermhead. A natural occurring mutation in the *Hook1* gene causing a C-terminal truncated protein leading to the *azh* phenotype (abnormal spermatozoan headshape) (Meistrich 1990, Mendoza-Lujambio 2002).

However, the results of the performed experiments did not give any hint of an interaction between these two proteins. They did not interact in the yeast two-hybrid assay, which is one argument against a physical interaction of both molecules (Figure 43). If both molecules would interact directly in a common pathway or mechanism, the deletion of both genes could lead to a more severe phenotype than that observed in Hook1[azh/azh]-mice although a more severe phenotype in the double knockout could also have other reasons. Anyway, the Hook1[azh/azh]/ Irgc^{-/-}-mice did not show a phenotype different from that of Hook1[azh/azh]-mice (Figure 44). Hence the obtained results do not give any indications for an interaction between Hook1 and Irgc.

In mouse and human the quasi-GTPase *IRGQ* was shown earlier to be located in close proximity to *IRGC* on the respective chromosomes (Bekpen 2005). It now seems that this linkage is universally the case in mammals (Julia Hunn personal communication). In all species where *IRGC* and *IRGQ* were identified and could be mapped they are located very close to each other on the same chromosome with the chromosomal synteny marker *Plaur* between them (Figure 6). This lead to the assumption, that IRGQ may function as some kind of regulator of other IRG proteins, in particular of IRGC (Bekpen 2005). Interaction would take place in a dimer-like structure. The paradigm for this assumption is Rap1GAP (Daumke 2004). Rap1GAP is a GAP (GTPase activating protein) for the Ras-like guanine-nucleotide-binding protein Rap1. It is probably derived from a GTPase ancestor and thus retains the structure of the G domain, although it is not functional anymore. For *IRGQ* a similar evolutionary origin is possible. Mammalian *IRGQ*s have radically modified G1, G3 and G4 motifs in their G domain and have certainly lost their GTPase function. Nevertheless, this does not exclude a regulatory function of IRGQ. It would act either in a GAP-like way as activator or could also mediate an inhibitory effect on IRGs.

Because no experimental data on *Irgq* existed, the expression pattern of the gene was analyzed. The gene is universally transcribed in the mouse with transcripts detected in all tissues investigated (Figure 46). Indeed this is a striking difference to the very restricted transcription profile of *Irgc*. If Irgq is an Irgc-specific regulator a similar expression pattern would be expected.

Direct interaction between Irgc and Irgq was analyzed by a yeast two-hybrid assay. However, no interaction between both proteins was observed in this assay (Figure 45). Taken together the obtained data do not support the assumption that Irgq is a regulator of Irgc. Although transcription of Irgq was shown, it is not known yet whether these transcripts are translated into protein. Further investigations of the role of Irgq would require an antiserum against this protein. Then the crucial question, whether the transcript is also translated into protein could be answered.

Whether Irgc and Irgq interact or not, the question remains why they are linked so closely throughout mammalian evolution. Further investigations have to show whether the conserved linkage between *IRGC* and *IRGQ* is based on their function or whether they were not separated yet by recombination because they are located so close to each other on the respective chromosome.

4.7   Past, presence and future of IRGC

From the evolutionary point of view *IRGC* is an exceptional gene among the family of *IRG* genes. No other *IRG* gene in mammals shows such a strong conservation. During the course of mammalian evolution *IRGC* is the only constant factor in the family of *IRG* genes. While the genes of the other *IRG* subfamilies are subjected to repeated duplications, diversification and loss, the status of the *IRGC* clade remains with one highly conserved gene per species unchanged.

The cause for the significant difference in the evolutionary history of the *IRG* genes is most likely to be found in their respective functions. While IRGC is involved in the conserved mechanism of spermatogenesis, the other IRG proteins act as resistance factors and evolution stimulated the diversification of these genes in response to the threat of infections by pathogens. Although these two functional assignments are not related to each other, the molecular mechanism by which the IRG proteins mediate their specific function may be similar. Although major progress in understanding the function of IRG proteins has been made in recent years, the molecular mechanism of IRG mediated resistance is not resolved yet. Therefore it seemed to be a promising attempt to study the molecular mechanism of the IRGC mediated function in the testis and transfer the results to the immunity model of other IRG proteins. Unfortunately the lack of an obvious phenotype in the Irgc deficient mice did not allow further conclusions on the role of Irgc in spermatogenesis.

A profound understanding of the mechanism of the action of IRG proteins is crucial to answer the question, whether IRG proteins developed as resistance factors and were adopted by spermatogenesis or vice versa. Since higher primates possess only IRGC it has to mediate its function independently of any other IRG protein. The IRG mediated resistance, in contrast, is mediated by a complex network of interactions between different IRG proteins. Therefore it is tempting to speculate that the function mediated by the single protein was the primary function and was the basis for the evolution of the complex resistance system.

The genes closest related to the *IRGC* genes are the *IRGC-like* genes. Interestingly mouse, rat and humans have lost any *IRGC-like* genes and the phylogenetic distribution of these genes will become clearer with progressing genome sequencing projects. Members of this clade have been discovered recently also outside the mammals in reptiles (*Anolis carolinensis*) and amphibians (*Ambystoma tigrinum*) (Julia Hunn personal communication) indicating that the *IRGC-like* genes are most likely relatively ancient *IRG* genes. Since the *IRGC-like* genes are the only *IRG* genes which are present in mammals and other classes of vertebrates, they may represent the ancestral gene for all mammalian *IRG* genes. Two lines of development

departed from this ancestral gene. While one line led to the formation of IRGC, which has not changed since the origination of mammals, the other line led to the formation of the *IRG* resistance system. Thus it would be interesting to know whether the *IRGC-like* genes are regarding their functional properties rather like the *IRGC* genes or the other *IRG* genes. The divergence within the *IRGC-like* genes is considerably higher than within the *IRGC* genes (Julia Hunn personal communication). This could indicate a possible immune function. Therefore it is essential to analyze whether they are inducible by interferons, which would suggest a role in immunity.

With the same approach the fish genes have to be analyzed. After it was shown that a subset of zebrafish *IRG* genes are interferon-inducible (Dirk Sieger, Cornelia Stein personal communication), the next question to be resolved is, whether fish IRG proteins are also involved in other functions, which are not related to immunity. The most promising tissue to start this search for non-immunity related functions of fish IRG proteins would be the testis.

5.   Appendix

5.1 Appendix I. List of all ES cell injections into blastocysts.

(B) : *Bruce4* ES cell clones derived from C57BL/6

(F1) : V6.5 ES cell clones derived from F1 of C57BL/6 x 129sv/Jae breeding

injection date	ES cell clone	strain of embryo donors	blastocystes injected / transfered	transfers / pregnant	offspring / chimeras	chimerism
06.02.03	1G12 (B)	CB20	13 /13	1 / 1	4 / 2	#66 70 % ♂ #67 30 % ♀
05.03.03	2A6 (B)	CB20	27 / 27	3 / 1	4 / 2*	*80%, 50 % both died
06.03.03	1B10 (B)	CB20	28 / 28	3 / 3	3* / 1	#77 50 % ♀ *many pubs eaten
27.08.03	2C2 (B)	CB20	8 / 8	1 / 1	all eaten	-
28.08.03	3E3 (B)	CB20	24 / 24	2 / 2	4 / 1 4 / 0	#3 40 % ♂
04.09.03	2C2 (B)	CB20	14 / 14	2 / 1	8 / 2	#4 80 % ♀ #5 50 % ♂
21.01.04	B2H5 (F1)	CB20	20 / 10	1 / 0	-	-
22.01.04	B1H2 (F1)	CB20	24 / 24	3 / 1	4 / 3	#13 90% ♂ germline transmission #14 80% ♂ germline transmission #15 50% ♂
11.02.04	B3E5 (F1)	CB20	67 / 28	2 / 1	2* / 0	*some maybe eaten
12.02.04	B1E3 (F1)	CB20 C57BL/6	39 / 16 37 / 26	1 / 1 2 / 2	abort abort 1* / 0	*some maybe eaten
31.03.04	B1F6 (F1)	CB20	17 / 17	2 / 2	3* / 0 2 / 0	*all eaten
01.04.04	B3E5 (F1)	CB20	10 / 10	1 / 1	6 / 3*	*1 died #45 85 % ♂ germline transmission #46 75 % ♀ germline transmission
28.04.04	B1F6 (F1)	CB20	30 / 28	3 / 1	4/ 2	# 60 % ♂ # 10 % ♀
29.04.04	B1H2 (F1)	C57BL/6	42 / 42	4 /1	3 / 1	# 100 % ♂
Total: 14			400 / 315	31 / 17	45 / 17	

5.2 Appendix II. List of all IRGC ESTs detected in the databases.

M: male, F: female

Species	Nr	Accession nr	Tissue	Sex, age	Length
Mus musculus	1	BY748210	NOD-derived CD11c +ve dendritic cells	-	715 bp
	2	CJ232199	Pool	mixed	674 bp
	3	CJ096897	Pool	mixed	656 bp
	4	BB615720	testis	M, adult	606 bp
	5	AV270586	testis	M, adult	618 bp
	6	CB274179	round spermatids	M 60 days	546 bp
	7	BX517297	testis	M 9 months	568 bp
	8	CF104767	round spermatids	M 60 days	530 bp
	9	CA464745	testis	M,	874 bp
	10	AI595504	testis	M, 10-12 weeks	498 bp
	11	AI595232	testis	M, 10-12 weeks	445 bp
	12	AA492644	testis	M, 10-12 weeks	446 bp
	13	AI507025	testis	M, 10-12 weeks	427 bp
	14	AI615330	testis	M, 10-12 weeks	383 bp
	15	CN838993	testis	M	419 bp
	16	AI036789	testis	M, adult	413 bp
	17	BU938355	testis	M,	390 bp
	18	BF152667	testis	M, 5 months	333 bp
	19	BF152824	testis	M, 5 months	362 bp
	20	BY198273	B6-derived CD11c +ve dendritic cells	-	383 bp
	21	AI507049	testis	M, 10-12 weeks	302 bp
	22	BY534053	NOD-derived CD11c +ve dendritic cells	-	403 bp
	23	AI427794	testis	M, 10-12 weeks	304 bp
	24	BY525225	NOD-derived CD11c +ve dendritic cells	-	409 bp
	25	BY087970	pooled	-	383 bp
	26	BF152741	testis	M 5 months	243 bp
	27	AI614196	testis	M, 10-12 weeks	328 bp
	28	BY095213	pooled	-	398 bp
	29	BX638993	-	-	206 bp
	30	AA061392	testis	M, 10-12 weeks	172 bp
	31	AA492703	testis	M, 10-12 weeks	242 bp
	32	AA106441	testis	M, 10-12 weeks	121 bp
	33	BY455469	pooled	-	424 bp
	34	AA065423	testis	M, 10-12 weeks	111 bp
	35	CJ139276	B6 derived CD11c +ve dendritic cells	-	400 bp
	36	BY202622	B6 derived CD11c +ve dendritic cells	-	358 bp
	37	AA492614	testis	M, 10-12 weeks	95 bp
Homo sapiens	1	BM554106	brain medulla	-	1036 bp
	2	BX359457	placenta	F	943 bp
	3	BX337259	placenta	F	981 bp
	4	BI825481	brain medulla	-	838 bp
	5	BI520032	brain medulla	-	857 bp
	6	BI826173	brain medulla	-	805 bp
	7	BI520533	brain medulla	-	847 bp
	8	BI520261	brain medulla	-	873 bp
	9	BI828881	brain medulla	-	859 bp
	10	BG705154	brain hippocampus	-	874 bp
	11	BI830526	brain medulla	-	896 bp
	12	BG773495	testis	M	724 bp
	13	AA861068	testis	M	780 bp
	14	BI826126	brain medulla	-	680 bp
	15	BG722126	testis	M	699 bp
	16	BI828394	brain medulla	-	675 bp
	17	BG771757	testis	M	920 bp
	18	BI828548	brain medulla	-	629 bp
	19	BX103486	testis	M	645 bp
	20	BG722800	testis	M	614 bp
	21	BG723426	testis	M	727 bp
	22	BI828552	brain medulla	-	569 bp
	23	AW593346	pooled (lung, testis, B-cell)	-	565 bp
	24	AI026913	testis	M	524 bp
	25	AA447543	testis	M	780 bp
	26	AI372028	pooled germ cell tumors	-	476 bp
	27	AI684805	pooled (lung, testis, B-cell)	-	563 bp
	28	AI122717	testis	M	446 bp
	29	AI017139	testis	M	503 bp

	30	AA431984	testis	M	593 bp
	31	AI476720	pooled (lung, testis, B-cell)	-	465 bp
	32	BE044223	pooled (lung, testis, B-cell)	-	442 bp
	33	AW418643	pooled (lung, testis, B-cell)	-	428 bp
	34	AI150286	testis	M	464 bp
	35	AA918216	pooled (lung, testis, B-cell)	-	468 bp
	36	DB462403	testis	M	488 bp
	37	AW294021	lung	-	404 bp
	38	DB526649	testis	M	454 bp
	39	AI283570	pooled (lung, testis, B-cell)	-	386 bp
	40	AW873559	pooled (lung, testis, B-cell)	-	379 bp
	41	AW181969	pooled (lung, testis, B-cell)	-	416 bp
	42	AW592970	pooled (lung, testis, B-cell)	-	449 bp
	43	AI125548	testis	-	379 bp
	44	BE044235	pooled (lung, testis, B-cell)	-	375 bp
	45	BF115492	brain glioblastoma	-	381 bp
	46	BE044186	pooled (lung, testis, B-cell)	-	374 bp
	47	BE550422	pooled germ cell tumors	-	375 bp
	48	BE503483	pooled germ cell tumors	-	370 bp
	49	AA974680	pooled (lung, testis, B-cell)	-	385 bp
	50	AA994056	pooled (lung, testis, B-cell)	-	432 bp
	51	BE044229	pooled (lung, testis, B-cell)	-	340 bp
	52	DB461236	testis	M	408 bp
	53	BE041516	pooled (lung, testis, B-cell)	-	331 bp
	54	AA628142	testis	M	381 bp
	55	AA953413	pooled (lung, testis, B-cell)	-	295 bp
	56	AA909114	pooled (lung, testis, B-cell)	-	309 bp
	57	AW104933	pooled (lung, testis, B-cell)	-	278 bp
	58	AA854988	testis	M	350 bp
	59	AA992982	testis	M	272 bp
	60	BX369977	placenta	F	264 bp
	61	AI218365	pooled (lung, testis, B-cell)	-	322 bp
	62	BX348869	placenta	F	254 bp
	63	AA335595	epididymus	M, adult	217 bp
	64	AA448525	testis	M	247 bp
	65	AA884883	pooled (lung, testis, B-cell)	-	211 bp
	66	AW779121	pooled (lung, testis, B-cell)	-	244 bp
	67	AA926841	pooled (lung, testis, B-cell)	-	151 bp
	68	AA970662	pooled (lung, testis, B-cell)	-	96 bp
	69	AA906221	pooled (lung, testis, B-cell)	-	133 bp
	70	AA738056	pooled germ cell tumors	-	100 bp
	71	AA935622	pooled (lung, testis, B-cell)	-	91 bp
	72	AA917036	pooled (lung, testis, B-cell)	-	73 bp
Bos taurus	1	DT836443	liver	F, 6 months	837
	2	DT838127	liver	F, 6 months	861
	3	DT848387	liver	F, 6 months	795
	4	DT842144	liver	F, 6 months	754
	5	DT844821	liver	F, 6 months	733
	6	DT837202	liver	F, 6 months	836
	7	DT840242	liver	F, 6 months	420
Macaca nemestrina	1	EB519615	ovary	F, young adult	808
	2	EB518936	ovary	F, young adult	824
	3	DY750065	testis	M, young adult	728
	4	EB520540	ovary	F, young adult	830
	5	DY743765	testis	M, young adult	797
	6	DY747096	testis	M, young adult	700
	7	DY745613	testis	M, young adult	705
	8	DY755323	ovary	F, young adult	738
	9	EB518177	ovary	F, young adult	864
	10	EB517680	ovary	F, young adult	858
	11	DY750066	testis	M, young adult	678
	12	EB517681	ovary	F, young adult	829
	13	DY759992	ovary	F, young adult	716
	14	DY745097	testis	M, young adult	716
	15	DY746816	testis	M, young adult	717
	16	EB518935	ovary	F, young adult	865
	17	DY745356	testis	M, young adult	735
	18	EB524862	ovary	F, young adult	848
	19	EB520541	ovary	F, young adult	841
	20	EB523154	ovary	F, young adult	885
	21	EB525106	ovary	F, young adult	783
	22	EB524861	ovary	F, young adult	841
	23	DY745457	testis	M, young adult	739

	24	EB523153	ovary	F, young adult	808
	25	DY745098	testis	M, young adult	683
	26	EB525105	ovary	F, young adult	791
	27	DY745455	testis	M, young adult	765
	28	EB518176	ovary	F, young adult	835
	29	DY745355	testis	M, young adult	757
	30	DY746050	testis	M, young adult	662
	31	DY750067	testis	M, young adult	752
	32	DY748346	testis	M, young adult	638
	33	DY747095	testis	M, young adult	613
	34	DY748347	testis	M, young adult	700
	35	DY746818	testis	M, young adult	677
	36	DY759991	ovary	F, young adult	623
	37	DY745614	testis	M, young adult	578
	38	DY746049	testis	M, young adult	681
	39	DY748180	testis	M, young adult	631
	40	DY748179	testis	M, young adult	704
	41	DY755322	ovary	M, young adult	700
	42	EB519616	ovary	M, young adult	737
	43	DY747354	testis	M, young adult	531
	44	DY747353	testis	M, young adult	597
Canis familiaris	1	CX988596	testis	M	799
	2	CX989998	testis	M	840
	3	CX989526	testis	M	814
	4	CX985303	testis	M	834
	5	CX985975	testis	M	803
	6	CX991954	testis	M	852
	7	BM537262	testis cells	M	585
	8	CX993880	testis	M	635
	9	CX990304	testis	M	613
	10	CX986297	testis	M	598
	11	DN341250	testis	M	464
	12	CX991177	testis	M	711
	13	CX984764	testis	M	518
	14	CX986228	testis	M	543
Rattus norvegicus	1	CK653113	testis	M, 8 weeks	853
	2	CK469249	testis	M, 8 weeks	766
	3	CK470037	testis	M, 8 weeks	777
	4	CK600500	testis	M, 8 weeks	848
	5	CK653335	testis	M, 8 weeks	850
	6	CK653485	testis	M, 8 weeks	813
	7	CK603648	testis	M, 8 weeks	783
	8	CK470449	testis	M, 8 weeks	778
	9	CK469950	testis	M, 8 weeks	745
	10	CK470952	testis	M, 8 weeks	768
	11	CK653357	testis	M, 8 weeks	803
	12	CK471007	testis	M, 8 weeks	838
	13	CK653168	testis	M, 8 weeks	801
	14	CK471134	testis	M, 8 weeks	730
	15	CK470665	testis	M, 8 weeks	739
	16	CK595840	testis	M, 8 weeks	785
	17	CK653471	testis	M, 8 weeks	829
	18	CK469166	testis	M, 8 weeks	820
	19	CK595604	testis	M, 8 weeks	844
	20	CV115369	testis	M, 8 weeks	746
	21	CK652897	testis	M, 8 weeks	833
Sus scrofa	1	CV876013	testis	M, 1 year	631
	2	CV875009	testis	M, 1 year	646
	3	CX063332	testis	M, 1 year	639
	4	CV877305	testis	M, 1 year	633
	5	CX057625	testis	M, 1 year	672
	6	CV870591	testis	M, 1 year	484
	7	CX059393	testis	M, 1 year	617
	8	CV876822	testis	M, 1 year	475
	9	CX064612	testis	M, 1 year	647
	10	CX058998	testis	M, 1 year	611
	11	CX060027	testis	M, 1 year	552
	12	CX065385	testis	M, 1 year	620
	13	CX057748	testis	M, 1 year	611
	14	CV873933	testis	M, 1 year	408
Felis catus	1	AW646927	testis	M	419

6.   References

Accola M.A., B. Huang, A. Al Masri, and M.A. McNiven. 2002. The antiviral dynamin family member, MxA, tubulates lipids and localizes to the smooth endoplasmic reticulum. *J Biol Chem*. 277(24):21829-35.

Aebi M., J. Fah, N. Hurt, C.E. Samuel, D. Thomis, L. Bazzigher, J. Pavlovic, O. Haller, and P. Staeheli. 1989. cDNA structures and regulation of two interferon-induced human Mx proteins. *Mol Cell Biol*. 9(11):5062-72.

Ahituv N., Y. Zhu, A. Visel, A. Holt, V. Afzal, L.A. Pennacchio, and E.M. Rubin. 2007. Deletion of Ultraconserved Elements Yields Viable Mice. *PLoS Biol*. 5(9):e234.

Alexenko A.P., J. Mao, M.R. Ellersieck, A.M. Davis, J.J. Whyte, C.S. Rosenfeld, and R.M. Roberts. 2007. The Contrasting Effects of Ad Libitum and Restricted Feeding of a Diet Very High in Saturated Fats on Sex Ratio and Metabolic Hormones In Mice. *Biol Reprod*. Epub ahead of print

Altschul S.F., W. Gish, W. Miller, E.W. Myers, and D.J. Lipman. 1990. Basic local alignment search tool. *J Mol Biol*. 215(3):403-10.

Anderson S.L., J.M. Carton, J. Lou, L. Xing, and B.Y. Rubin. 1999. Interferon-induced guanylate binding protein-1 (GBP-1) mediates an antiviral effect against vesicular stomatitis virus and encephalomyocarditis virus. *Virology*. 256(1):8-14.

Ando T., M. Yamasaki, and K. Suzuki. 1973. Protamines. Isolation, characterization, structure and function. *Mol Biol Biochem Biophys*. 12,1–114.

Angata T. 2006. Molecular diversity and evolution of the Siglec family of cell-surface lectins. *Mol Divers*. 10(4):555-66.

Ausubel F.M., R. Brent, R.E. Kingston, D.D. Moore, J.G. Seidman, J.A. Smith, and K. Struhl. 1998. Current protocols in molecular biology. John Wiley & Sons. Inc.

Baba T., S. Azuma, S. Kashiwabara, and Y. Toyoda. 1994. Sperm from mice carrying a targeted mutation of the acrosin gene can penetrate the oocyte zona pellucida and effect fertilization. *J Biol Chem*. 269(50):31845-9.

Bagshaw R.D., D.J. Mahuran, and J.W. Callahan. 2005. A proteomic analysis of lysosomal integral membrane proteins reveals the diverse composition of the organelle. *Mol Cell Proteomics*. 4(2):133-43.

Balhorn R., S. Weston, C. Thomas, and A. J. Wyrobek. 1984. DNA packaging in mouse spermatids. Synthesis of protamine variants and four transition proteins. *Exp. Cell Res.* 150: 298–308.

Barr F.A., M. Puype, J. Vandekerckhove, and G. Warren. 1997. GRASP65, a protein involved in the stacking of Golgi cisternae. *Cell*. 91(2):253-62.

Barr F.A., N. Nakamura, and G. Warren. 1998. Mapping the interaction between GRASP65 and GM130, components of a protein complex involved in the stacking of Golgi cisternae. *EMBO J*. 17(12):3258-68.

Bauer H., J. Willert, B. Koschorz, and B.G. Herrmann. 2005. The t complex-encoded GTPase-activating protein Tagap1 acts as a transmission ratio distorter in mice. *Nat Genet*. 37(9):969-73.

Bauer H., N. Veron, J. Willert, and B.G. Herrmann. 2007. The t-complex-encoded guanine nucleotide exchange factor Fgd2 reveals that two opposing signaling pathways promote transmission ratio distortion in the mouse. *Genes Dev*. 21(2):143-7.

Bekpen C., J.P. Hunn, C. Rohde, I. Parvanova, L. Guethlein, D.M. Dunn, E. Glowalla, M. Leptin, and J.C. Howard. 2005. The interferon-inducible p47 (IRG) GTPases in vertebrates: Loss of the cell-autonomous resistance mechanism in the human lineage. *Genome Biology* 6:R92 doi:10.1186/gb-2005-6-11-r92

Bernstein-Hanley I., J. Coers, Z.R. Balsara, G.A. Taylor, M.N. Starnbach, and W.F. Dietrich. 2006. The p47 GTPases Igtp and Irgb10 map to the *Chlamydia trachomatis* susceptibility locus Ctrq-3 and mediate cellular resistance in mice. *Proc Natl Acad Sci USA*. 103: 14092–14097.

Blanco-Rodriguez J., and C. Martinez-Garcia. 1999. Apoptosis is physiologically restricted to a specialized cytoplasmic compartment in rat spermatids. *Biol Reprod*. 61(6):1541-7.

Blendy J.A., K.H. Kaestner, G.F. Weinbauer, E. Nieschlag, and G. Schutz. 1996. Severe impairment of spermatogenesis in mice lacking the CREM gene. *Nature*. 380(6570):162-5.

Boehm U., L. Guethlein, T. Klamp, K. Ozbek, A. Schaub, A. Fütterer, K. Pfeffer, and J.C. Howard. 1998. Two families of GTPases dominate the complex cellular response to interferon-γ. *J Immunol*. 161:6715–6723.

Boehm, U., T. Klamp, M. Groot, and J.C. Howard. 1997. Cellular responses to interferon-gamma. *Annu. Rev. Immunol.* 15, 749-795.

Boer P.H., C.N. Adra, Y.F. Lau, and M.W. McBurney. 1987. The testis-specific phosphoglycerate kinase gene pgk-2 is a recruited retroposon. *Mol Cell Biol*. 7(9):3107-12.

Bowles J., G. Schepers, and P. Koopman. 2002. Phylogeny of the SOX family of developmental transcription factors based on sequence and structural indicators. *Dev Biol* 227:239–255.

Braun R.E. 2000. Temporal control of protein synthesis during spermatogenesis. *Int J Androl*. 23 Suppl 2:92-4.

Brinster R.L. 2002. Germline stem cell transplantation and transgenesis. *Science*. 296(5576):2174-6.

Brohmann H., S. Pinnecke, and S. Hoyer-Fender. 1997 Identification and characterization of new cDNAs encoding outer dense fiber proteins of rat sperm. *J Biol Chem*. 272(15):10327-32.

Bucher P. 1990. Weight matrix descriptions of four eukaryotic RNA polymerase II promoter elements derived from 502 unrelated promoter sequences. *J Mol Biol*. 212(4):563-78.

Budde L.M., C. Wu, C. Tilman, I. Douglas, and S. Ghosh. 2002. Regulation of IkappaBbeta expression in testis. *Mol Biol Cell*. 13(12):4179-94.

Burmester S., and S. Hoyer-Fender. 1996. Transcription and translation of the outer dense fiber gene (Odf1) during spermiogenesis in the rat. A study by in situ analyses and polysome fractionation. *Mol Reprod Dev*. 45(1):10-20.

Butcher B.A, R.I. Greene, S.C. Henry, K.L. Annecharico, J.B. Weinberg, E.Y. Denkers, A. Sher, and G.A.. Taylor. 2005. p47 GTPases regulate *Toxoplasma gondii* survival in activated macrophages. *Infect Immun.* 73: 3278–3286.

Carlow, D., J. Marth, I. Clark-Lewis, and H. Teh. 1995. Isolation of a gene encoding a developmentally regulated T cell-specific protein with a guanine nucleotide triphosphate-binding motif. *J. Immunol.* 154:1724.

Carlow D.A., S.J. Teh, and H.S. Teh. 1998. Specific antiviral activity demonstrated by TGTP, a member of a new family of interferon-induced GTPases. *J Immunol*. 161(5):2348-55.

Carrera A., G.L. Gerton, and S.B. Moss. 1994. The major fibrous sheath polypeptide of mouse sperm: structural and functional similarities to the A-kinase anchoring proteins. *Dev Biol.* 165:272-284

Carter C.C., V.Y. Gorbacheva, and D.J. Vestal. 2005. Inhibition of VSV and EMCV replication by the interferon-induced GTPase, mGBP-2: differential requirement for wild-type GTP binding domain. *Arch Virol*. 150(6):1213-20.

Chemes H. 1986. The phagocytic function of Sertoli cells: a morphological, biochemical, and endocrinological study of lysosomes and acid phosphatase localization in the rat testis. *Endocrinology*. 119(4):1673-81.

Cheng Y.S, M.F. Becker-Manley, T.P. Chow, and D.C. Horan. 1985. Affinity purification of an interferon-induced human guanylate-binding protein and its characterization. *J Biol Chem*. 260(29):15834-9.

Cheng Y.S., R.J. Colonno, and F.H. Yin 1983. Interferon Induction of Fibroblasts Proteins with Guanylate Binding Activity. *J Biol Chem*. 258(12):7746-50.

Cheng Y.S., C.E. Patterson, and P. Staeheli. 1991. Interferon-induced guanylate-binding proteins lack an N(T)KXD consensus motif and bind GMP in addition to GDP and GTP. *Mol Cell Biol*. 11(9):4717-25.

Clermont Y., and M. Trott. 1969. Duration of the cycle of the seminiferous epithelium in the mouse and hamster determined by means of 3H-thymidine and radioautography. *Fertil Steril*. 20(5):805-17.

Collazo, C.M., G.S. Yap, G.D. Sempowski, K.C. Lusby, L. Tessarollo, G.F. Woude, A. Sher, and G.A. Taylor. 2001. Inactivation of LRG-47 and IRG-47 reveals a family of interferon gamma-inducible genes with essential, pathogen-specific roles in resistance to infection. *J Exp Med.* 194: 181–188.

Conklin D. 2001. Interferon-epsilon. U.S. patent 6,329,175

Dadoune J.P. 2003. Expression of mammalian spermatozoal nucleoproteins. *Microsc Res Tech*. 61(1):56-75.

Dadoune J.P., J.P. Siffroi, and M.F. Alfonsi. 2004. Transcription in haploid male germ cells. *Int Rev Cytol*. 237:1-56.

Daumke O., M. Weyand, P.P. Chakrabarti, I.R. Vetter, and A. Wittinghofer. 2004 The GTPase-activating protein Rap1GAP uses a catalytic asparagine. *Nature*. 429(6988):197-201.

Deghmane A.E., H. Soulhine, H. Bach, K. Sendide, S. Itoh, A. Tam, S. Noubir, A. Talal, R. Lo, S. Toyoshima, Y. Av-Gay, and Z. Hmama. 2007. Lipoamide dehydrogenase mediates retention of coronin-1 on BCG vacuoles, leading to arrest in phagosome maturation. *J Cell Sci*. 120(Pt 16):2796-806.

Denny P, S. Swift, F. Connor, and A. Ashworth. 1992. An SRY-related gene expressed during spermatogenesis in the mouse encodes a sequence-specific DNA-binding protein. *EMBO J*. 11(10):3705-12

de Rooij D.G., and P. de Boer. 2003. Specific arrests of spermatogenesis in genetically modified and mutant mice. *Cytogenet. Genome Res*. 103:267-276.

Dorn, A., J. Bollekens, A. Staub, C. Benoist, and D. Mathis. 1987. A multiplicity of CCAAT box-binding proteins. *Cell*. 50:863-872.

Eddy E.M. 2002. Male germ cell gene expression. *Recent Prog Horm Res*. 57:103-28.

Ehman K.D., and M.E. Scott. 2002. Female mice mate preferentially with non-parasitized males. *Parasitology*. 125(Pt 5):461-6.

Fajardo M.A., H.S. Haugen, C.H. Clegg, and R.E. Braun. 1997. Separate elements in the 3' untranslated region of the mouse protamine 1 mRNA regulate translational repression and activation during murine spermatogenesis. *Dev Biol*. 191:42–52

Fawcett D.W., S. Ito, and D. Slautterback. 1959. The occurrence of intercellular bridges in groups of cells exhibiting synchronous differentiation. *J Biophys Biochem Cytol*. 5(3):453-60.

Fellenberg F., T.B. Hartmann, R. Dummer, D. Usener, D. Schadendorf, and S. Eichmuller. 2004. GBP-5 splicing variants: New guanylate-binding proteins with tumor-associated expression and antigenicity. *J Invest Dermatol*. 122(6):1510-7.

Feng C.G., C.M. Collazo-Custodio, M. Eckhaus, S. Hieny, Y. Belkaid, K. Elkins, D. Jankovic, G.A. Taylor, and A. Sher. 2004. Mice deficient in LRG-47 display increased susceptibility to mycobacterial infection associated with the induction of lymphopenia. *J Immunol*. 172: 1163–1168.

Foulkes N.S., B. Mellstrom, E. Benusiglio, and P. Sassone-Corsi. 1992. Developmental switch of CREM function during spermatogenesis: from antagonist to activator. *Nature*. 355(6355):80-4.

Fujii T., K. Tamura, K. Masai, H. Tanaka, Y. Nishimune, and H. Nojima. 2002. Use of stepwise subtraction to comprehensively isolate mouse genes whose transcription is up-regulated during spermiogenesis. *EMBO Rep*. 3(4):367-72.

Fujii T., K. Tamura, N.G. Copeland, D.J. Gilbert, N.A. Jenkins, K. Yomogida, H. Tanaka, Y. Nishimune, H. Nojima, and Y. Abiko. 1999. Sperizin is a murine RING zinc-finger protein specifically expressed in Haploid germ cells. *Genomics*. 57(1):94-101.

Fulcher K.D., C. Mori, J.E. Welch, D.A. O'Brien, D.G. Klapper, and E.M. Eddy. 1995. Characterization of Fsc1 cDNA for a mouse sperm fibrous sheath component. *Biol Reprod* 52:41-49.

Ghosh A., G.J. Praefcke, L. Renault, A. Wittinghofer, and C. Herrmann. 2006. How guanylate-binding proteins achieve assembly-stimulated processive cleavage of GTP to GMP. *Nature*. 440(7080):101-4.

Ghosh A., R. Uthaiah, J.C. Howard, C. Herrmann, and E. Wolf. 2004. Crystal structure of IIGP1: a paradigm for interferon-inducible p47 resistance GTPases. *Mol Cell*. 15:727–739. doi: 10.1016/j.molcel.2004.07.017.

Gilly M., M.A. Damore, and R. Wall. 1996 A promoter ISRE and dual 5' YY1 motifs control IFN-gamma induction of the IRG-47 G-protein gene. *Gene*. 179(2):237-44.

Gilly M., and R. Wall. 1992. The IRG-47 gene is IFN-gamma induced in B cells and encodes a protein with GTP-binding motifs. *J Immunol*. 148(10):3275-81.

Giorgini F., H.G. Davies, and R.E. Braun. 2001. MSY2 and MSY4 bind a conserved sequence in the 3' untranslated region of protamine 1 mRNA in vitro and in vivo. *Mol Cell Biol*. 21(20):7010-9.

Giorgini F., H.G. Davies, and R.E. Braun. 2002. Translational repression by MSY4 inhibits spermatid differentiation in mice. *Development*. 129(15):3669-79.

Gorbacheva V.Y., D. Lindner, G.C. Sen, and D.J. Vestal. 2002. The interferon (IFN)-induced GTPase, mGBP-2. Role in IFN-gamma-induced murine fibroblast proliferation.*J Biol Chem*. 277(8):6080-7.

Grimm D., P. Staeheli, M. Hufbauer, I. Koerner, L. Martinez-Sobrido, A. Solorzano, A. Garcia-Sastre, O. Haller, and G. Kochs. 2007. Replication fitness determines high virulence of influenza A virus in mice carrying functional Mx1 resistance gene. *Proc Natl Acad Sci U S A*. 104(16):6806-11.

Guenzi E., K. Topolt, C. Lubeseder-Martellato, A. Jorg, E. Naschberger, R. Benelli, A. Albini, and M. Sturzl. 2003. The guanylate binding protein-1 GTPase controls the invasive and angiogenic capability of endothelial cells through inhibition of MMP-1 expression. *EMBO J*. 22(15):3772-82.

Guenzi E., K. Topolt, E. Cornali, C. Lubeseder-Martellato, A. Jorg, K. Matzen, C. Zietz, E. Kremmer, F. Nappi, M. Schwemmle, C. Hohenadl, G. Barillari, E. Tschachler, P. Monini, B.

Ensoli, and M. Sturzl. 2001. The helical domain of GBP-1 mediates the inhibition of endothelial cell proliferation by inflammatory cytokines. *EMBO J*. 20(20):5568-77.

Gutierrez M.G., S.S. Master, S.B. Singh, G.A. Taylor, M.I. Colombo, and V. Deretic. 2004. Autophagy is a defense mechanism inhibiting BCG and Mycobacterium tuberculosis survival in infected macrophages. *Cell*. 17;119(6):753-66.

Haller O., P. Staeheli, and G. Kochs. 2007. Interferon-induced Mx proteins in antiviral host defense. *Biochimie*. 89(6-7):812-8.

Halonen S.K., G.A. Taylor, and L.M. Weiss. 2001. Gamma interferon-induced inhibition of Toxoplasma gondii in astrocytes is mediated by IGTP. *Infect Immun*. 69(9):5573-6.

Halonen S.K., T. Woods, K. McInnerney, and L.M. Weiss. 2006. Microarray analysis of IFN-gamma response genes in astrocytes. *J Neuroimmunol*. 175(1-2):19-30.

Han B.H., D.J. Park, R.W. Lim, J.H. Im, and H.D. Kim. 1998. Cloning, expression, and characterization of a novel guanylate-binding protein, GBP3 in murine erythroid progenitor cells. *Biochim Biophys Acta*. 1384(2):373-86.

Hauptmann R., and P. Swetly. 1985. A novel class of human type I interferons. *Nucleic Acids Res*. 13(13):4739-49.

Hawthorne S.K., R.R. Busanelli, and K.C. Kleene. 2006. The 5' UTR and 3' UTR of the sperm mitochondria-associated cysteine-rich protein mRNA regulate translation in spermatids by multiple mechanisms in transgenic mice. *Dev Biol*. 297(1):118-26.

Hefti H.P., M. Frese, H. Landis, C. Di Paolo, A. Aguzzi, O. Haller, and J. Pavlovic. 1999. Human MxA protein protects mice lacking a functional alpha/beta interferon system against La crosse virus and other lethal viral infections. *J Virol*. 73(8):6984-91.

Herrmann B.G., B. Koschorz, K. Wertz, K.J. McLaughlin, and A. Kispert. 1999. A protein kinase encoded by the t complex responder gene causes non-mendelian inheritance. *Nature*. 402(6758):141-6.

Heydecke D., D. Meyer, F. Ackermann, B. Wilhelm, T. Gudermann, and I. Boekhoff. 2006. The multi PDZ domain protein MUPP1 as a putative scaffolding protein for organizing signaling complexes in the acrosome of mammalian spermatozoa. *J Androl*. 27(3):390-404.

Hirshfield A.N. 1991. Development of follicles in the mammalian ovary. *Int Rev Cytol.* 124:43–101

Horisberger M.A., and H.K. Hochkeppel. 1987. IFN-alpha induced human 78 kD protein: purification and homologies with the mouse Mx protein, production of monoclonal antibodies, and potentiation effect of IFN-gamma. *J Interferon Res.* 7(4):331-43.

Horowitz E., Z. Zhang, B.H. Jones, S.B. Moss, C. Ho, J.R. Wood, X. Wang, M.D. Sammel, and J.F. Strauss 3rd. 2005. Patterns of expression of sperm flagellar genes: early expression of genes encoding axonemal proteins during the spermatogenic cycle and shared features of promoters of genes encoding central apparatus proteins. *Mol Hum Reprod.* 11(4):307-17.

Huh J.R., S.Y. Vernooy, H. Yu, N. Yan, Y. Shi, M. Guo, and B.A. Hay. 2004. Multiple apoptotic caspase cascades are required in nonapoptotic roles for Drosophila spermatid individualization. *PLoS Biol.* 2(1):E15.

Jackson, S.M., J. Ericsson, R. Mantovani, and P.A. Edwards. 1998. Synergistic activation of transcription by nuclear factor Y and sterol regulatory element binding protein. *J. Lipid Res.* 39, pp. 767–776.

James P., J. Halladay, and E.A. Craig. 1996. Genomic Libraries and a Host Strain Designed for Highly Efficient Two-Hybrid Selection in Yeast. *Genetics.* 144(4):1425-1436

Janzen C., G. Kochs, and O. Haller. 2000. A monomeric GTPase-negative MxA mutant with antiviral activity. *J Virol.* 74(17):8202-6.

Jesch S.A., T.S. Lewis, N.G. Ahn, and A.D. Linstedt. 2001. Mitotic phosphorylation of Golgi reassembly stacking protein 55 by mitogen-activated protein kinase ERK2. *Mol Biol Cell.* 12(6):1811-7.

Jimenez A., R. Oko, J.A. Gustafsson, G. Spyrou, M. Pelto-Huikko, and A. Miranda-Vizuete. 2002. Cloning, expression and characterization of mouse spermatid specific thioredoxin-1 gene and protein. *Mol Hum Reprod.* 8(8):710-8.

Jin H.K., T. Yamashita, K. Ochiai, O. Haller, and T. Watanabe. 1998. Characterization and expression of the Mx1 gene in wild mouse species. *Biochem Genet.* 36(9-10):311-22.

Kabeya Y., N. Mizushima, T. Ueno, A. Yamamoto, T. Kirisako, T. Noda, E. Kominami, Y. Ohsumi, and T. Yoshimori. 2000. LC3, a mammalian homologue of yeast Apg8p, is localized in autophagosome membranes after processing. *EMBO J.* 19, pp. 5720–5728.

Kaiser F., S.H. Kaufmann, and J. Zerrahn. 2004. IIGP, a member of the IFN inducible and microbial defense mediating 47 kDa GTPase family, interacts with the microtubule binding protein hook3. *J Cell Sci.* 117(Pt 9): 1747-56

Kanai Y, M. Kanai-Azuma, T. Noce, T.C. Saido, T. Shiroishi, Y. Hayashi, and K. Yazaki. 1996. Identification of two Sox17 messenger RNA isoforms, with and without the high mobility group box region, and their differential expression in mouse spermatogenesis. *J Cell Biol.* 133(3):667-81.

Kanai-Azuma M., Y. Kanai, J.M. Gad, Y. Tajima, C. Taya, M. Kurohmaru, Y. Sanai, H. Yonekawa, K. Yazaki, P.P. Tam, and Y. Hayashi. 2002. Depletion of definitive gut endoderm in Sox17-null mutant mice. *Development.* 129(10):2367-79.

Kankova S., P. Kodym, D. Frynta, R. Vavrinova, A. Kubena, and J. Flegr. 2007. Influence of latent toxoplasmosis on the secondary sex ratio in mice. *Parasitology.* Epub ahead of print

Kashiwabara S., J. Noguchi, T. Zhuang, K. Ohmura, A. Honda, S. Sugiura, K. Miyamoto, S. Takahashi, K. Inoue, A. Ogura, and T. Baba. 2002. Regulation of spermatogenesis by testis-specific, cytoplasmic poly(A) polymerase TPAP. *Science.* 298(5600):1999-2002.

Kashiwabara S., T. Baba, M. Takada, K. Watanabe, Y. Yano, and Y. Arai. 1990. Primary structure of mouse proacrosin deduced from the cDNA sequence and its gene expression during spermatogenesis. *J Biochem.* 108(5):785-91.

Kerr J.B., and D.M. de Kretser. 1974. Proceedings: The role of the Sertoli cell in phagocytosis of the residual bodies of spermatids. *Reprod Fertil.* 36(2):439-40.

Kimmins S., N. Kotaja, I. Davidson, and P. Sassone-Corsi. 2004. Testis-specific transcription mechanisms promoting male germ-cell differentiation. *Reproduction.* 128(1):5-12.

Klamp T., U. Boehm, D. Schenk, K. Pfeffer, and J.C. Howard. 2003. A giant GTPase, very large inducible GTPase-1, is inducible by IFNs. *J Immunol.* 171(3):1255-65.

Kleene K.C. 1984. Translational regulation and deadenylation of a protamine mRNA during spermatogenesis in the mouse. *Dev. Biol*. 105:455-464

Kleene K.C. 2003. Patterns, mechanisms, and functions of translation regulation in mammalian spermatogenic cells. *Cytogenet Genome Res*. 103(3-4):217-24.

Klemm U., W.M. Maier, S. Tsaousidou, I.M. Adham, K. Willison, and W. Engel. 1990. Mouse preproacrosin: cDNA sequence, primary structure and postmeiotic expression in spermatogenesis. *Differentiation*. 42(3):160-6.

Klionsky D.J., J.M. Cregg, W.A. Dunn Jr., S.D. Emr, Y. Sakai, I.V. Sandoval, A. Sibirny, S. Subramani, M. Thumm, M. Veenhuis, and Y. Ohsumi. 2003. A unified nomenclature for yeast autophagy-related genes. *Dev. Cell* 5, pp. 539–545.

Kochs G., M. Haener, U. Aebi, and O. Haller. 2002a. Self-assembly of human MxA GTPase into highly ordered dynamin-like oligomers. *J Biol Chem*. 277(16):14172-6.

Kochs G., C. Janzen, H. Hohenberg, and O. Haller. 2002b. Antivirally active MxA protein sequesters La Crosse virus nucleocapsid protein into perinuclear complexes. *Proc Natl Acad Sci U S A*. 99(5):3153-8.

Kochs G., and O. Haller. 1999a. GTP-bound human MxA protein interacts with the nucleocapsids of Thogoto virus (Orthomyxoviridae). *J Biol Chem*. 274(7):4370-6.

Kochs G., and O. Haller. 1999b. Interferon-induced human MxA GTPase blocks nuclear import of Thogoto virus nucleocapsids. *Proc Natl Acad Sci U S A*. 96(5):2082-6.

Koga R., S. Hamano, H. Kuwata, K. Atarashi, M. Ogawa, H. Hisaeda, M. Yamamoto, S. Akira, K. Himeno, M. Matsumoto, and K. Takeda. 2006. TLR-dependent induction of IFN-beta mediates host defense against *Trypanosoma cruzi*. *J Immunol.* 177: 7059–7066.

Kontgen F., G. Süss, C. Stewart, M. Steinmetz, and H. Bluethmann. 1993. Targeted disruption of the MHC class II Aa gene in C57BL/6 mice. *Int Immunol*. 5(8):957-64.

Kota R.S., J.C. Rutledge, K. Gohil, A. Kumar, R.I. Enelow, and C.V. Ramana. 2006. Regulation of gene expression in RAW 264.7 macrophage cell line by interferon-gamma. *Biochem Biophys Res Commun*. 342(4):1137-46.

Kotaja N., D. De Cesare, B. Macho, L. Monaco, S. Brancorsini, E. Goossens, H. Tournaye, A. Gansmuller, and P. Sassone-Corsi. 2004. Abnormal sperm in mice with targeted deletion of the act (activator of cAMP-responsive element modulator in testis) gene. *Proc Natl Acad Sci U S A*. 101(29):10620-5.

Kotenko S.V., G. Gallagher, V.V. Baurin, A. Lewis-Antes, M. Shen, N.K. Shah, J.A. Langer, F. Sheikh, H. Dickensheets, and R.P. Donnelly. 2003. IFN-lambdas mediate antiviral protection through a distinct class II cytokine receptor complex. *Nat Immunol*. 4(1):69-77.

Krajewski S., M. Krajewska, and J.C. Reed. 1996. Immunohistochemical analysis of *in vivo* patterns of Bak expression, a proapoptotic member of the Bcl-2 protein family. *Cancer Res*. 56:2849–2855.

Kueng P., Z. Nikolova, V. Djonov, A. Hemphill, V. Rohrbach, D. Boehlen, G. Zuercher, A.C. Andres, and A. Ziemiecki. 1997. A novel family of serine/threonine kinases participating in spermiogenesis. *J Cell Biol*. 139(7):1851-9.

Kumar S., C. Mitnik, G. Valente, and G. Floyd-Smith. 2000. Expansion and molecular evolution of the interferon-induced 2'-5' oligoadenylate synthetase gene family. *Mol Biol Evol*. 17(5):738-50.

LaFleur D.W., B. Nardelli, T. Tsareva, D. Mather, P. Feng, M. Semenuk, K. Taylor, M. Buergin, D. Chinchilla, V. Roshke, G. Chen, S.M. Ruben, P.M. Pitha, T.A. Coleman, and P.A. Moore. 2001. Interferon-kappa, a novel type I interferon expressed in human keratinocytes. *J Biol Chem*. 276(43):39765-71.

Lafuse, W., D. Brown, L. Castle, and B. Zwilling. 1995. Cloning and characterization of a novel cDNA that is IFN-γ-induced in mouse peritoneal macrophages and encodes a putative GTP-binding protein. *J. Leukoc. Biol.* 57:477.

Lambert R. 2007. Breeding Strategies for Maintaining Colonies of Laboratory Mice – A Jackson Laboratory Resource Manual. The Jackson Laboratory.

Leblond C.P., and Y. Clermont. 1952. Spermiogenesis of rat, mouse, hamster and guinea pig as revealed by the periodic acid-fuchsin sulfurous acid technique. *Am J Anat*. 90(2):167-215.

Lefebvre V., P. Li, and B. de Crombrugghe. 1998. A new long form of Sox5 (L-Sox5), Sox6 and Sox9 are coexpressed in chondrogenesis and cooperatively activate the type II collagen gene. *EMBO J*. 17(19):5718-33.

Lefevre F., M. Guillomot, S. D'Andrea, S. Battegay, and C. La Bonnardiere. 1998. Interferon-delta: the first member of a novel type I interferon family. *Biochimie*. 80(8-9):779-88.

Lenhard B., A. Sandelin, L. Mendoza, P. Engstrom, N. Jareborg, and W.W. Wasserman. 2003. Identification of conserved regulatory elements by comparative genome analysis. *J Biol*. 2(2):13.

Leung T., B.E. How, E. Manser, and L. Lim. 1993. Germ cell beta-chimaerin, a new GTPase-activating protein for p21rac, is specifically expressed during the acrosomal assembly stage in rat testis. *J Biol Chem*. 268(6):3813-6.

Lichtenfels A.J., J.B. Gomes, P.C. Pieri, S.G. El Khouri Miraglia, J. Hallak, and P.H. Saldiva. 2006. Increased levels of air pollution and a decrease in the human and mouse male-to-female ratio in Sao Paulo, Brazil. *Fertil Steril*. 87(1):230-2.

Lin Q., A. Sirotkin, and A.I. Skoultchi. 2000. Normal spermatogenesis in mice lacking the testis-specific linker histone H1t.*Mol Cell Biol*. 20(6):2122-8.

Lindenmann J., C.A. Lane, and D. Hobson. 1963. The resistance of A2g mice to myxoviruses. *J Immunol*. 90:942-51.

Ling Y.M., M.H. Shaw, C. Ayala, I. Coppens, G.A. Taylor, D.J. Ferguson, and G.S. Yap. 2006. Vacuolar and plasma membrane stripping and autophagic elimination of *Toxoplasma gondii* in primed effector macrophages. *J Exp Med.* 203: 2063–2071.

Liu D., J.M. Brockman, B. Dass, L.N. Hutchins, P. Singh, J.R. McCarrey, C.C. MacDonald, and J.H. Graber. 2007. Systematic variation in mRNA 3'-processing signals during mouse spermatogenesis. *Nucleic Acids Res*. 35(1):234-46.

Luan Z., Y. Zhang, A. Liu, Y. Man, L. Cheng, and G. Hu. 2002. A novel GTP-binding protein hGBP3 interacts with NIK/HGK. *FEBS Lett*. 530(1-3):233-8.

Lyon M.F. 2003. Transmission ratio distortion in mice. *Annu Rev Genet*. 37:393-408.

MacDonald C.C., and J.L. Redondo. 2002. Reexamining the polyadenylation signal: were we wrong about AAUAAA? *Mol Cell Endocrinol.* 190(1-2):1-8.

MacMicking J.D. 2004. IFN-inducible GTPases and immunity to intracellular pathogens. *Trends Immunol.* 25(11):601-9.

MacMicking J.D. 2005. Immune control of phagosomal bacteria by p47 GTPases. *Curr Opin Microbiol.* 8(1):74-82.

MacMicking J., G.A. Taylor, and J. McKinney. 2003. Immune control of tuberculosis by IFN-gamma-inducible LRG-47. *Science*. 302:654–659. doi: 10.1126/science.1088063.

Mandal A., S. Naaby-Hansen, M.J. Wolkowicz, K. Klotz, J. Shetty, J.D. Retief, S.A. Coonrod, M. Kinter, N. Sherman, F. Cesar, C.J. Flickinger, and J.C. Herr. 1999. FSP95, a testis-specific 95-kilodalton fibrous sheath antigen that undergoes tyrosine phosphorylation in capacitated human spermatozoa. *Biol Reprod.* 61(5):1184-97.

Mannan A.U., K. Nayernia, C. Mueller, P. Burfeind, I.M. Adham, and W. Engel. 2003. Male mice lacking the Theg (testicular haploid expressed gene) protein undergo normal spermatogenesis and are fertile. *Biol Reprod.* 69(3):788-96.

Mantovani R. 1998. A survey of 178 NF-Y binding CCAAT boxes. *Nucleic Acids Res.* 26(5):1135-43.

Martens S, K. Sabel, R. Lange, R. Uthaiah, E. Wolf, and J.C. Howard. 2004. Mechanisms regulating the positioning of mouse p47 resistance GTPases LRG-47 and IIGP1 on cellular membranes: retargeting to plasma membrane induced by phagocytosis. *J Immunol*.173:2594–2606.

Martens S., I. Parvanova, J. Zerrahn, G. Griffiths, G. Schell, G. Reichmann, and J.C. Howard. 2005. Disruption of *Toxoplasma gondii* Parasitophorous Vacuoles by the Mouse p47-Resistance GTPases. *PLoS Pathog.* 1(3): e24. doi: 10.1371/journal.ppat.0010024.

Martens S., and J. Howard. 2006 The interferon-inducible GTPases. *Annu Rev Cell Dev Biol.* 22:559-89.

Matsui T., M. Kanai-Azuma, K. Hara, S. Matoba, R. Hiramatsu, H. Kawakami, M. Kurohmaru, P. Koopman, and Y. Kanai. 2006. Redundant roles of Sox17 and Sox18 in postnatal angiogenesis in mice. *J Cell Sci*. 119(Pt 17):3513-26.

Matzuk M.M., and D.J. Lamb. 2002. Genetic dissection of mammalian fertility pathways. *Nat Cell Biol.* Suppl:s41-9.

McCarrey J.R., and K. Thomas. 1987. Human testis-specific PGK gene lacks introns and possesses characteristics of a processed gene. *Nature*. 326(6112):501-5.

Meier E., J. Fah, M.S. Grob, R. End, P. Staeheli, and O. Haller. 1988. A family of interferon-induced Mx-related mRNAs encodes cytoplasmic and nuclear proteins in rat cells. *J Virol*. 62(7):2386-93.

Meistrich M.L., K. Kasai, P. Olds-Clarke, G.R. MacGregor, A.D. Berkowitz, and K.S. Tung. 1994. Deficiency in fertilization by morphologically abnormal sperm produced by azh mutant mice. *Mol Reprod Dev*. 37(1):69-77.

Meistrich M.L., P.K. Trostle-Weige, and L.D. Russell. 1990. Abnormal manchette development in spermatids of azh/azh mutant mice. *Am J Anat*. 188(1):74-86.

Melen K., T. Ronni, B. Broni, R.M. Krug, C.H. von Bonsdorff, and I. Julkunen. 1992. Interferon-induced Mx proteins form oligomers and contain a putative leucine zipper. *J Biol Chem*. 267(36):25898-907.

Mendoza-Lujambio I., P. Burfeind, C. Dixkens, A. Meinhardt, S. Hoyer-Fender, W. Engel, and J. Neesen. 2002. The Hook1 gene is non-functional in the abnormal spermatozoon head shape (azh) mutant mouse. *Hum Mol Genet*. 11(14):1647-58.

Miranda-Vizuete A., K. Tsang, Y. Yu, A. Jimenez, M. Pelto-Huikko, C.J. Flickinger, P. Sutovsky, and R. Oko. 2003. Cloning and developmental analysis of murid spermatid-specific thioredoxin-2 (SPTRX-2), a novel sperm fibrous sheath protein and autoantigen. *J Biol Chem*. 278(45):44874-85.

Miyairi I., V.R. Tatireddigari, O.S. Mahdi, L.A. Rose, R.J. Belland, L. Lu, R.W. Williams, and G.I. Byrne. 2007. The p47 GTPases Iigp2 and Irgb10 regulate innate immunity and inflammation to murine Chlamydia psittaci infection. *J Immunol*. 179(3):1814-24.

Modiano N., Y.E. Lu, and P. Cresswell. 2005. Golgi targeting of human guanylate-binding protein-1 requires nucleotide binding, isoprenylation, and an IFN-gamma-inducible cofactor. *Proc Natl Acad Sci U S A*. 102(24):8680-5.

Mogensen K.E., M. Lewerenz, J. Reboul, G. Lutfalla, and G. Uze. 1999. The type I interferon receptor: structure, function, and evolution of a family business. *J Interferon Cytokine Res*. 19(10):1069-98.

Mori C., J.E. Welch, Y. Sakai, and E.M. Eddy. 1992. In situ localization of spermatogenic cell-specific glyceraldehyde 3-phosphate dehydrogenase (Gapd-s) messenger ribonucleic acid in mice. *Biol Reprod*. 46(5):859-68.

Mori H., D. Shimizu, R. Fukunishi, and A.K. Christensen. 1982. Morphometric analysis of testicular Leydig cells in normal adult mice. *Anat Rec*. 204(4):333-9.

Mosmann T.R., and R.L. Coffman. 1989. TH1 and TH2 cells: different patterns of lymphokine secretion lead to different functional properties. *Annu Rev Immunol*. 7:145-73.

Müller W., R. Kühn, and K. Rajewsky. 1991. Major histocompatibility complex class II hyperexpression on B cells in interleukin 4-transgenic mice does not lead to B cell proliferation and hypergammaglobulinemia. *Eur J Immunol*. 21(4):921-5.

Nantel F., L. Monaco, N.S. Foulkes, D. Masquilier, M. LeMeur, K. Henriksen, A. Dierich, M. Parvinen, and P. Sassone-Corsi. 1996. Spermiogenesis deficiency and germ-cell apoptosis in CREM-mutant mice. *Nature*. 380(6570):159-62.

Nelander S., E. Larsson, E. Kristiansson, R. Mansson, O. Nerman, M. Siqvardsson, P. Mostad, and P. Lindahl. 2005. Predictive screening for regulators of conserved functional gene modules (gene batteries) in mammals. *BMC Genomics*. 6(1):68

Nelson D.E., D.P. Virok, H. Wood, C. Roshick, R.M. Johnson, W.M. Whitmire, D.D. Crane, O. Steele-Mortimer, L. Kari, G. McClarty, and H.D. Caldwell. 2005. Chlamydial IFN-gamma immune evasion is linked to host infection tropism. *Proc Natl Acad Sci*. USA 102: 10658–10663.

Neun R., M.F. Richter, P. Staeheli, and M. Schwemmle. 1996. GTPase properties of the interferon-induced human guanylate-binding protein 2. *FEBS Lett*. 390(1):69-72.

Nguyen T.T., Y. Hu, D.P. Widney, R.A. Mar, and J.B. Smith. 2002 Murine GBP-5, a new member of the murine guanylate-binding protein family, is coordinately regulated with other GBPs in vivo and in vitro. *J Interferon Cytokine Res*. 22(8):899-909.

Niimi T., Y. Hayashi, S. Futaki, and K. Sekiguchi. 2004. SOX7 and SOX17 regulate the parietal endoderm-specific enhancer activity of mouse laminin alpha1 gene. *J Biol Chem*. 279(36):38055-61.

Noteborn M., H. Arnheiter, L. Richter-Mann, H. Browning, and C. Weissmann. 1987. Transport of the murine Mx protein into the nucleus is dependent on a basic carboxy-terminal sequence. *J Interferon Res.* 7(5):657-69.

Oakberg E.F. 1956. A description of spermiogenesis in the mouse and its use in analysis of the cycle of the seminiferous epithelium and germ cell renewal. *Am J Anat*. 99(3):391-413.

Oko R. 1998. Occurrence and formation of cytoskeletal proteins in mammalian spermatozoa. *Andrologia*. 30(4-5):193-206.

Olszewski M.A., J. Gray, and D.J. Vestal. 2006. In silico genomic analysis of the human and murine guanylate-binding protein (GBP) gene clusters. *J Interferon Cytokine Res*. 26(5):328-52.

Oritani K., K.L. Medina, Y. Tomiyama, J. Ishikawa, Y. Okajima, M. Ogawa, T. Yokota, K. Aoyama, I. Takahashi, P.W. Kincade, and Y. Matsuzawa. 2000. Limitin: An interferon-like cytokine that preferentially influences B-lymphocyte precursors. *Nat Med*. 6(6):659-66.

Parkes M., J.C. Barrett, N.J. Prescott, M. Tremelling, C.A. Anderson, S.A. Fisher, R.G. Roberts, E.R: Nimmo, F.R. Cummings, D. Soars, H. Drummond, C.W. Lees, S.A. Khawaja, R. Bagnall, D.A. Burke, C.E. Todhunter, T. Ahmad, C.M. Onnie, W. McArdle, D. Strachan, G. Bethel, C. Bryan, C.M. Lewis, P. Deloukas, A. Forbes, J. Sanderson, D.P. Jewell, J. Satsangi, J.C. Mansfield; Wellcome Trust Case Control Consortium, L. Cardon, and C.G. Mathew. 2007. Sequence variants in the autophagy gene IRGM and multiple other replicating loci contribute to Crohn's disease susceptibility. *Nat Genet*. 39(7):830-2.

Parvanova I. 2005. Analysis of the role of the p47 GTPase IIGP1 in Resistance against Intracellular Pathogens. Dissertation.

Pavlovic J., O. Haller, and P. Staeheli. 1992. Human and mouse Mx proteins inhibit different steps of the influenza virus multiplication cycle. *J Virol*. 66(4):2564-9.

Pestka S., C.D. Krause, and M.R. Walter. 2004. Interferons, interferon-like cytokines, and their receptors. *Immunol Rev*. 202:8-32.

Platanias L.C. 2005. Mechanisms of type-I- and type-II-interferon-mediated signalling. *Nat Rev Immunol*. 5(5):375-86.

Praefcke G.J., and H.T. McMahon. 2004. The dynamin superfamily: universal membrane tubulation and fission molecules? *Nat Rev Mol Cell Biol*. 5(2):133-47.

Praefcke G.J., M. Geyer, M. Schwemmle, H. Robert Kalbitzer, and C. Herrmann. 1999. Nucleotide-binding characteristics of human guanylate-binding protein 1 (hGBP1) and identification of the third GTP-binding motif. *J Mol Biol*. 292(2):321-32.

Prakash B., G.J. Praefcke, L. Renault, A. Wittinghofer, and C. Herrmann. 2000. Structure of human guanylate-binding protein 1 representing a unique class of GTP-binding proteins. *Nature*. 403(6769):567-71.

Puddu P., M. Carollo, I. Pietraforte, F. Spadaro, M. Tombesi, C. Ramoni, F. Belardelli, and S. Gessani. 2005. IL-2 induces expression and secretion of IFN-gamma in murine peritoneal macrophages. *J Leukoc Biol*. 78(3):686-95.

Reichelt M., S. Stertz, J. Krijnse-Locker, O. Haller, and G. Kochs. 2004. Missorting of LaCrosse virus nucleocapsid protein by the interferon-induced MxA GTPase involves smooth ER membranes. *Traffic*. 5(10):772-84.

Reith W., C.-A. Seigrist, B. Durand, E. Barras, and B. Mach. 1994. Function of major histocompatibility complex class II promoters requires cooperative binding between factors RFX and NF-Y. *Proc. Natl. Acad. Sci. USA* 91, 554–558.

Richter M.F., M. Schwemmle, C. Herrmann, A. Wittinghofer, and P. Staeheli. 1995. Interferon-induced MxA protein. GTP binding and GTP hydrolysis properties. *J Biol Chem*. 270(22):13512-7.

Rideout W.M. 3rd, T. Wakayama, A. Wutz, K. Eggan, L. Jackson-Grusby, J. Dausman, R. Yanagimachi, and R. Jaenisch. 2000. Generation of mice from wild-type and targeted ES cells by nuclear cloning. *Nat Genet*. 24(2):109-10.

Roberts R.M. 2007. Interferon-tau, a Type 1 interferon involved in maternal recognition of pregnancy. *Cytokine Growth Factor Rev*. Epub ahead of print

Robertsen B., J. Zou, C. Secombes, and J.A. Leong. 2006. Molecular and expression analysis of an interferon-gamma-inducible guanylate-binding protein from rainbow trout (Oncorhynchus mykiss). *Dev Comp Immunol*. 30(11):1023-33.

Robzyk K., and Y. Kassir. 1992. A simple and highly efficient procedure for rescuing autonomous plasmids from yeast. *Nucleic Acids Res*. 20(14):3790.

Rohde C. 2003. Studien über die in der Maus und dem Menschen konservierte p47 GTPase Cinema. Diplomarbeit

Russell L.D. 1979. Spermatid-Sertoli tubulobulbar complexes as devices for elimination of cytoplasm from the head region late spermatids of the rat. *Anat Rec*. 194(2):233-46.

Russel L.D., R.A. Ettlin, A.P. Sinha Hikim, and E.D. Clegg. 1991. Histological and histopathological evaluation of the testis. Cache River Press, Clearwater.

Sad S., R. Marcotte, and T.R. Mosmann. 1995. Cytokine-induced differentiation of precursor mouse CD8+ T cells into cytotoxic CD8+ T cells secreting Th1 or Th2 cytokines. *Immunity*. 2(3):271-9.

Saitou N., and M. Nei. 1987. The neighbor-joining method: a new method for reconstructing phylogenetic trees. *Mol Biol Evol*. 4(4):406-25.

Sambrook J., E.F. Fritsch, and T. Maniatis. 1989. Molecular Cloning. Cold Spring Harbour Laboratory Press.

Sandelin A., W.W. Wasserman, and B. Lenhard. 2004. ConSite: web-based prediction of regulatory elements using cross-species comparison. *Nucleic Acids Res*. 32(Web Server issue):W249-52.

Sanger F., S. Nicklen, and A.R. Coulson. 1977. DNA sequencing with chain-terminating inhibitors. *Proc Natl Acad Sci U S A*. 74(12):5463-7.

Santiago, H.C., C.G. Feng, A. Bafica, E. Roffe, R.M. Arantes, A. Cheever, G. Taylor, L.Q. Vieira, J. Aliberti, R.T. Gazzinelli, and A. Sher. 2005. Mice deficient in LRG-47 display enhanced susceptibility to *Trypanosoma cruzi* infection associated with defective hemopoiesis and intracellular control of parasite growth. *J Immunol*. 175: 8165–8172.

Sassone-Corsi P. 1998. CREM: a master-switch governing male germ cells differentiation and apoptosis. *Semin Cell Dev Biol*. 9(4):475-82.

Schug J. 2003. Current Protocols in Bioinformatics - Using TESS to Predict Transcription Factor Binding Sites in DNA Sequence. John Wiley & Sons, Inc.

Schwemmle M., and P. Staeheli. 1994. The interferon-induced 67-kDa guanylate-binding protein (hGBP1) is a GTPase that converts GTP to GMP. *J Biol Chem*. 269(15):11299-305.

Schwenk F., U. Baron, and K. Rajewsky. 1995. A cre-transgenic mouse strain for the ubiquitous deletion of loxP-flanked gene segments including deletion in germ cells. *Nucleic Acids Res*. 23(24):5080-1.

Sheppard P., W. Kindsvogel, W. Xu, K. Henderson, S. Schlutsmeyer, T.E. Whitmore, R. Kuestner, U. Garrigues, C. Birks, J. Roraback, C. Ostrander, D. Dong, J. Shin, S. Presnell, B. Fox, B. Haldeman, E. Cooper, D. Taft, T. Gilbert, F.J. Grant, M. Tackett, W. Krivan, G. McKnight, C. Clegg, D. Foster, and K.M. Klucher. 2003. IL-28, IL-29 and their class II cytokine receptor IL-28R. *Nat Immunol*. 4(1):63-8.

Shiratsuchi A., M. Umeda, Y. Ohba, and Y. Nakanishi. 1997. Recognition of phosphatidylserine on the surface of apoptotic spermatogenic cells and subsequent phagocytosis by Sertoli cells of the rat. *J Biol Chem*. 272(4):2354-8.

Shorter J., R. Watson, M.E. Giannakou, M. Clarke, G. Warren, and F.A. Barr. 1999. GRASP55, a second mammalian GRASP protein involved in the stacking of Golgi cisternae in a cell-free system. *EMBO J*. 18(18):4949-60.

Singh S.B., A.S. Davis, G.A. Taylor, and V. Deretic. 2006. Human IRGM induces autophagy to eliminate intracellular mycobacteria. *Science*. 313(5792):1438-41.

Smits P., P. Li, J. Mandel, Z. Zhang, J.M. Deng, R.R. Behringer, B. de Crombrugghe, and V. Lefebvre. 2001. The transcription factors L-Sox5 and Sox6 are essential for cartilage formation. *Dev Cell*. 1(2):277-90.

Sohn J., J. Natale, L.J. Chew, S. Belachew, Y. Cheng, A. Aguirre, J. Lytle, B. Nait-Oumesmar, C. Kerninon, M. Kanai-Azuma, Y. Kanai, and V. Gallo. 2006. Identification of Sox17 as a transcription factor that regulates oligodendrocyte development. *J Neurosci*. 26(38):9722-35.

Somboonthum P., H. Ohta, S. Yamada, M. Onishi, A. Ike, Y. Nishimune, and M. Nozaki. 2005. cAMP-responsive element in TATA-less core promoter is essential for haploid-specific gene expression in mouse testis. *Nucleic Acids Res*. 33(10):3401-11.

Sorace, J., R. Johnson, D. Howard, and B. Drysdale. 1995. Identification of an endotoxin and IFN-inducible cDNA: possible identification of a novel protein family. *J. Leukoc. Biol.* 58:477.

Sprando R.L., and L.D. Russell. 1987. Comparative study of cytoplasmic elimination in spermatids of selected mammalian species. *Am J Anat*. 178(1):72-80.

Staeheli P., M. Prochazka, P.A. Steigmeier, and O. Haller. 1984. Genetic control of interferon action: mouse strain distribution and inheritance of an induced protein with guanylate-binding property. *Virology*. 137(1):135-42.

Staeheli P., and O. Haller. 1985. Interferon-induced human protein with homology to protein Mx of influenza virus-resistant mice. *Mol Cell Biol*. 5(8):2150-3.

Staeheli P., O. Haller, W. Boll, J. Lindenmann, and C. Weissmann. 1986. Mx protein: constitutive expression in 3T3 cells transformed with cloned Mx cDNA confers selective resistance to influenza virus. *Cell*. 44(1):147-58.

Staeheli P., and J.G. Sutcliffe. 1988. Identification of a second interferon-regulated murine Mx gene. *Mol Cell Biol*. 8(10):4524-8.

Tam P.P., M. Kanai-Azuma, and Y. Kanai. 2003. Early endoderm development in vertebrates: lineage differentiation and morphogenetic function. *Curr Opin Genet Dev*. 13(4):393-400.

Tamura K., J. Dudley, M. Nei, and S. Kumar. 2007. MEGA4: Molecular Evolutionary Genetics Analysis (MEGA) software version 4.0. *Molecular Biology and Evolution* 10.1093/molbev/msm092.

Tanaka H., N. Iguchi, C. Egydio de Carvalho, Y. Tadokoro, K. Yomogida, and Y. Nishimune. 2003. Novel actin-like proteins T-ACTIN 1 and T-ACTIN 2 are differentially expressed in the cytoplasm and nucleus of mouse haploid germ cells. *Biol Reprod*. 69(2):475-82.

Tanaka H., and T. Baba. 2005. Gene expression in spermiogenesis. *Cell Mol Life Sci*. 62(3):344-54.

Taveau M., D. Stockholm, S. Marchand, C. Roudaut, M. Le Bert, and I. Richard. 2004. Bidirectional transcriptional activity of the Pgk1 promoter and transmission ratio distortion in Capn3-deficient mice. *Genomics*. 84(3):592-5.

Tay J., and J.D. Richter. 2001. Germ cell differentiation and synaptonemal complex formation are disrupted in CPEB knockout mice.*Dev Cell*. 1(2):201-13.

Taylor G., M. Jeffers, D. Largaespada, N. Jenkins, N. Copeland, G. Vande Woude. 1996. Identification of a novel GTPase, the inducibly expressed GTPase, that accumulates in response to interferon-ɣ. *J. Biol. Chem.* 271:20399

Taylor G.A., C.M. Collazo, G.S. Yap, K. Nguyen, T.A. Gregorio, L.S. Taylor, B. Eagleson, L. Secrest, E.A. Southon, S.W. Reid, L. Tessarollo, M. Bray, D.W. McVicar, K.L. Komschlies, H.A. Young, C.A. Biron, A. Sher, and G.F. Vande Woude. 2000. Pathogen-specific loss of host resistance in mice lacking the IFN-gamma-inducible gene IGTP. *Proc Natl Acad Sci U S A*. 97(2):751-5.

Taylor G.A., R. Stauber, S. Rulong, E. Hudson, V. Pei, G.N. Pavlakis, J.H. Resau, and G.F. Vande Woude. 1997. The inducibly expressed GTPase localizes to the endoplasmic reticulum, independently of GTP binding. *J Biol Chem*. 272:10639–10645. doi: 10.1074/jbc.272.16.10639.

Taylor G.A. 2007. IRG proteins: key mediators of interferon-regulated host resistance to intracellular pathogens. *Cell Microbiol*. 9(5):1099-107.

Terskikh A.V., M.C. Easterday, L. Li, L. Hood, H.I. Kornblum, D.H. Geschwind, and I.L. Weissman. 2001. From hematopoiesis to neuropoiesis: evidence of overlapping genetic programs. *Proc Natl Acad Sci U S A*. 98(14):7934-9.

Thomas M.A., and B. Lemmer. 2005. HistoGreen: a new alternative to 3,3'-diaminobenzidine-tetrahydrochloride-dihydrate (DAB) as a peroxidase substrate in immunohistochemistry?. *Brain Res Brain Res Protoc*. 14(2):107-18.

Torres R., and R. Kühn. 1997. Laboratory protocols for conditional gene targeting. *Oxford university press*.

Trinchieri G. 1995. Interleukin-12: a proinflammatory cytokine with immunoregulatory functions that bridge innate resistance and antigen-specific adaptive immunity. *Annu Rev Immunol*. 13:251-76.

Trivers R.L., and D.E. Willard. 1973. Natural selection of parental ability to vary the sex ratio of offspring. *Science*. 179(68):90-2.

Uthaiah R., G.J.M. Praefcke, J.C. Howard, and C. Herrmann. 2003. IIGP-1, a interferon-γ inducible 47 kDa GTPase of the mouse, is a slow GTPase showing co-operative enzymatic activity and GTP-dependent multimerisation. *J Biol Chem*. 278:29336–29343. doi: 10.1074/jbc.M211973200.

van Pesch V., H. Lanaya, J.C. Renauld, and T. Michiels. 2004. Characterization of the murine alpha interferon gene family. *J Virol*. 78(15):8219-28.

Venezia T.A., A.A. Merchant, C.A. Ramos, N.L. Whitehouse, A.S. Young, C.A. Shaw, and M.A. Goodell. 2004. Molecular signatures of proliferation and quiescence in hematopoietic stem cells. *PLoS Biol*. 2(10):e301.

Vergouwen R.P., S.G. Jacobs, R. Huiskamp, J.A. Davids, and D.G. de Rooij. 1993. Postnatal development of testicular cell populations in mice. *J Reprod Fertil*. 99(2):479-85.

Vestal D.J. 2005. The guanylate-binding proteins (GBPs): proinflammatory cytokine-induced members of the dynamin superfamily with unique GTPase activity. *J Interferon Cytokine Res*. 25(8):435-43.

Vestal D.J., V.Y. Gorbacheva, and G.C. Sen. 2000. Different subcellular localizations for the related interferon-induced GTPases, MuGBP-1 and MuGBP-2: implications for different functions? *J Interferon Cytokine Res*. 20(11):991-1000.

Vijayaraghavan S., G.A. Liberty, J. Mohan, V.P. Winfrey, G.E. Olson, and D.W. Carr. 1999. Isolation and molecular characterization of AKAP110, a novel, sperm-specific protein kinase A-anchoring protein. *Mol Endocrinol*. 13(5):705-17.

Wang Y., J. Seemann, M. Pypaert, J. Shorter, and G. Warren. 2003. A direct role for GRASP65 as a mitotically regulated Golgi stacking factor. *EMBO J*. 22(13):3279-90.

Weber J.E., and L.D. Russell. 1987. A study of intercellular bridges during spermatogenesis in the rat. *Am J Anat.* 180(1):1-24.

Weir J.A. 1960. A Sex Ratio Factor in the House Mouse That Is Transmitted by the Male. *Genetics*. 45(11):1539-52.

Welch J.E., P.R. Brown, D.A. O'Brien, and E.M. Eddy. 1995. Genomic organization of a mouse glyceraldehyde 3-phosphate dehydrogenase gene (Gapd-s) expressed in post-meiotic spermatogenic cells. *Dev Genet*. 16(2):179-89.

Wellcome Trust Case Control Consortium. 2007. Genome-wide association study of 14,000 cases of seven common diseases and 3,000 shared controls. *Nature*. 447(7145):661-78.

Wilson M., and P. Koopman. 2002. Matching SOX: partner proteins and co-factors of the SOX family of transcriptional regulators. *Curr Opin Genet Dev*. 12(4):441-6.

Wright K.L., T. L. Moore, B.J. Vilen, A.M. Brown, and J.P.-Y. Ting. 1995. Major histocompatibility complex class II-associated invariant chain gene expression is up-regulated by cooperative interactions of Sp1 and NF-Y. *J. Biol. Chem.* 270, pp. 20978–20986.

Wynn T.A., C.M. Nicolet, and D.M Paulnock. 1991. Identification and characterization of a new gene family induced during macrophage activation. *J Immunol*. 147(12):4384-92

Yan W., L. Ma, K.H. Burns, and M.M. Matzuk. 2003. HILS1 is a spermatid-specific linker histone H1-like protein implicated in chromatin remodeling during mammalian spermiogenesis. *Proc Natl Acad Sci U S A*. 100(18):10546-51.

Zerrahn J., U.E. Schaible, V. Brinkmann, U. Guhlich, und S.H. Kaufmann. 2002. The IFN-inducible Golgi- and endoplasmic reticulum- associated 47-kDa GTPase IIGP is transiently expressed during listeriosis. *J Immunol.* 168(7):3428-36.

Zhang H.M., J. Yuan, P. Cheung, H. Luo, B. Yanagawa, D. Chau, N. Stephan-Tozy, B.W. Wong, J. Zhang, J.E. Wilson, B.M. McManus, and D. Yang. 2003. Overexpression of interferon-gamma-inducible GTPase inhibits coxsackievirus B3-induced apoptosis through the activation of the phosphatidylinositol 3-kinase/Akt pathway and inhibition of viral replication. *J Biol Chem.* 278(35):33011-9.

Zhao M., C.R. Shirley, Y.E. Yu, B. Mohapatra, Y. Zhang, E. Unni, J.M. Deng, N.A. Arango, N.H. Terry, M.M. Weil, L.D. Russell, R.R. Behringer, and M.L. Meistrich. 2001. Targeted disruption of the transition protein 2 gene affects sperm chromatin structure and reduces fertility in mice. *Mol Cell Biol.* 21(21):7243-55.

Zhong J., A.H. Peters, K. Kafer, and R.E. Braun. 2001. A highly conserved sequence essential for translational repression of the protamine 1 messenger rna in murine spermatids. *Biol Reprod.* 64(6):1784-9.

Zocco M.A., E. Carloni, M. Pescatori, N. Saulnier, A. Lupascu, E.C. Nista, M. Novi, M. Candelli, V. Cimica, S. Mihm, G. Gasbarrini, G. Ramadori, and A. Gasbarrini. 2006. Characterization of gene expression profile in rat Kupffer cells stimulated with IFN-alpha or IFN-gamma. *Dig Liver Dis.* 38(8):563-77.

7.   Summary

The Immunity-related GTPases (IRG), also known as p47 GTPases, are important factors mediating resistance against different intracellular pathogens. In the mouse there are at least 23 different *IRG* genes. Most of them are located in clusters on chromosome 11 and 18, but one family member, *Irgc* (*CINEMA*), is an isolated gene on chromosome 7. Humans, in contrast, possess only one full-length *IRG* gene called *IRGC*, which is an orthologue of the isolated mouse gene *Irgc*, and one truncated gene called *IRGM*. The high sequence conservation and clear orthology between man and mouse justified an investigation into the the function of IRGC in a mouse model.

IRGC is highly conserved in mammals and orthologues were detected in all subclasses. Although an obvious orthologue of *IRGC* was not detected outside the mammals, the reptile *Anolis carolinensis* possesses an *IRG* gene that is clearly IRGC-related.

Irgc is expressed only in haploid spermatids during spermatogenesis in the testis. This expression pattern seems to be conserved in all mammals. Expression is driven by a conserved promoter containing the transcription factor binding sites for Sox5, Sox17 and NF-Y. In contrast to most other *IRG* genes the promoter of *IRGC* does not contain any ISRE or GAS sites mediating interferon-γ induction. *IRGC* expression was not induced in mouse or human cell lines after interferon-stimulation or *in vivo* after infection with *Listeria monocytogenes*.

Irgc deficient mice were generated and analyzed. However deficiency of Irgc did not have any morphological effect on spermatogenesis and the Irgc-deficient mice were completely fertile.

In order to detect interaction partners of Irgc, a yeast two-hybrid screen of a cDNA library from testis was performed. Two putative interaction partners were detected, the eukaryotic release factor 1 (eRF1) and a testis-specific splice variant of the Golgi reassembly and stacking protein 2 (GORASP2).

From the data obtained it was concluded that IRGC is not a resistance factor like the interferon-inducible IRG proteins, but mediates some yet unknown function in spermatogenesis. Despite the strong conservation of IRGC a phenotype in Irgc deficient mice could not be detected yet.

8.   Zusammenfassung

Die Immunity-related GTPasen IRG sind wichtige Faktoren des zell-unabhängigen angeborenen Immunsystems zur Abwehr von intrazellulären Pathogenen. Die Maus verfügt über mindestes 23 verschiedene *IRG* Gene. Die meisten sind in Clustern auf den Chromosomen 11 und 18 lokalisiert, aber ein Gen mit dem Namen *Irgc* (*CINEMA*) liegt als isoliertes Gen auf Chromosom 7. Der Mensch verfügt im Gegensatz zur Maus nur über ein komplettes *IRG* Gen namens *IRGC*, das ein Ortholog des Gens *Irgc* in der Maus ist. Zusätzlich besitzt der Mensch noch das verkürzte Gen *IRGM*. Um die Rolle der IRG Proteine im Menschen zu verstehen ist es von entscheidender Bedeutung die Funktion von Irgc in der Maus zu analysieren.

IRGC ist stark konserviert in Mammaliern und Orthologe finden sich in allen *Mammalia*-Unterklassen. Außerhalb der *Mammalia* wurde kein eindeutiges *IRGC* Ortholog identifiziert, aber das Reptil *Anolis carolinensis* besitzt ein *IRG* Gen, das eindeutig *IRGC* verwandt ist.

Irgc wird nur während der Spermatogenese in haploiden Spermatiden im Hoden exprimiert. Dieses Expressionsmuster scheint in allen Mammaliern konserviert zu sein. Die Expression wird von einem konservierten Promoter mit Transkriptionsfaktor-Bindestellen für Sox5, Sox17 und NF-Y reguliert.

Im Gegensatz zu den meisten anderen *IRG* Genen enthält der Promoter von *IRGC* weder ISRE noch GAS Motive, die Interferon-γ induzierte Expression vermitteln. Die Expression von *IRGC* konnte in verschiedenen murinen und menschlichen Zelllinien durch Stimulation mit Interferonen nicht induziert werden. Ebenso induziert die Infektion von Mäusen mit *Listeria monocytogenes in vivo* keine *Irgc* Expression.

Um die Funktion von Irgc zu analysieren wurden Irgc defiziente Mäuse generiert. Die Untersuchung dieser Mäuse zeigte, dass das Fehlen von Irgc keine morphologischen Auswirkungen auf die Spermatogenese hat und die entsprechenden Mäuse fruchtbar sind.

Zur Identifizierung von möglichen Interaktionspartnern wurde ein cDNA Bank aus dem Hoden mit dem Yeast Two-Hybrid System analysiert. Dabei wurden zwei putative Partner von Irgc identifiziert. Den eukaryotische Terminations (Release) Faktor 1 (eRF1) und eine Hoden-spezifische Spleissvariante von GORASP2 (Golgi reassembly and stacking protein 2).

Die Ergebnisse dieser Arbeit lassen darauf schließen, dass IRGC im Gegensatz zu den anderen IRG Proteinen kein Bestandteil des zellautonomen Immunsystems ist, sondern eine

noch nicht bekannte Funktion in der Spermatogenese ausführt. Trotz der starken Konserviertheit von IRGC konnte bis jetzt kein Phänotyp in Irgc defizienten Mäusen entdeckt werden.

9. Danksagung

Natasa Papic und Niko Pawlowski danke ich für die Unterstützung bei meinen Ausflügen in die Biochemie.

Gaby, Rita, Bettina und Steffi danke ich für ihre Hilfe.

Michael Knittler danke ich für seine Hilfe bei allen Fragen und motivierenden Worte.

Außerdem danke ich allen anderen aktuellen und ehemaligen Mitgliedern der Arbeitsgruppen Howard und Knittler.

Den Mitgliedern der Arbeitsgruppen Langer, Praefcke und Dohmen danke ich für das wunderbare Arbeitsklima auf unserer Etage.

Für das Zustandekommen dieser Arbeit haben auch viele Menschen außerhalb des Labors einen wichtigen Beitrag geleistet. Ich bedanke mich bei…

…meinen Brüdern und Freunden Alexander und Sebastian…

…Ete, Rasta, Ömmes, Gerd & Andrea, Jens, Lustig für alles…

…Werner, Ralf, Frank & Friederike und allen, die ich hier vergessen habe…

…Roger, Bruce, Mark, Bruce, Eric, Joe, Farin für musikalische Inspiration…

…Jörg Claren, Kommilitone, Weggefährte, Horizonterweiterer und guter Freund...

…Kerstin dafür, dass sie mit mir einen Kaffee trinken war…

Besonders möchte ich mich bei meinen Eltern für die liebevolle Unterstützung während des ganzen Weges durchs Studium bedanken und ohne deren Hilfe diese Arbeit nicht möglich gewesen wäre.

10.   Erklärung

Ich versichere, dass ich die von mir vorgelegte Dissertation selbständig angefertigt, die benutzten Quellen und Hilfsmittel vollständig angegeben und die Stellen der Arbeit – einschließlich Tabellen, Karten und Abbildungen -, die anderen Werken im Wortlaut oder dem Sinn entnommen sind, in jedem Einzelfall als Entlehnung kenntlich gemacht habe; dass diese Dissertation noch keiner anderen Fakultät oder Universität zur Prüfung vorgelegen hat; dass sie – abgesehen von unten angegebenen Teilpublikationen – noch nicht veröffentlicht worden ist sowie, dass ich eine solche Veröffentlichung vor Abschluß des Promotionsverfahrens nicht vornehmen werde. Die Bestimmungen dieser Promotionsordnung sind mir bekannt.

Die von mir vorgelegte Dissertation ist von Herrn Prof. Dr. Jonathan C. Howard betreut worden.

_____

Teilpublikationen:

Bekpen C., J.P. Hunn, C. Rohde, I. Parvanova, L. Guethlein, D.M. Dunn, E. Glowalla, M. Leptin, and J.C. Howard. 2005. The interferon-inducible p47 (IRG) GTPases in vertebrates: loss of the cell autonomous resistance mechanism in the human lineage. *Genome Biol.* 6(11):R92.

11.   Lebenslauf

Name:	Christoph Rohde
Geburtsdatum:	7. Januar 1977
Geburtsort:	Köln
Staatsangehörigkeit:	deutsch
Familienstand:	ledig

Ausbildung

1983-1987	Besuch der Fortuna-Grundschule in Bergheim-Oberaußem
1987-1996	Besuch des Erftgymnasiums in Bergheim/Erft
1996	Allgemeine Hochschulreife
1996-1997	Grundwehrdienst
WS 1997/1998	Immatrikulation an der Mathematisch-Naturwissenschaftlichen Fakultät der Universität zu Köln. Diplomstudiengang: Biologie
2002-2003	Diplomarbeit Biologie (Fachrichtung Genetik) am Institut für Genetik der Universität zu Köln, Abteilung von Prof. Dr. Jonathan C. Howard
ab Juni 2003	Promotionsstudiengang Biologie (Fachrichtung Genetik) am Institut für Genetik, Universität zu Köln, Abteilung von Prof. Dr. Jonathan C. Howard